Studies on saccharothriolides, phenyl-substituted 10-membered macrolides from a rare actinomycete *Saccharothrix* sp. and precursor-directed *in situ* synthesis of saccharothriolide analogs

2016

盧　　山

Table of Contents

Chapter 2

Plausible Biosynthetic Pathway of Saccharothriolides and Isolation of a Key Precursor "Precursor A"

Chapter 3

Precursor-Directed *in situ* Synthesis of Saccharothriolide Analogs and their Structure-Activity Relationship Study

GENERAL INTRODUCTION

Actinomycetes, as a great resource for the discovery of bioactive natural products, have been well studied in the past years. Of all reported bioactive compounds of microbial origin, 45% are produced by actinomycetes. Until now, many of the successful antibiotic products on the market are produced by such actinomycetes; rifamycins are produced by *Amycolatopsis mediterranei*, erythromycin by *Saccharopolyspora erythraea*, teicoplanin by *Actinoplanes teichomyceticus*, vancomycin by *Amycolatopsis orientalis* and gentamicin from *Micromonopsora purpurea*. [1-3]

Streptomyces is the largest genus of actinomycetes. Since the discovery of streptomycin, a large number of antibiotics have been discovered from *Streptomyces* such as neomycin, nystatin, amphotericin B, and natamycin. However, since *Streptomyces* has been well studied, it becomes harder and harder to discover interesting natural products with new structure and new bioactivity. The focus of industrial screening has therefore moved to less exploited genera of rare actinomycetes. Rare actinomycetes (or non-streptomycete actinomycetes) are regarded as the actinomycete strains whose isolation frequency determined by conventional methods is much lower than that of the streptomycete strains. Investigation of these so called 'rare' actinomycetes will hopefully lead us to discover new bioactive natural products.[1,2]

Saccharothrix sp., one of the rare actinomycetes, was first reported from a soil sample collected in Australia in 1984.[4] Dozens of bioactive natural products with a structural and biological diversity have been isolated from this genus: for example, a naphthoquinone derivative sacchathridine A which was reported as a prostaglandin release inhibitor,[5] 16-membered macrolides tianchimycins A and B,[6] cytotoxic 20-membered macrolides ammocidins A-D,[7,8] antibacterial galacardins A and B,[9] and antitumor rebeccamycin.[10-14] (Figure 1)

In the course of our chemical screening for novel microbe metabolites, we found that the culture extract of *Saccharothrix* sp. A1506 contains novel metabolites and discovered a variety of phenyl-substituted 10-membered macrolides, designated as saccharothriolides (**Chapter 1**). Structure analyses implied the presence of common biosynthetic precursors, including precursor A (**Chapter 2**). Identification of precursor A allowed us to generate new saccharothriolide analogs by precursor-directed *in situ* synthesis (PDSS) method (**Chapter 3**). In this thesis, isolation and generation of unique metabolites by exploring rare resources and PDSS method are described.

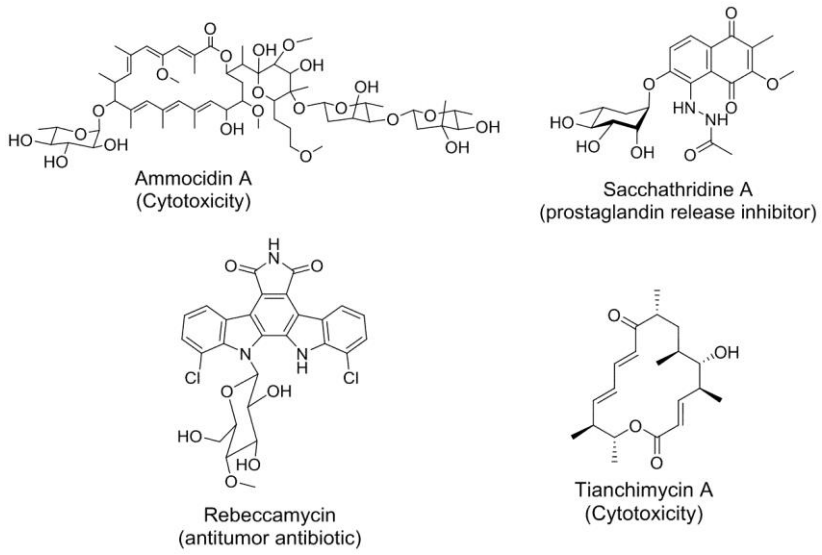

Figure 1. Examples of bioactive natural products from genus *Saccharothrix*.

Chapter 1

Isolation, Structure Elucidation, and Biological Activities of Saccharothriolides A-F, Produced by a Rare Actinomycete *Saccharothrix* sp. A1506

1. Introduction

Expanding natural chemical diversity is an important way for drug leads discovery, since natural products can possess highly potent and/or selective biological activities.[15,16] Over 10,000 bioactive secondary metabolites have been identified from a variety of actinomycetes.[17] In discovery programs, however, compounds identified as active substances from bioassay-guided isolation are often known substances.[18] To avoid this problem, rare actinomycetes are being explored as potential sources for discovering novel classes of bioactive compounds.[19] The genus *Saccharothrix* is considered to be a rare actinomycete. A growing number of novel bioactive metabolites including antibiotics and cytotoxic compounds have been reported from this genus.[5-14]

The Medium-sized macrolides are a class of natural products that consist of a large macrocyclic lactone ring (8- to 16-membered lactones rings). Among them, the 14-, 15-, and 16-membered macrolides are a widely used family of antibiotics, and some of them are developed as FDA-approved pharmaceutical drugs, such as Azithromycin, Clarithromycin, Erythromycin, Fidaxomicin and Telithromycin. Unlike the 14-, 15-, and 16-membered macrolides, naturally occurring 10-membered macrolides, such as saccharothriolides family, are categorized as rare species of organic molecules which has not been well studied. Since many of them have interesting and potent activities, including cytotoxic, phytotoxic, antimalarial, antifungal, antibacterial, and anti-microfilament activities. It should be stressed that further investigations may provide further insight into their biological roles in the treatment of diseases.[20-21] On the other hand, chemically constructing 10-membered lactone is not straightforward, and is frequently more difficult to achieve than that of other macrocyclic lactones, therefore this challenging class of natural products has been stimulating chemists to develop new methodologies for the total synthesis of 10-membered macrolides.[22]

Chemical screening is an alternative to identify novel metabolites without any information of bioactivity.[23-26] We surveyed more than 30,000 microbe cultures by LC-MS analysis to find novel metabolites, and isolated six new 10-membered macrolides, saccharothriolides A-F (**1-6**) from the rare actinomycete *Saccharothrix* sp. A1506.[27-28] Saccharothriolides A-F (**1-6**) possessed unique phenyl-substituted 10-membered

macrolide structures (Figure 2). They could be biosynthesized from an aryl acid and all sp^3 carbons on the lactone ring possess chirality. Their chemical structures were deduced by extensive spectroscopic analyses including advanced universal NMR database method and HR-ESI-MS data. The absolute configurations were determined by the modified Mosher's method and TDDFT-calculation of ECD spectra. Saccharothriolides A, B, D and E had an aryl amine substituent in the lactone ring through a C-N bond, while saccharothriolide C possessed a hydroxy group at C-7. Saccharothriolides D and E were determined to be C-2 epimers of saccharothriolides A and B, respectively. Saccharothriolide F was identified to be a demethylated congener of saccharothriolides A and D at the C-2 position. Unexpectedly, two pairs of C-2 epimers were isolated from the same actinomycete extract, and these epimers showed different cytotoxicity against the human fibrosarcoma HT1080 cells.

The discovery of an array of new phenyl-substituted 10-membered macrolides demonstrates the potential of this genus *Saccharothrix* as drug discovery resources.

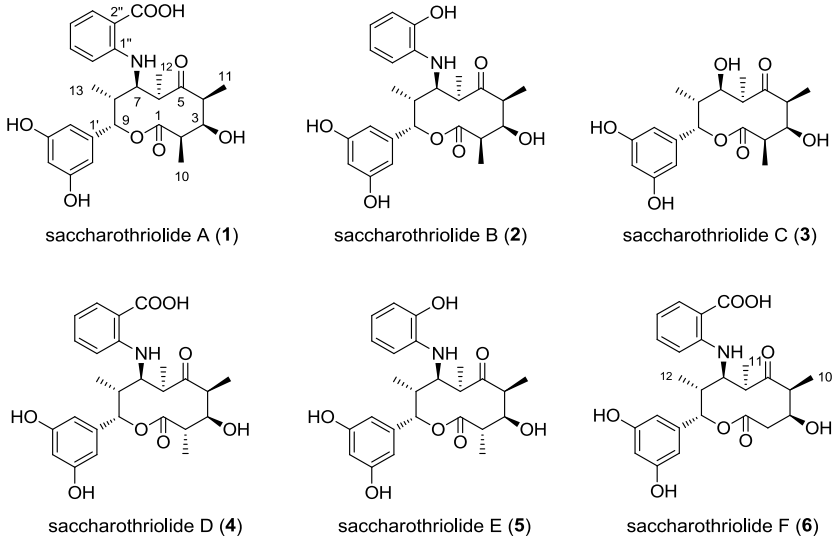

Figure 2. Chemical structures of saccharothriolides A-F (**1-6**).

2. Results and Discussion

2.1 Extraction and Isolation

I surveyed more than 30,000 microbe cultures by LC-MS analysis to identify novel metabolites from a culture broth of a rare actinomycete *Saccharothrix* sp. A1506. *Saccharothrix* sp. A1506 was isolated from a soil sample collected in Yamanashi Prefecture, Japan. The culture broth of *Saccharothrix* sp. (6 L) was extracted with *n*-BuOH, and then concentrated to afford a crude residue (5.44 g). This residue was separated by repeated column chromatography on silica gel to give 35 fractions. This metabolite, designated saccharothriolide A (**1**), was isolated from combined fractions 23 to 25, and exhibited an MS signal (*m/z* 486.2134 $[M+H]^+$) with no previous report and a UV absorption at 345 nm characteristic to anthranilic acid.

Further analysis of the LC-MS data of each fraction revealed the presence of five congeners, saccharothriolides B-F (**2-6**). We detected metabolites **2** and **3** as saccharothriolide congeners; the MS signal of **2** was 14 mass units less than **1** (C=O vs CH_2), while the MS signal of **3** indicated the absence of the anthranilic acid of **1**. In the fractions that contained metabolite **1**, we detected two related metabolites **4** and **6** that showed UV absorption similar to that of metabolite **1**, but were less hydrophobic. In the same manner, compound **5** was identified as a saccharothriolide congener because its UV absorption and MS signal were similar to that of metabolite **2** (Figure 3).

By LC-MS-guided isolation, we purified metabolites **1** (24.7 mg), **2** (5.4 mg), **3** (17.8 mg), **4** (4.98 mg), **5** (0.90 mg) and **6** (1.38 mg) (Scheme 1).

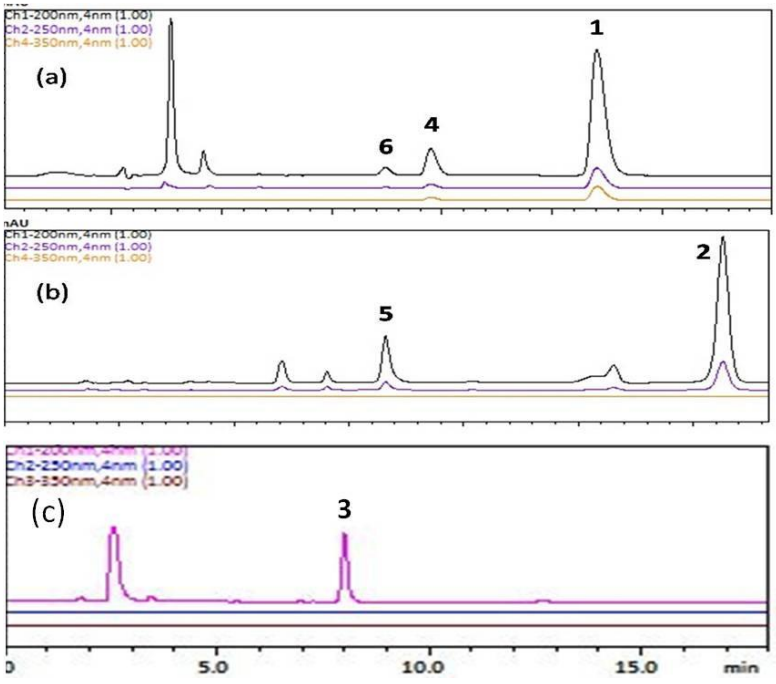

Figure 3. HPLC analysis of saccharothriolides A (**1**), B (**2**), C (**3**), D (**4**), E (**5**), and F (**6**).

(a) HPLC chromatogram obtained for a fraction containing **1**, **4** and **6** (PEGASIL ODS SP100, ϕ4.6×250 mm, 40% MeCN, 1.0 mL/min);

(b) HPLC chromatogram obtained for a fraction containing **2** and **5** (PEGASIL ODS SP100, ϕ4.6×250 mm, 40% MeCN, 1.0 mL/min);

(c) HPLC chromatogram obtained for a fraction containing **3** (PEGASIL ODS SP100, ϕ4.6×250 mm, 30% MeCN, 1.0 mL/min).

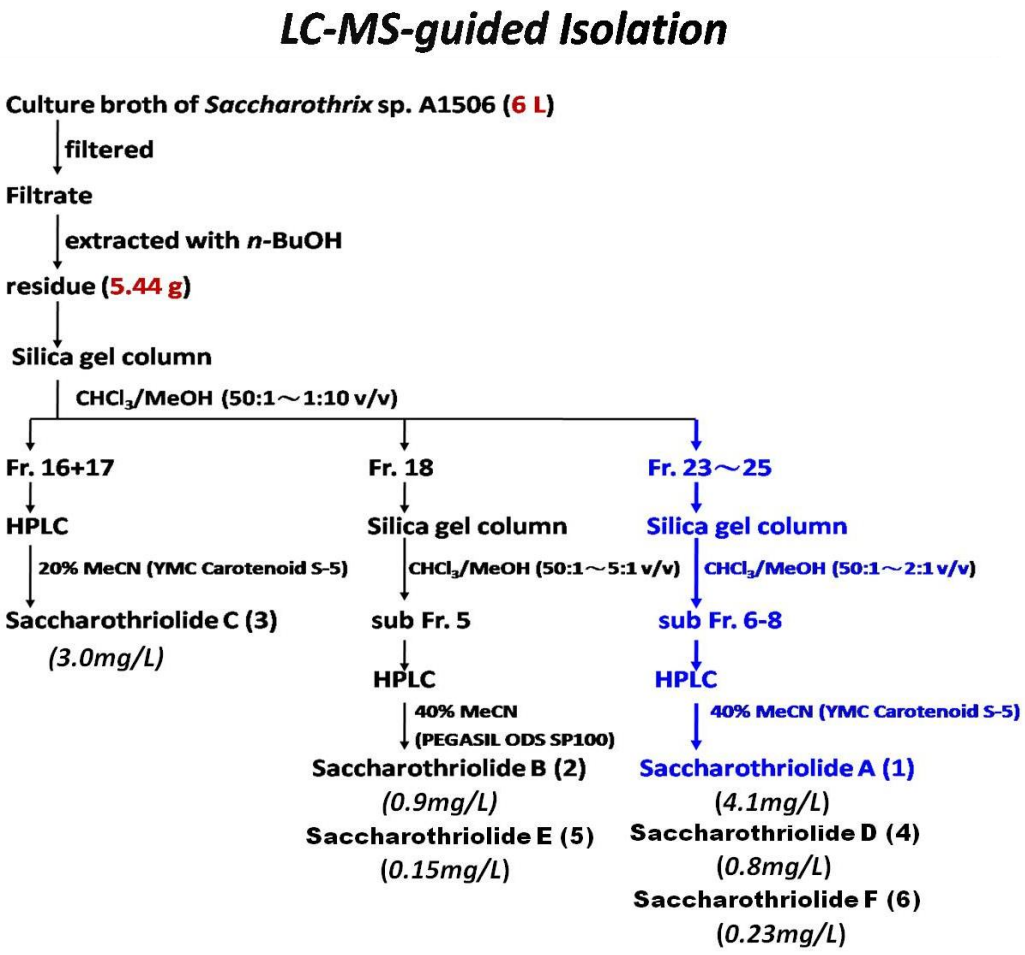

Scheme 1. Isolation procedure of saccharothriolides A-F (**1**-**6**)

Table 1. ^{1}H NMR data for saccharothriolides A-F (**1-6**) in methanol-d_4

position	δ_H, m, *J* (Hz)					
	1	**2**	**3**	**4**	**5**	**6**
2	2.88, qd, 6.9, 3.4	2.88, qd, 6.9, 3.4	2.85, brs	2.47, dq, 9.7, 6.9	2.47, dq, 9.7, 6.9	2.78, dd, 15.8, 4.3 (2a)
						2.47, dd, 15.8, 11.2 (2b)
3	3.79, brs	3.80, d, 2.3	3.78, brs	4.40, dd, 9.7, 2.9	4.40,dd, 9.7, 3.4	4.81, d, 10.3
4	3.28, q, 7.5	3.29, qd, 7.5, 1.2	3.27, brs	3.26, qd, 6.3, 3.4	3.25, qd, 6.9, 3.4	3.28, overlap
6	3.43, q, 6.9	3.42, qd, 6.9, 2.3	3.20, brs	3.51, q, 6.9	3.48, qd, 7.5, 1.7	3.50, m
7	3.66, brs	3.51, dd, 4.0, 2.3	3.63, brs	3.67, brs	3.53, brs	3.68, brs
8	2.19, qd, 6.9, 5.2	2.24, qd, 7.5, 4.0	2.10, brs	2.10, qd, 7.5, 2.9	2.16, qd, 6.9, 2.9	2.12, m
9	5.50, brs	5.55, brs	5.59, brs	5.37, brs	5.38, brs	5.41, brs
10	1.20, d, 6.9	1.20, d, 6.9	1.19, d, 6.9	1.45, d, 6.9	1.45, d, 7.5	1.10, d, 6.9
11	1.46, d, 7.5	1.46, d, 7.5	1.42, d, 7.5	1.09, d, 6.3	1.08, d, 6.9	1.33, d, 6.9
12	1.35, d, 6.9	1.39, d, 6.9	1.42, d, 7.5	1.32, d, 6.9	1.35, d, 7.5	1.05, d, 7.5
13	1.09, d, 6.9	1.04, d, 7.5	0.92, d, 6.9	1.05, d, 7.5	1.02, d, 6.9	-
2'/6'	5.87, s	5.87, d, 2.3	6.10, s	5.87, s	5.89, d, 1.7	5.89, s
4'	6.06, s	6.06, t, 2.3	6.14, t, 2.3	6.05, s	6.06, t, 2.3	6.04, s
3"	7.95, brs	6.73, d, 8.1	-	7.93, d, 6.3	6.73, dd, 8.0, 1.2	7.93, d, 4.6
4"	6.57, t, 5.7	6.48, t, 6.5	-	6.55, t, 6.9	6.46, td, 7.5, 1.2	6.55, t, 5.7
5"	7.31, t, 7.5	6.70, t, 7.5	-	7.27, t, 7.5	6.69, td, 7.5, 1.2	7.26, t, 7.5
6"	6.66, d, 8.6	6.47, d, 7.0	-	6.62, d, 8.6	6.44, d, 8.0	6.63, d, 8.6

Table 2. ^{13}C NMR data for saccharothriolides A-F (**1-6**) in methanol-d_4

position	δ_C					
	1	**2**	**3**	**4**	**5**	**6**
1	173.8, C	173.9, C	173.8, C	173.3, C	173.3, C	169.8, C
2	46.3, CH	46.4, CH	46.3, CH	44.4, CH	44.3, CH	39.0, CH_2
3	81.4, CH	81.3, CH	80.8, CH	73.9, CH	73.8, CH	68.8, CH
4	50.8, CH	50.9, CH	51.2, CH	52.2, CH	52.3, CH	51.9, CH
5	224.6, C	225.8, C	224.7, C	216.3, C	217.4, C	216.9, C
6	43.7, CH	43.8, CH	44.1, CH	42.2, CH	42.1, CH	42.8, CH
7	62.2, CH	63.5, CH	80.1, CH	61.5, CH	62.7, CH	61.6, CH
8	43.1, CH	42.8, CH	47.3, CH	43.8, CH	43.2, CH	43.6, CH
9	74.3, CH	74.1, CH	73.1, CH	74.6, CH	74.5, CH	75.4, CH
10	14.1, CH_3	14.0, CH_3	14.0, CH_3	16.7, CH_3	16.7, CH_3	8.7, CH_3
11	18.4, CH_3	18.3, CH_3	18.2, CH_3	9.0, CH_3	8.9, CH_3	19.0, CH_3
12	20.3, CH_3	20.4, CH_3	20.3, CH_3	19.2, CH_3	19.3, CH_3	11.1, CH_3
13	10.7, CH_3	10.9, CH_3	10.3, CH_3	11.1, CH_3	11.3, CH_3	-
1'	144.9, C	145.0, C	144.5, C	144.4, C	144.5, C	144.4, C
2'/6'	104.7, CH	104.8, CH	105.0, CH	104.6, CH	104.7, CH	104.6, CH
3'/5'	159.5, C	159.5, C	159.7, C	159.6, C	159.5, C	159.5, C
4'	102.3, CH	102.2, CH	102.4, CH	102.3, CH	102.3, CH	102.2, CH
1"	151.7, C	138.2, C	-	151.5, C	138.3, C	151.2, C
2"	113.7, C	146.0, C	-	117.5, C	146.1, C	n.i.[a]
3"	134.1, CH	115.2, CH	-	133.9, CH	115.1, CH	133.9, CH
4"	115.6, CH	117.4, CH	-	115.5, CH	117.3, CH	115.5, CH
5"	135.6, CH	121.6, CH	-	134.9, CH	121.6, CH	134.6, CH
6"	111.8, CH	111.1, CH	-	111.7, CH	110.9, CH	111.7, CH
2"-COOH	173.8, C	-	-	173.3, C	-	172.7, C

[a] no information

2.2 Structure Elucidation

2.2.1 Structure Elucidation of Saccharothriolide A (1)

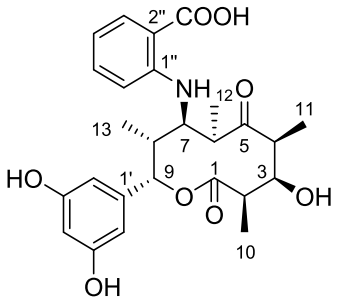

Saccharothriolide A (1)

Saccharothriolide A (**1**) was obtained as a light yellow oil with $[\alpha]_D^{20}$ +18.0 (*c* = 0.74, MeOH). The molecular formula was determined to be $C_{26}H_{31}NO_8$ by HR-ESI-MS (*m/z* 486.2134 $[M+H]^+$, calcd 486.2128), indicating the presence of 12 degrees of unsaturation. The IR spectrum showed absorptions corresponding to hydroxy (3327 cm^{-1}), ester carbonyl (1732 cm^{-1}), and ketone (1679 cm^{-1}) groups. The ^1H NMR spectrum of **1** displayed seven aromatic protons (δ 7.95, 7.31, 6.66, 6.57, 6.06×2, 5.87 ppm) and an oxymethine proton (δ 5.50 ppm) in addition to four aliphatic methyl signals (δ 1.09, 1.20, 1.35, 1.46 ppm) and six methine protons (δ 2.19, 2.88, 3.28, 3.43, 3.66, 3.79 ppm). The ^{13}C NMR spectrum included 26 carbon signals corresponding to four aliphatic methyls (δ 10.7, 14.1, 18.4, 20.3), seven aliphatic methines including two carbons adjacent to an oxygen atom (δ 74.3 and 81.4) and one carbon adjacent to a nitrogen atom (δ 62.2), twelve aromatic carbons and three carbonyl carbons (δ 173.8×2, 224.6) (Table 1 and 2).

^1H-^1H COSY experiment revealed the presence of three spin systems: CH_3-10/H-2/H-3/H-4/CH_3-11, CH_3-12/H-6/H-7/H-8/CH_3-13/H-9, and H-3”/H-4”/H-5”/H-6” (Figure 4). HMBC correlations from CH_3-11 to C-5, and from CH_3-12 to C-5 connected C-4 and C-6 through a ketone group. HMBC correlations from both H-3 and H-9 to carbonyl C-1 connected C-2 and C-9 through an ester bond, leading to the formation of the 10-membered lactone ring (Figure 4). The formation of the lactone ring was further supported by the observation of the down-field shifted chemical shift for H-9 (δ_H5.50). The meta-disubstituted benzene ring was determined on the basis of the HMBC correlations from H-4’ to C-2’/C-6’, and from H-2’/H-6’ to C-3’/C-5’. This benzene ring was connected to C-9 due to the HMBC correlations from H-9 to aromatic carbons C-1’ and C-2’/6’. The presence of anthranilic acid suggested by the characteristic UV absorption (Figure S3)[29] was confirmed by HMBC correlations from H-6” (δ_H 6.66)

to C-2" (δ_C 113.7), and from H-3" (δ_H 7.95) to C-1" (δ_C 151.7) and 2"-COOH (δ_C 173.8), along with the $^1H-^1H$ COSY correlations from H-3" to H-6" (Figure 4). The anthranilic acid was connected to the lactone ring at C-7 through an NH group, which was deduced by the up-field shifted chemical shift for C-7 (δ_C 62.2) and the presence of a free carboxylic acid (δ_C 173.8). This connection was further confirmed by the mutual NOESY correlations among H-6", H-7, and H-8 (Figure 4).

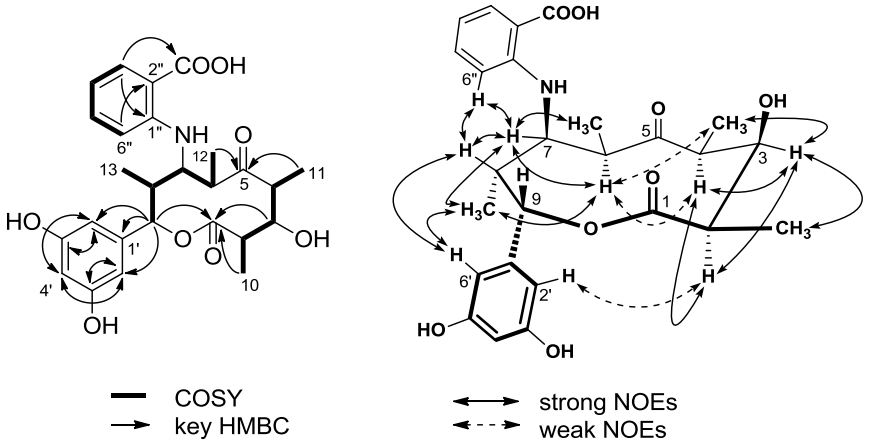

Figure 4. $^1H-^1H$ COSY (left, bold) correlations and selected HMBC (left, arrow) and NOESY (right) correlations in saccharothriolide A (**1**).

The relative stereochemistry of metabolite **1** was deduced from the NOESY data (Figure 4). NOESY cross peaks between H-2 and H-4 indicated that they are placed in the same α face, whereas NOESY correlations between H-3 and H-2, H-4, CH_3-10, and CH_3-11suggested the α configuration of H-3. NOESY correlations between H-6 and H-4(weak), CH_3-11(weak), and CH_3-13 indicated an α configuration for these protons. A β configuration for H-8 was then determined. Correlations between H-7 and H-6, H-8, CH_3-12, and CH_3-13 suggested that H-7 has an α configuration. Finally, NOESY correlations between the aromatic proton H-6' and H-8, and CH_3-13, together with a weak correlation from the aromatic proton H-2' to H-2, revealed the β orientation of H-9. Thus, the relative configurations were deduced to be 2*R**, 3*R**, 4*S**, 6*R**, 7*R**, 8*R**, 9*S**.

Macrolides can exist in several conformations, which can be a potential cause of mis-interpretation of the NOESY data. We next analyzed the relative stereochemistry of **1** by the advanced statistical Universal NMR Database (UDB) approach, originally developed by Kishi and co-workers.[30-32] Reductive opening of the lactone of **1** with $LiAlH_4$ furnished a linear product **7** (Figure 5). The ^{13}C NMR data for the two tetrad segments, C3-C6 and C5-C2, were subjected to the statistical UDB analysis. The

difference between the adjusted NMR data of the tetrad segments in **7** and Kishi's database was calculated to reveal that both sequences have an *anti-anti-anti* configuration (Table S1-4), which was in good agreement with the NOESY data in **1**.

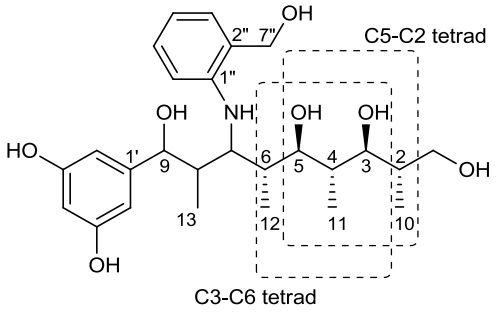

Figure 5. Analysis of the stereochemistry of compound **7** (C3-C6 and C5-C2 tetrads) by the statistical UDB approach.

The absolute stereochemistry was determined by the modified Mosher's method (Figure 6).[33] Phenolic hydroxy groups and carboxylic acid of **1** were first protected by methylation with CH_3I to yield a tri-methyl derivative **8**. The methylated derivative **8** was treated with (*R*)- and (*S*)-MTPA chloride to afford (*S*)- and (*R*)-MTPA esters of **8**, respectively. The $\Delta\delta$ (δ_S-δ_R) values for the protons flanking the C-3 chiral center revealed the 3*R* absolute configuration, which in turn concluded the absolute configurations of **1** as 2*R*, 3*R*, 4*S*, 6*R*, 7*R*, 8*R*, 9*S*.

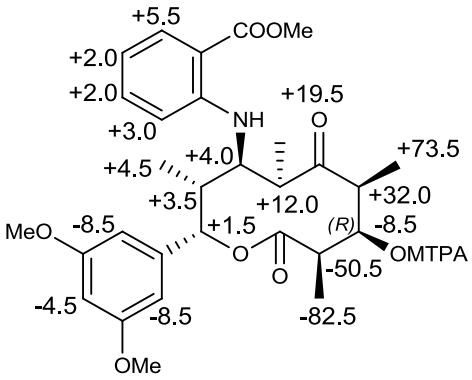

Figure 6. $\Delta\delta$ (δ_S-δ_R) values (in Hz) for the MTPA esters of **8**.

The modified Mosher's method is sometimes not applicable to axial hydroxy groups.[34] In order to confirm the above results, we finally measured the CD spectrum of **1**, which was compared with the electronic circular dichroism (ECD) spectrum calculated by time-dependent density functional theory (TDDFT). As shown in Figure 7, the experimental CD spectrum showed a Cotton effect at 199 ($\Delta\varepsilon$, +15.0), 227 ($\Delta\varepsilon$, −25.0)

and 355 ($\Delta\varepsilon$, +3.46)nm, all of which were observed in the ECD spectrum calculated for the stereochemistry of 2*R*, 3*R*, 4*S*, 6*R*, 7*R*, 8*R*, 9*S*. We also calculated $^{3}J_{\text{H-H}}$ values for the stable conformer, which were almost the same to those of the measured ones (Table S5).

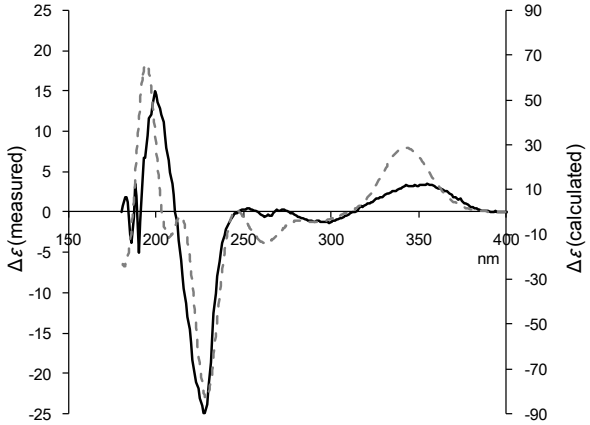

Figure 7. Experimental ECD (solid line) and calculated ECD (dotted line) spectra of saccharothriolide A (**1**). ECD was calculated for 2*R*, 3*R*, 4*S*, 6*R*, 7*R*, 8*R*, 9*S*.

Thus, the absolute configuration of **1** was unambiguously established by two independent methods.

2.2.2 Structure Elucidation of Saccharothriolide B (2)

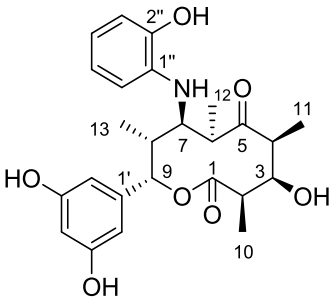

Saccharothriolide B (2)

To find congeners of saccharothriolide A (**1**), we investigated the LC-MS data of the crude broth extract. We detected a metabolite whose ion peak was observed at *m/z* 458.2162 ($[M+H]^+$), revealing the molecular formula of $C_{25}H_{31}NO_7$. This metabolite, designated as saccharothriolide B (**2**), contained one nitrogen atom the same as **1**, but the molecular size was 28 Da smaller than **1**. Metabolite **2** was obtained as a light yellow oil with $[\alpha]_D^{20}$ -81.2 (*c* = 0.36, MeOH).

The ^1H and ^{13}C NMR data of **2** were very similar to those of **1** (Table 1 and 2), with the exception of the disappearance of the carboxylic acid. The obvious downfield shift of C-2" (δ_C 113.7 in **1**, δ_C 146.0 in **2**) and an upfield shift of C-1" and C-3" (δ_C 151.7 in **1**, δ_C138.2 in **2** and δ_C 134.1 in **1**, δ_C 115.2 in **2**, respectively) were observed, accompanied by a marked upfield shift of H-3" and H-5" (δ_H 7.95 in **1**, δ_H 6.73 in **2** and δ_H 7.31 in **1**, δ_H 6.70 in **2**, respectively), which suggested that **2** possessed a phenolic hydroxy group instead of a carboxylic acid at C-2". This was in agreement with the fact that **2** was 28Da smaller than **1**. The planar structure was deduced by the COSY, HMQC and HMBC data (Figure 8). Detailed analysis of the NOESY spectrum of **2** revealed that the relative stereochemistry was the same as that of **1** (Figure 8): 2*R**, 3*R**, 4*S**, 6*R**, 7*R**, 8*R**, 9*S**.

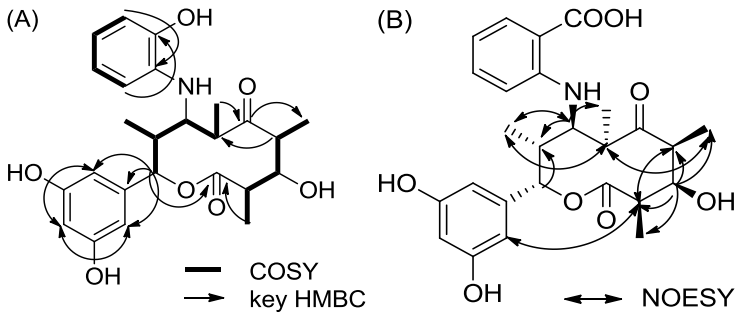

Figure 8. ^1H-^1H COSY and key HMBC correlations (A), and selected NOESY correlations (B) in saccharothiolide B (**2**).

The absolute stereochemistry of **2** was determined by measurement and calculation of ECD. The ECD was calculated for the absolute stereochemistry the same as **1**. The calculated ECD spectrum overlapped well with the experimental CD spectrum (Figure 9), concluding that the absolute stereochemistry of **2** was 2*R*, 3*R*, 4*S*, 6*R*, 7*R*, 8*R*, 9*S*.

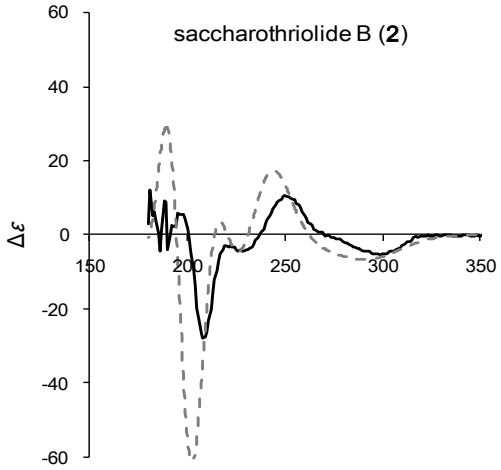

Figure 9. Experimental ECD (solid line) and calculated ECD (dotted line) spectra for saccharothriolide B (**2**). ECD spectra were calculated for 2*R*, 3*R*, 4*S*, 6*R*, 7*R*, 8*R*, 9*S*.

2.2.3 Structure Elucidation of Saccharothriolide C (3)

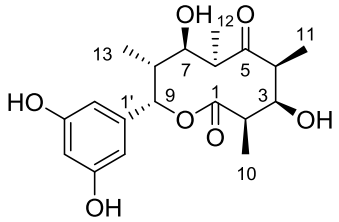

Saccharothriolide C (3)

Saccharothriolides A (**1**) and B (**2**) have an aminoaryl substitution at C-7, suggesting the presence of a common precursor for them, i.e., Michael addition of nucleophilic amines to the corresponding precursor can afford the metabolites **1** and **2**. For investigating this possibility, we surveyed the LC-MS data of the culture broth to identify saccharothriolide C (**3**). Metabolite C (**3**) was obtained as a light yellow oil with $[\alpha]_D^{20}$ -111.8 (*c* = 0.58, MeOH). The HR-ESI-MS data that gave an $[M+Na]^+$ ion peak at m/z 389.1586 ($[M+Na]^+$, calcd 389.1576) revealed the molecular formula of $C_{19}H_{26}O_7$. The ^1H and ^{13}C NMR data of **3** were similar to those of **1** and **2** (Table 1 and 2), except for the

absence of a set of aromatic proton and carbon signals corresponding to the amino aryl groups substituted at C-7. Instead, metabolite **3** possessed a hydroxy group at C-7, supported by the downfield shift of the carbon signal of C-7 (δ_C80.1). The planar structure was elucidated by detailed analysis of the 2D NMR data, while the NOESY data indicated the same relative configuration with those of **1** and **2** (Figure 10). As expected, the absolute stereochemistry of **3** was the same as those of **1** and **2**, because the calculated ECD spectrum for the stereochemistry of 2*R*, 3*R*, 4*S*, 6*R*, 7*R*, 8*R*, 9*S* showed a high similarity to that of the measured one (Figure 11).

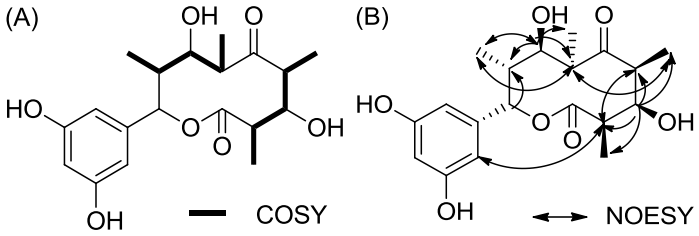

Figure 10. ^{1}H-^{1}H COSY correlations (A), and selected NOESY correlations (B) in saccharothiolide C (**3**).

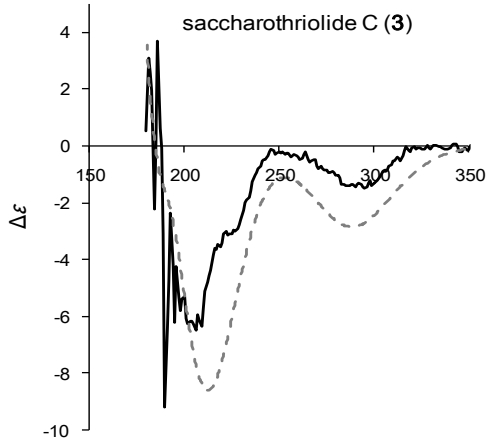

Figure 11. Experimental ECD (solid line) and calculated ECD (dotted line) spectra for saccharothriolide C (**3**). ECD spectra were calculated for 2*R*, 3*R*, 4*S*, 6*R*, 7*R*, 8*R*, 9*S*.

2.2.4 Structure Elucidation of Saccharothriolide D (4)

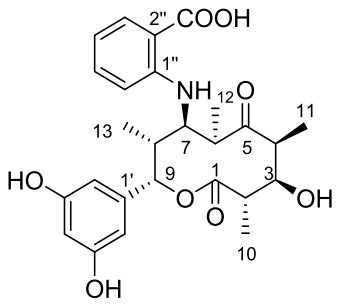

Saccharothriolide D (4)

Saccharothriolide D (**4**) was obtained as a light-yellow oil. The molecular formula was determined to be $C_{26}H_{31}NO_8$ by HR-ESI-MS, the same as that of saccharothriolide A (**1**). The characteristic UV absorption at 341 nm revealed the presence of an anthranilic acid moiety, also present in **1**. The ^{1}H and ^{13}C NMR spectra were also similar to those of **1**, except for slight differences in chemical shifts for atoms in the right part of the lactone ring (Table 1 and 2). The ^{1}H NMR chemical shifts corresponding to H-2 and CH_3-11 in compound **4** were shifted upfield, while those for H-3 and CH_3-10 were shifted downfield compared with compound **1** (Figure S1). Comparison of the ^{13}C NMR spectra of compounds **4** and **1** revealed the differences in the chemical shifts of C-3, C-5, CH_3-10 and CH_3-11 (Figure S1). The ^{1}H-^{1}H COSY experiment revealed the presence of three spin systems; CH_3-10/H-2/H-3/H-4/CH_3-11, CH_3-12/H-6/H-7/H-8/CH_3-13, and H-3”/H-4”/H-5”/H-6” (Figure 12). HMBC correlations from H-6/CH_3-11/CH_3-12 to C-5 connected C-4 and C-6 through a ketone group. HMBC correlations from H-2/CH_3-10 to carbonyl C-1, and from CH_3-13 to C-9, combined with the down-field shifted chemical shift of H-9 (δ_H5.37), connected C-2 and C-9 through an ester bond, leading to the formation of the 10-membered lactone ring (Figure 12). The meta-disubstituted benzene ring was connected to C-9 based on the HMBC correlations from aromatic protons H-2’/6’ to C-9. Taken together, the planar structure of **4** was revealed to be identical to that of **1** and thus compound **4** is a diastereomer of saccharothriolide A (**1**).

The relative stereochemistry of **4** was determined from the NOESY and $^{3}J_{H\text{-}H}$ data (Figure 12). NOESY cross peaks between H-3 and H-4/H-6/CH_3-10/CH_3-13, and between H-6 and CH_3-13 suggested that they were placed in the same α-face. The NOESY correlations between H-7 and H-6/H-8/CH_3-12/CH_3-13 indicated that H-7 also has an α configuration, while the β-orientation of H-9 was revealed by the correlation between the aromatic proton H-6’ and H-8/CH_3-13. The NOESY correlations described above were also observed for metabolite **1**. However, contrary to the case of **1**, no NOESY correlation

was detected between H-2 and H-4/aromatic proton H-2'. Instead, H-2 exhibited a NOESY correlation with CH_3-11, and the aromatic proton H-2' and CH_3-10 showed a NOESY correlation, which led to the identification of the β-orientation of H-2 and the α-orientation of CH_3-10 (Figure 12). Thus, **4** was revealed to be a C-2 epimer of saccharothriolide A (**1**). This result was supported by the $^3J_{H\text{-}H}$ values: values in the left half of the lactone ring were similar between metabolites **4** and **1**, whereas there was an apparent difference in the $^3J_{H2\text{-}H3}$ value (9.7 Hz in **4** and 3.4 Hz in **1**).

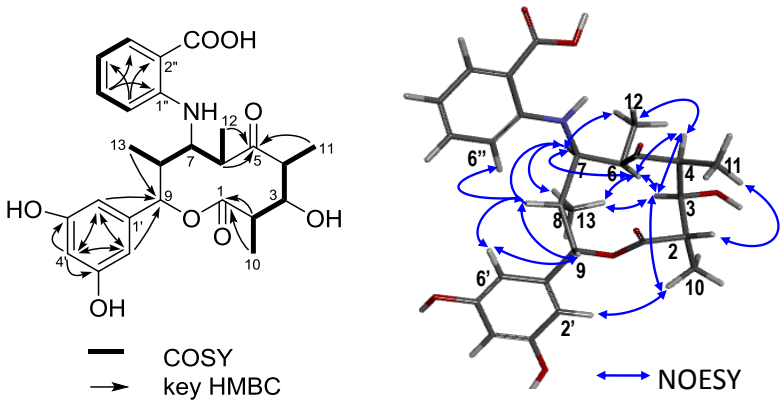

Figure 12. ^{1}H-^{1}H COSY (left, bold) correlations and selected HMBC (left, arrow) and NOESY (right) correlations in saccharothriolide D (**4**).

The absolute stereochemistry of **4** was determined by comparing the ECD spectra of **4** and **1**. The ECD spectrum of **4** showed characteristic Cotton effects at 201 (Δε, +19.2), 227 (Δε, –27.4), and 347 (Δε, +5.1) nm, which were also observed in the spectrum of **1** (Figure 13). Thus, the absolute configuration of **4** was established to be 2*S*, 3*R*, 4*S*, 6*R*, 7*R*, 8*R*, 9*S*.

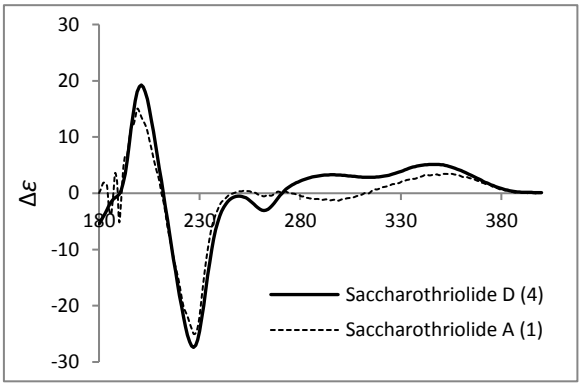

Figure 13. Experimental ECD spectra of saccharothriolide D (**4**) (solid line) and saccharothriolide A (**1**) (dotted line).

2.2.5 Structure Elucidation of Saccharothriolide E (5)

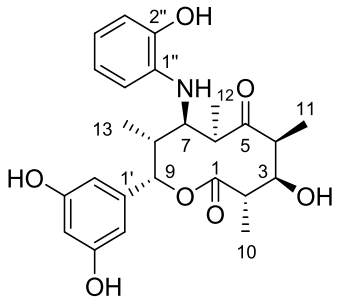

Saccharothriolide E (5)

Saccharothriolide E (**5**) was obtained as a light yellow oil. The molecular formula was determined by HR-ESI-MS to be $C_{25}H_{31}NO_7$, the same as that of saccharothriolide B (**2**). The ^{1}H and ^{13}C NMR data of **5** resembled those of **2**, while differences were observed for the chemical shifts of H-2, H-3, CH_3-10, CH_3-11 (Table 1 and 2, Figure S1). Additionally, the chemical shifts of the lactone ring were very similar to those of **4**. From these results, **5** was deduced to be an epimer of **2** at C-2. The proposed structure was confirmed by detailed analysis of the NOESY spectrum of **5** (Figure 14). The relative configuration of the C-2/C-3 was proven to be same as that of **4** on the basis of the similar NOESY correlations and coupling constants. Therefore, the relative configuration of **5** was deduced to be 2*S**, 3*R**, 4*S**, 6*R**, 7*R**, 8*R**, 9*S**. The ECD spectrum of **5** was almost identical to that of **2** (Figure 15), indicating the absolute stereochemistry was 2*S*, 3*R*, 4*S*, 6*R*, 7*R*, 8*R*, 9*S*.[35]

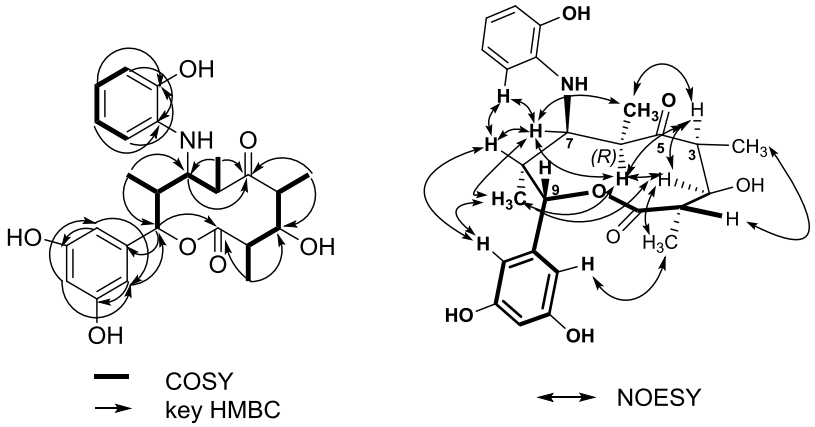

Figure 14. ^{1}H-^{1}H COSY and key HMBC correlations (a), and selected NOESY correlations (b) of saccharothriolide E (**5**).

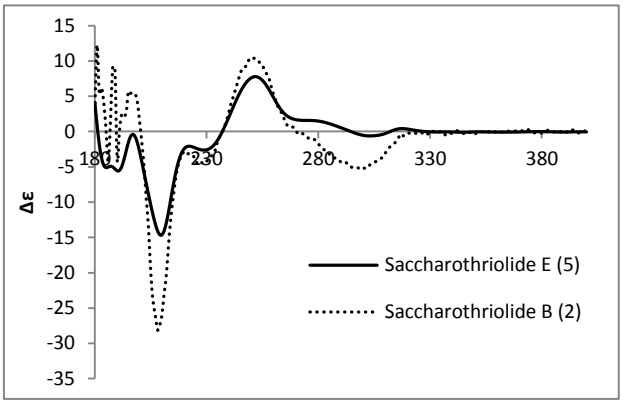

Figure 15. Experimental ECD spectra of saccharothriolide E (**5**) (solid line) and saccharothriolide B (**2**) (dotted line).

2.2.6 Structure Elucidation of Saccharothriolide F (6)

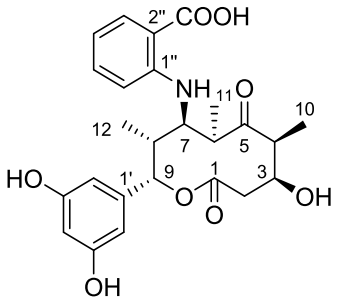

Saccharothriolide F (6)

Saccharothriolide F (**6**) was obtained as a light-yellow oil. HR-ESIMS data for **6** showed an ion peak at *m/z* 472.1981 $[M+H]^+$, indicating the molecular formula of $C_{25}H_{29}NO_8$, which was smaller than saccharothriolide D (**4**) by a CH_2 unit. The UV absorption at 343 nm suggested that metabolite **6** also had an anthranilic acid. The ^1H and ^{13}C NMR spectra of **6** were similar to those of **4** (Table 1 and 2, Figure S1), except for the absence of signals corresponding to CH-2 and CH_3-10 in **4**, and the presence of a methylene signal (δ_H2.78 ppm; δ_C39.0 ppm). These data suggested that **6** should be a demethylated analogue of **1** and **4**. The relative configuration of six stereocenters in the 10-membered lactone ring was established on the basis of the $^1H–^1H$ coupling constant values and NOESY data (Figure 16). The absolute stereochemistry of **6** was determined as 3*S*, 4*S*, 6*R*, 7*R*, 8*R*, 9*S*, since the ECD spectrum (Figure 17) of **6** showed high similarity to that of **4**.

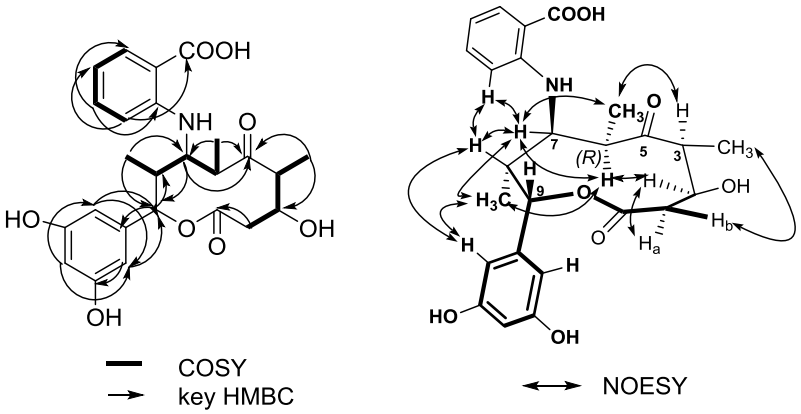

Figure 16. ^{1}H-^{1}H COSY and key HMBC correlations (a), and selected NOESY correlations (b) of saccharothriolide F (**6**).

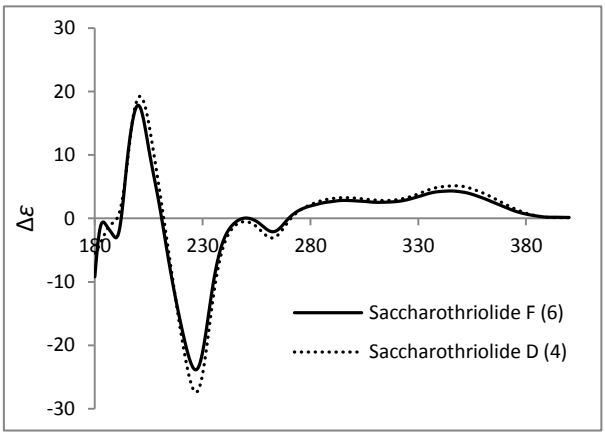

Figure 17. Experimental ECD spectra of saccharothriolide F (**6**) (solid line) and saccharothriolide D (**4**) (dotted line).

2.3 Biological Activities

2.3.1 Cytotoxicity

To analyze the structure-activity relationship (SAR) of these 10-membered macrolides, we examined the cytotoxicity of saccharothriolides A-F (**1**-**6**) against the human fibrosarcoma HT1080 cells (Figure 18).

Only saccharothriolide B (**2**) showed moderate cytotoxicity (IC_{50} value, 13.9 μM) against HT1080 cells. Saccharothriolide E (**5**) showed weak toxicity (IC_{50} value, 29.2 μM), but it was still less potent than the C-2 epimer (**2**). Other saccharothriolides A (**1**) and D (**4**) were inactive even at 100 μM, and F (**6**) showed weak (IC_{50} value, 66.4 μM) toxicity, all of which have an anthranilic acid substituted at C-7. Saccharothriolide C (**3**) was inactive, also indicating the importance of the functional group substituted on C-7.

The availability of saccharothriolides **1**-**6** enabled a structure-activity relationship study that revealed the importance of the phenolic hydroxy group at C-2" and the involvement of the stereochemistry of C-2 for the inhibition of human fibrosarcoma HT1080 cell growth. These results indicate that saccharothriolides are capable of regulating their biological activities by modifying the functional group at C-7 position.

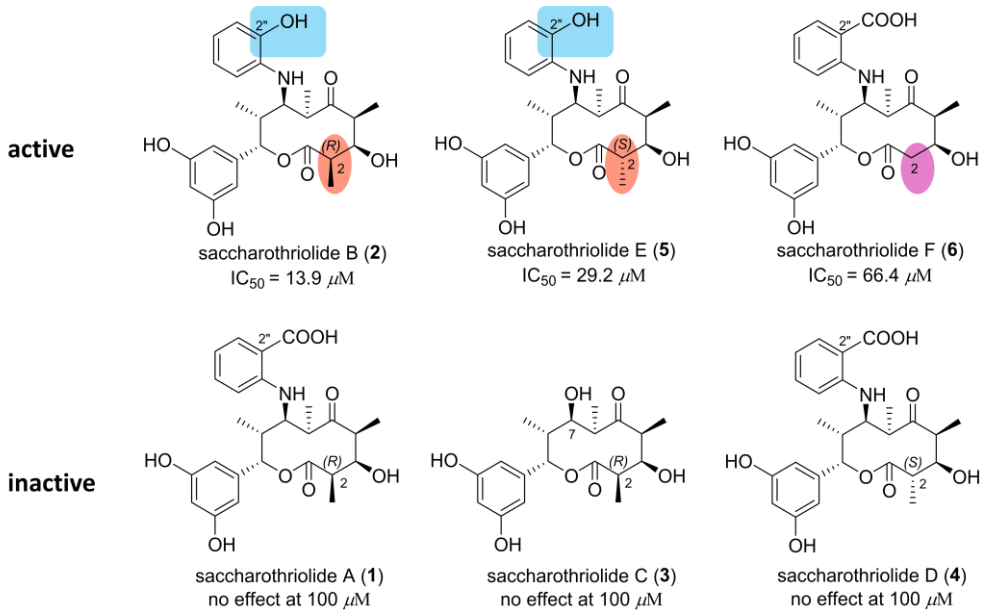

Figure 18. Cytotoxicity of saccharothriolides A-F against human fibrosarcoma HT1080 cells.

2.3.2 Antibacterial Activity

The saccharothriolides A-C (**1**-**3**) were tested in an agar diffusion assay for their antibacterial activity against *Staphylococcus aureus*, *Bacillus subtilis*, *Escherichia coli* and *Pseudomonas aeruginosa*, and compared with the control compounds, (penicillin, streptomycin, and the solvent methanol, Figure 19). Only saccharothriolide B (**2**) showed weak antibacterial activity at 50 μg per disc against *Staphylococcus aureus*.

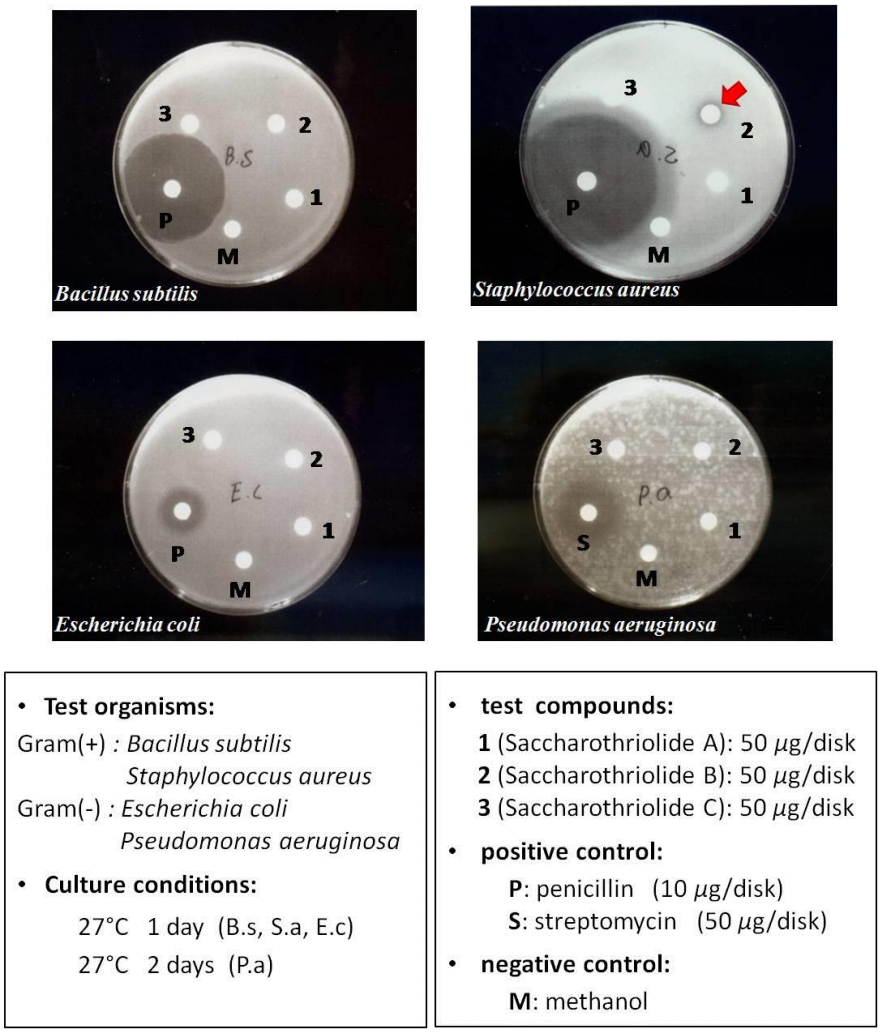

Figure 19. Antibacterial activity of saccharothriolides A-C.

3. Experimental Section

3.1 General Procedures

Optical rotations were measured using the sodium D line (589 nm) at 20°C in methanol. UV spectra were recorded in methanol on a spectrophotometer. IR spectra were measured using an FTIR spectrometer equipped with a ZnSe ATR plate. High resolution ESI-MS spectra were recorded on LC-IT-TOF MS. NMR spectra were recorded on a 500 MHz instrument. ^{1}H and ^{13}C chemical shifts are shown relative to the residual solvent: δ_H 3.31 and δ_C 49.15 for methanol-d_4. Chemical shifts (δ) are shown in parts per million (ppm), and coupling constants (J) are in hertz (Hz). CD spectra were recorded using a CD spectrometer with a 1mm pathlength cell.

3.2 Fermentation, Extraction and Isolation

Saccharothrix sp. A1506 was isolated from a soil sample collected in Yamanashi Prefecture, Japan. A frozen stock culture of the strain A1506 was inoculated into 250-mL Erlenmeyer flasks, each containing 25 mL of a seed medium consisting of 2% potato starch (Tobu Tokachi Nosan Kako Agricultural Cooperative Assoc., Hokkaido, Japan), 2% glucose (Junsei Chemical, Tokyo, Japan), 2% soy bean powder (SoyPro, J-Oil Mills, Tokyo, Japan), 0.5% yeast extract powder (Oriental Yeast, Tokyo, Japan), 0.25% NaCl (Junsei Chemical), 0.32% $CaCO_3$ (Wako Pure Chemical Industries, Osaka, Japan), 0.0005% $CuSO_4 \cdot 5H_2O$ (Wako), 0.0005% $ZnSO_4 \cdot 7H_2O$ (Wako), and 0.0005% $MnCl_2 \cdot 4H_2O$ (Junsei Chemical) for 3 days at 28°C on a rotary shaker at 220 r.p.m. (pH 7.4). The seed culture (0.5 ml) was transferred into 500-mL Erlenmeyer flasks containing 50 mL of the same medium but with the addition of 0.05% L-Tryptophan, which were cultivated for 4 days at 28°C on a rotary shaker at 220 r.p.m.

The whole culture broth (6 L) was extracted with *n*-BuOH to afford a residue (5.44 g) after concentration *in vacuo*. The residue was subjected to column chromatography on silica gel and eluted with $CHCl_3$/MeOH (50:1, 20:1, 10:1, 5:1, 2:1, and 1:10 v/v) to give 35 fractions. Fractions 16 and 17 were combined and subjected to RP-HPLC (YMC Carotenoid, ϕ20×250 mm, 20% MeCN, 8.0 mL/min) to yield metabolite **3** (17.8 mg, rt = 46.2 min). The fraction 18 was separated by silica gel column chromatography with $CHCl_3$/MeOH (50:1, 20:1, 10:1, and 5:1 v/v), to give 6 subfractions. The subfraction 5 was subjected to RP-HPLC (PEGASIL ODS SP100, ϕ10×250 mm, 40% MeCN, 2.0 mL/min) to yield metabolites **2** (5.4 mg, 34.1 min) and **5** (0.90 mg, 22.2 min), respectively. The fractions 23 to 25 were combined and fractionated by silica gel column chromatography with $CHCl_3$/MeOH (50:1, 20:1, 10:1, 5:1, and 2:1 v/v), to give 11

subfractions. Subfractions 6 to 8 were combined and subjected to RP-HPLC (YMC Carotenoid, ϕ20×250 mm, 40% MeCN, 8.0 mL/min) to give metabolites **1** (24.7 mg, 28.5 min), **4** (4.98 mg, 15.3 min) and **6** (1.38 mg, 14.0 min), respectively.

Saccharothriolide A (1): light yellow oil; $[\alpha]_D^{20}$ +18.0 (*c* = 0.74, MeOH); UV (MeOH) λ_{max} (log ε) 259 (4.17), 345 (3.76) nm; CD (*c* 4.56 ×10^{-4} M, MeOH) λ_{max} ($\Delta\varepsilon$) 199 (+15.01), 227 (–25.0), 355 (+3.46) nm; IR (neat) ν_{max} 3327, 2977, 2938, 1732, 1679, 1606, 1573, 1513, 1455, 1379, 1230, 1165cm^{-1}; ^1H and ^{13}C NMR data, see Table 1 and 2; HR-MS (ESI) $[M+H]^+$ *m/z* 486.2134 (calcd for $C_{26}H_{32}NO_8$, 486.2128).

Saccharothriolide B (2): light yellow oil; $[\alpha]_D^{20}$ -81.2 (*c* = 0.36, MeOH); UV (MeOH) λ_{max} (log ε) 248 (3.89) nm; CD (*c* 2.36 ×10^{-4} M, MeOH) λ_{max} ($\Delta\varepsilon$) 208 (–28.1), 250 (+10.5), 299 (-5.4)nm; IR (neat) ν_{max} 3373, 2976, 2937, 2879, 2319, 1732, 1675, 1606, 1514, 1452, 1172 cm^{-1}; ^1H and ^{13}C NMR data, see Table 1 and 2; HR-MS (ESI) $[M+H]^+$ *m/z* 458.2162 (calcd for $C_{25}H_{32}NO_7$, 458.2179).

Saccharothriolide C (3): light yellow oil; $[\alpha]_D^{20}$ -111.8 (*c* = 0.58, MeOH); UV(MeOH) λ_{max} (log ε) 278 (3.40) nm; CD (*c* 4.74 ×10^{-4} M, MeOH) λ_{max} ($\Delta\varepsilon$) 206 (–6.5), 290 (-1.5) nm; IR (neat) ν_{max} 3347, 2978, 2938, 1743, 1673, 1606, 1455, 1379, 1166 cm^{-1}; ^1H and ^{13}C NMR data, see Table 1 and 2; HR-MS (ESI) $[M+Na]^+$ *m/z* 389.1586 (calcd for $C_{19}H_{26}O_7Na$, 389.1576).

Saccharothriolide D (4): light yellow oil; $[\alpha]_D^{20}$ +95.8 (*c* = 0.33, MeOH); UV (MeOH) λ_{max} (log ε) 259 (4.32), 341 (3.87) nm; CD (*c* 6.84 ×10^{-4} M, MeOH) λ_{max} ($\Delta\varepsilon$) 201 (+19.2), 227 (–27.4), 347 (+5.1) nm; IR (neat) ν_{max} 3336, 2978, 2930, 1736, 1677, 1607, 1573, 1508, 1455, 1384, 1264, 1237, 1162 cm^{-1}; ^1H and ^{13}C NMR data, see Table 1 and 2; HR-MS (ESI) $[M+H]^+$ *m/z* 486.2107 (calcd for $C_{26}H_{32}NO_8$, 486.2128).

Saccharothriolide E (5): light yellow oil; $[\alpha]_D^{20}$ -6.3 (*c* = 0.06, MeOH); UV (MeOH) λ_{max} (log ε) 247 (4.46) nm; CD (*c* 6.56 ×10^{-4} M, MeOH) λ_{max} ($\Delta\varepsilon$) 210 (–14.6), 252 (+7.8) nm; IR (neat) ν_{max} 3394, 2978, 2940, 1742, 1684, 1607, 1518, 1461, 1268, 1161 cm^{-1}; ^1H and ^{13}C NMR data, see Table 1 and 2; HR-MS (ESI) $[M+H]^+$ *m/z* 458.2167 (calcd for $C_{25}H_{32}NO_7$, 458.2179).

Saccharothriolide F (6): light yellow oil; $[\alpha]_D^{20}$ + 19.8 (*c* = 0.09, MeOH); UV (MeOH) λ_{max} (log ε) 259 (4.27), 343 (3.81) nm; CD (*c* 6.52 ×10^{-4} M, MeOH) λ_{max} ($\Delta\varepsilon$) 200 (+17.8), 227 (-23.9), 345 (+4.3) nm; IR (neat) ν_{max} 3392, 2926, 1736, 1677, 1650, 1611, 1571, 1547, 1512, 1461, 1389, 1268, 1168 cm^{-1}; ^1H and ^{13}C NMR data, see Table 1 and 2; HR-MS (ESI) $[M+H]^+$ *m/z* 472.1981 (calcd for $C_{25}H_{30}NO_8$, 472.1971).

3.3 Reduced Derivative 7

To a solution of **1** (3.4 mg) in dry THF (0.4 mL) was added $LiAlH_4$ (30.2 mg), and the mixture was stirred at room temperature for 2 days. The solution was neutralized to pH 7 and extracted with ethyl acetate. The organic layers were combined, concentrated *in vacuo*, and fractionated by RP-HPLC (PEGASIL ODS SP100, ϕ10×250 mm, 25% CH_3CN, 8.0 mL/min) to afford **7** (0.7 mg, 19.8 %, Rt = 23.6 min). ^{1}H NMR (500 MHz, methanol-d_4) δ 3.59-3.46 (m, 2H, H-1), 1.85 (m, 1H, H-2), 3.45 (m, 1H, H-3), 1.96 (m, 1H, H-4), 3.57 (m , 1H, H-5), 2.24 (m, 1H, H-6), 3.79 (t, *J* = 4.8 Hz, 1H, H-7), 2.40 (m, 1H, H-8), 4.53 (d, *J* = 7.0 Hz, 1H, H-9), 0.99 (d, *J* = 7.0 Hz, 3H, H-10), 0.87 (d, *J* = 7.5 Hz, 3H, H-11), 1.03 (d, *J* = 7.5 Hz, 3H, H-12), 1.07 (d, *J* = 7.0 Hz, 3H, H-13), 6.25 (d, *J* = 2.0 Hz, 2H, H-2'/6'), 6.15 (t, *J* = 2.0 Hz, 1H, H-4'), 7.01 (dd, *J* = 7.5, 2.0 Hz, 1H, H-3"), 6.51 (t, *J* = 7.3 Hz, 1H, H-4"), 7.05 (ddd, *J* = 8.0, 8.0, 2.0 Hz, 1H, H-5"), 6.58 (d, *J* = 8.5 Hz, 1H, H-6"), 4.59 (d, *J* = 3.5 Hz, 2H, H-7"). ^{13}C NMR (500 MHz, methanol-d_4) δ 64.9 (C-1), 39.0 (C-2), 81.4 (C-3), 39.7 (C-4), 81.5 (C-5), 40.8 (C-6), 55.7 (C-7), 43.5 (C-8), 78.1 (C-9), 16.0 (C-10),16.2 (C-11), 16.0 (C-12), 10.9 (C-13),148.0 (C-1'), 106.8 (C-2'/6'), 159.4 (C-3'/5'), 102.4 (C-4'), 148.7 (C-1"), 125.6 (C-2"), 130.3 (C-3"), 116.7 (C-4"), 130.2 (C-5"), 113.0 (C-6"), 65.2 (C-7"). HR-MS (ESI) $[M+H]^+$ *m/z* 478.2719 (calcd for $C_{26}H_{40}NO_7$, 478.2805).

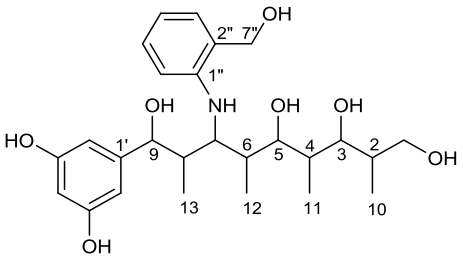

7

3.4 Methylated Derivative 8

To a solution of **1** (5.5 mg) in dry DMF (0.3 mL) was added CH_3I (9.6 μL) and K_2CO_3 (16.3 mg), and the mixture was stirred at room temperature for one week. The solution was neutralized to pH 7, which was extracted with ethyl acetate. The organic layers were combined, concentrated *in vacuo*, and subjected to RP-HPLC (PEGASIL ODS SP100, ϕ10×250 mm, 75% CH_3CN, 2.0 mL/min) to afford **8** (3.9 mg, 66.1%, Rt = 23.2 min). ^{1}H NMR (500 MHz, methanol-d_4) δ 2.91 (m, 1H, H-2), 3.81 (brs, 1H, H-3), 3.33 (m, 1H, H-4), 3.46 (m, 1H, H-6), 3.76 (brs, 1H, H-7), 2.26 (m, 1H, H-8), 5.48 (brs, 1H, H-9), 1.21 (d, *J* = 6.5 Hz, 3H, H-10), 1.49 (d, *J* = 7.5 Hz, 3H, H-11), 1.39 (d, *J* = 8.0 Hz, 3H, H-12), 1.09 (d, *J* = 7.0 Hz, 3H, H-13), 5.91 (s, 2H, H-2'/6'), 6.26 (s, 1H, H-4'), 7.96 (d, *J* = 7.5

Hz, 1H, H-3”), 6.61 (t, *J* = 7.8 Hz, 1H, H-4”), 7.37 (t, *J* = 7.5 Hz, 1H, H-5”), 6.73 (d, *J* = 8.5 Hz, 1H, H-6”), 3.94 (s, 3H, $COOCH_3$), 3.59 (s, 3H×2, OCH_3). HR-MS (ESI) $[M+H]^+$ *m/z* 528.2637 (calcd for $C_{29}H_{38}NO_8$, 528.2597).

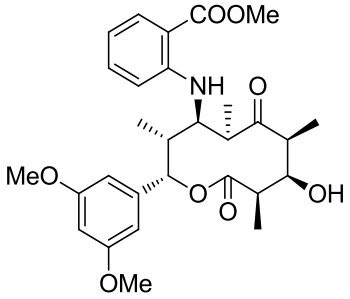

8

3.5 (*S*)-MTPA Ester of 8

To a solution of **8** (0.56 mg) in dry pyridine (0.1 mL) was added (*R*)-MTPA chloride (5 mg in 50 μL toluene), and the mixture was stirred at room temperature overnight. The reaction was stopped by adding H_2O, which was extracted with ethyl acetate. The organic layers were combined and concentrated *in vacuo*. The residue was subjected to RP-HPLC (PEGASIL ODS SP100, ϕ10×250 mm, 80% CH_3CN, 2.0 mL/min) to afford the (*S*)-MTPA ester of **8** (0.16 mg, 20.3 %, Rt = 53.1 min). ^{1}H NMR (500 MHz, methanol-d_4) δ 3.24 (m, 1H, H-2), 5.97 (brs, 1H, H-3), 3.58 (m, 1H, H-4), 3.54 (m, 1H, H-6), 3.77 (brs, 1H, H-7), 2.23 (m, 1H, H-8), 5.49 (brs, 1H, H-9), 1.02 (d, *J* = 7.0 Hz, 3H, H-10), 1.23 (d, *J* = 6.5 Hz, 3H, H-11), 1.35 (d, *J* = 6.5 Hz, 3H, H-12), 1.10 (d, *J* = 6.5 Hz, 3H, H-13), 5.97 (s, 2H, H-2’/6’), 6.27 (s, 1H, H-4’), 7.95 (d, *J* = 8.0 Hz, 1H, H-3”), 6.62 (t, *J* = 7.3 Hz, 1H, H-4”), 7.37 (t, *J* = 7.0 Hz, 1H, H-5”), 6.74 (d, *J* = 8.5 Hz, 1H, H-6”). HR-MS (ESI) $[M+H]^+$ *m/z* 744.2902 (calcd for $C_{39}H_{45}F_3NO_{10}$, 744.2996).

3.6 (*R*)-MTPA Ester of 8

To a solution of **8** (1.21 mg) in dry pyridine (0.2 mL) was added (*S*)-MTPA chloride (10 mg in 100μL toluene) and 4-DMAP (2.0 mg), and the mixture was stirred at room temperature overnight. The reaction was stopped by adding H_2O and extracted with ethyl acetate. The organic layers were combined and concentrated *in vacuo*. The residue was subjected to RP-HPLC (PEGASIL ODS SP100, ϕ10×250 mm, 85% CH_3CN, 2.0 mL/min) to afford the (*R*)-MTPA ester of **8** (0.69 mg, 40.4 %, Rt = 30.9 min). ^{1}H NMR (500 MHz, methanol-d_4) δ 3.34 (m, 1H, H-2), 5.99 (brs, 1H, H-3), 3.52 (m, 1H, H-4), 3.51 (m, 1H, H-6), 3.76 (brs, 1H, H-7), 2.22 (m, 1H, H-8), 5.49 (brs, 1H, H-9), 1.18 (d, *J* = 7.5 Hz, 3H, H-10), 1.09 (d, *J* = 7.5 Hz, 3H, H-11), 1.31 (d, *J* = 6.5 Hz, 3H, H-12), 1.09 (d, *J* = 7.5 Hz,

3H, H-13), 5.99 (s, 2H, H-2'/6'), 6.28 (s, 1H, H-4'), 7.94 (d, *J* = 7.0 Hz, 1H, H-3"), 6.61 (t, *J* = 7.5 Hz, 1H, H-4"), 7.36 (t, *J* = 7.3 Hz, 1H, H-5"), 6.73 (d, *J* = 8.0 Hz, 1H, H-6"). HR-MS (ESI) $[M+H]^+$ *m/z* 744.2932 (calcd for $C_{39}H_{45}F_3NO_{10}$, 744.2996).

3.7 Quantum Chemical ECD Calculation

Initial structures were constructed on Spartan'10 software (Wave function Inc.) based on information of NOESY correlations, and geometry optimization was carried out by means of Spartan'10 software on MMFF (Merck Molecular Force Field). Further optimization of the structures in methanol was performed using the Gaussian 09 program at B3LYP/6-31+G(d) with the polarizable continuum model (PCM). The optimized structures were shown in Figure S39. Optimization was confirmed by computation of frequency. Conformational distribution of the optimized structures was investigated on Spartan'10 software at PM3 level and suggested the absence of other major conformers (< 5%). Prediction of $^3J_{H\text{-}H}$ coupling constants at MPW1PW91/6-311+G(d,p) in methanol (PCM) and TDDFT calculations at B3LYP/6-31+G(d) in methanol (PCM) were performed on Gaussian 09 program. ECD spectra were generated using Gausssum 2.2 (sigma values: 0.4 eV for saccharothliolide A (**1**), 0.6 eV for saccharothliolide B (**2**), and 0.8 eV for saccharothliolide C (**3**).

3.8 Cytotoxicity Assay

Cytotoxicity of metabolites **1**-**6** against HT1080 cell lines was evaluated by a WST-8 colorimetric assay (Cell Counting Kit-8, Dojindo). Briefly, cells were cultured in 96-well plates (1500 cells/well) for 24 hours followed by exposure to metabolites **1-6** for 72 hours, and then the viability was assessed by WST-8. Adriamycin, a control reagent, showed IC_{50} value of 0.14 μM against HT1080 cells.

3.9 Antibacterial Assay

Growth inhibitory activity of metabolites **1**-**3** against bacteria was examined by paper disc method. The test organisms *Staphylococcus aureus*, *Bacillus subtilis*, *Escherichia coli* and *Pseudomonas aeruginosa* were suspended in NBRC 802 media (1% of polypepton, 0.2% of yeast extract and 0.1% of $MgSO_4 \cdot 7H_2O$) with 1% agar medium and overlaid on solid medium plates with 2% agarose. Metabolites **1**-**3** (50μg per disk), penicillin (10μg per disk) and streptomycin (10μg per disk) were loaded onto paper disks (ϕ6 mm) which were dried and placed on the agar plates. After incubation at 27 °C for one day, growth inhibitory zone was measured.

Chapter 2

Plausible Biosynthetic Pathway of Saccharothriolides and Isolation of a Key Precursor "Precursor A"

1. Introduction

Polyketide natural products are a structurally diverse group of highly oxygenated secondary metabolites biosynthesized by a complex cluster of enzymes known as a polyketide synthase (PKS).[36] Macrolide polyketides are an economically important class of polyketide natural products that have found widespread applications as therapeutic agents, such as epothilone family, spiramycin and pimaricin.[37] Macrolides are biosynthesized by type I modular polyketide synthase (PKS) pathways.[38]

2. Plausible Biosynthetic Pathway of Saccharothriolides A-F

Saccharothriolides are 10-membered macrolides. As in the case of other macrolides, saccharothriolides seem to be synthesized *via* polyketide biosynthetic pathway (Scheme 2). An aryl starter unit and four units of methyl-malonyl-CoA seem to be conjugated followed by cyclization to yield the precursors A-C. The aromatic unit-priming polyketide system has been found only in limited number of metabolites, *i.e*. soraphen A from *Sorangium cellulosum*[39], rifamycins from *Amycolatopsis rifamycinica*[40] and enterocin from *Streptomyces maritimus*[41] (Figure 20). The precursor A is likely attacked by an aminoaryl group to furnish metabolites **1** and **2**, or by a water molecule to furnish metabolite **3** (Scheme 2). In the same way, metabolites **4**-**6** strongly suggested the presence of other precursors B and C. In fact, the culture broth included a significant amount of anthranilic acid (23.5 mg) and 2-aminophenol (120.9 mg).[42]

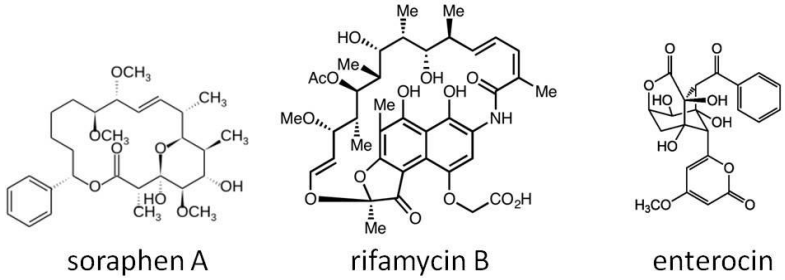

Figure 20. Chemical structures of soraphen A, rifamycin B and enterocin.

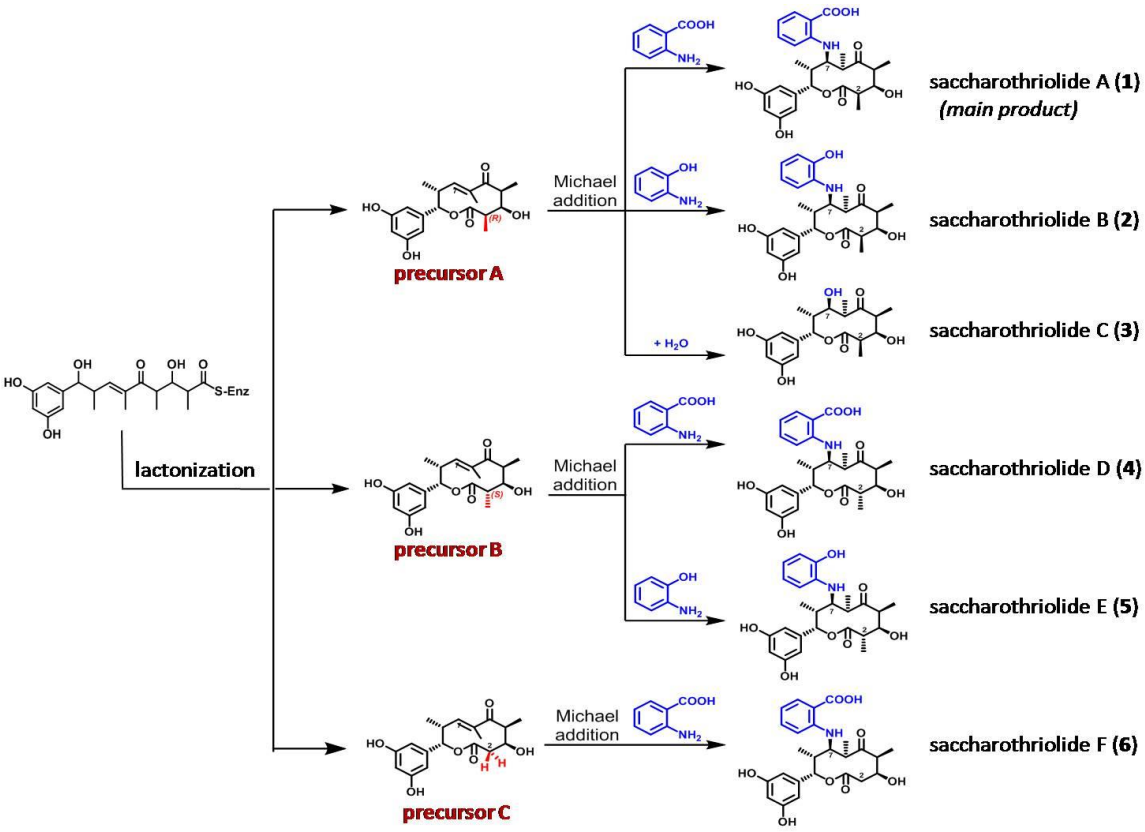

Scheme 2. Plausible biosynthetic pathway of saccharothriolides A-F (**1**-**6**).

3. Isolation of a Key Precursor "Precursor A"

We discovered six novel 10-membered macrolides saccharothriolides A-F (**1**-**6**) from a rare actinomycete *Saccharothrix* sp. A1506. Structural analysis implied their common biosynthetic origin, whereas we predict the presence of precursors A-C possessing α,β-unsaturated ketone. Although we explored the presence of precursors using the LC-MS data, ion peaks corresponding to the precursors were not found, probably due to the high reactivity of the α,β-unsaturated ketone. The main product saccharothriolides A is likely generated from the precursor metabolite A, so we focused on isolation of this key "precursor A" (Figure 21).

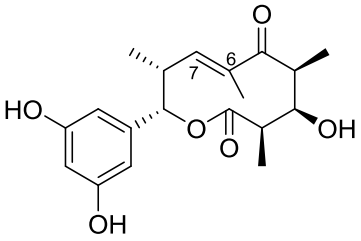

Figure 21. Chemical structure of precursor A (**9**).

Next, we have investigated the presence of precursor A by modifying the culture conditions. In fact, the culture broth included a significant amount of anthranilic acid and 2-aminophenol. Both of them could be generated from tryptophan, which was included in the culture media [43-45]. As we expected, saccharothriolides A and B were not detected when cultured in the absence of tryptophan. Instead, we could detect an ion peak corresponding to precursor A.

We prepared an EtOAc extract from a large-scale tryptophan-free culture of *Saccharothrix* sp. A1506. The 4-day culture broth of *Saccharothrix* sp. A1506 (5 L) was exhaustively extracted with EtOAc. The combined organic fraction was dried over anhydrous Na_2SO_4, filtered, and then evaporated to dryness *in vacuo* at low temperature to yield a 625.8 mg residue. The crude EtOAc extract was subjected to column chromatography on silica gel in MS-guided isolation and purified by HPLC, in which acidic or basic condition, and alcoholic solvents were not used. Finally, 3.16 mg precursor A was successfully isolated (Table 3).

Table 3. Products of *Saccharothrix* sp. in different culture and treatment conditions.

	precursor A	**saccharothriolides A and B**
Culture media	**Tryptophan-free** medium	**Tryptophan-supplemented** medium
Extraction solvent	EtOAc	BuOH
Isolation system	EtOAc/Hexane	MeOH/$CHCl_3$

4. Structure Elucidation of Precursor A

Precursor A (**9**) was obtained as a light-yellow oil. The molecular formula was determined to be $C_{19}H_{24}O_6$ by HR-ESI-MS. ^{1}H and ^{13}C NMR spectra suggested that precursor A was structurally close to saccharothriolides as expected (Table 4). The ^{1}H and ^{13}C NMR spectra of **9** were very similar to those of **3**, except for some differences in chemical shifts for atoms at positions 6 and 7 (Figure 22). Instead of sp^3 carbons of C-6 (δ_C 44.1) and C-7 (δ_C 80.1) in **3**, precursor A possessed a double bond, supported by the downfield shift of the proton and carbon signals (δ_C 140.3 at C6, and δ_H 6.35, δ_C146.9 at C-7). The planar structure was elucidated by detailed analysis of the 2D NMR data. The relative configuration of five stereocenters in the 10-membered lactone ring was established on the basis of the ^{1}H-^{1}H coupling constant values and NOESY data (Figure 22). The geometry of the double bond was determined to be *trans* based on the $J_{H7\text{-}H8}$ value of 8.0 Hz, and NOESY correlations of H-8 to CH_3-12, and H-7 to H-4 (Figure 23). The absolute stereochemistry of **9** was proven to be, 2*R*, 3*R*, 4*S*, 8*R*, and 9*S*, the same as that of **3** on the basis of the coupling constants and optical rotation values, which was in accordance with the reasonable biosynthetic hypothesis (Figure 24).

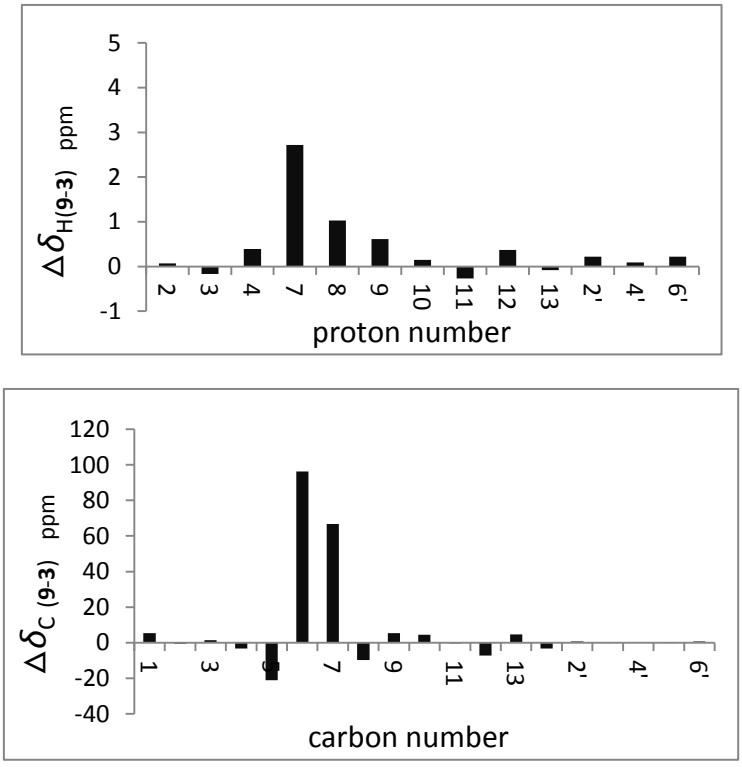

Figure 22**.** Differences between ^{1}H and ^{13}C NMR chemical shifts of precursor A (**9**) and saccharothriolide C (**3**).

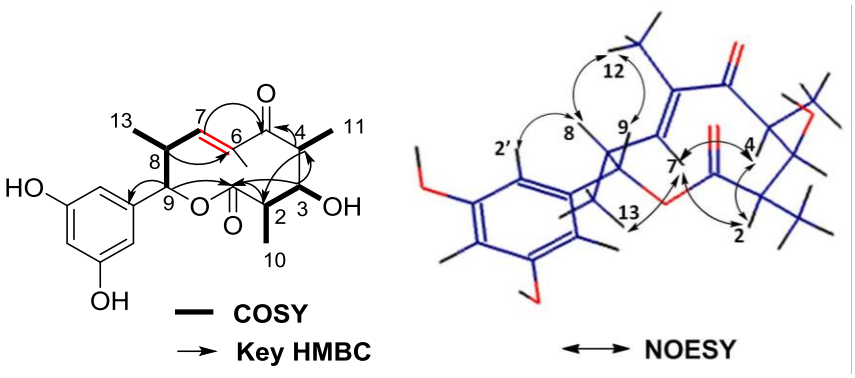

Figure 23. ^{1}H-^{1}H COSY (left, bold) correlations and selected HMBC (left, arrow) and NOESY (right) correlations in precursor A (**9**).

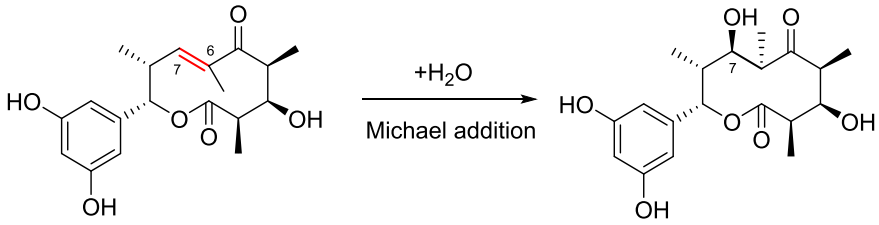

Figure 24. Plausible biosynthetic relationship between precursor A and saccharothriolides C.

Table 4. 1D and 2D NMR data for precursor A (**9**) in acetonitrile-d_3

no.	δ_H, m, J (Hz)	δ_C, m	COSY	HMBC	NOESY
1	-	179.1, C			
2	2.92, qd, 6.9, 1.7	45.7, CH	3, 10	C1, C10	3, 4, 7, 10
3	3.61, dd, 9.7, 1.7	82.3, CH	2, 3-OH	C1, C2, C4, C5, C10, C11	2, 10, 11
4	3.66, q, 6.9	48.0, CH	11	C2, C3, C5, C11	2, 7, 11
5	-	203.6, C			
6	-	140.3, C			
7	6.35, dd, 8.0, 1.2	146.9, CH	8	C5, C12	2, 4, 13
8	3.13, m	37.5, CH	7, 9, 13	C6, C7, C13	9, 12, 13, 2'/6'
9	6.2, d, 5.2	78.5, CH	8	C1, C8, C13, C1', C2'/6'	8, 12
10	1.34, d, 6.9	18.5, CH_3	2	C1, C2, C3	2, 3
11	1.15, d, 6.9	17.8, CH_3	4	C3, C4, C5	3, 4
12	1.79, d, 1.2	13.1, CH_3		C5, C6, C7	8, 9
13	0.84, d, 6.9	14.9, CH_3	8	C7, C8, C9	7, 8
1'	-	141.2, C			
2'	6.32, d, 2.3	105.7, CH		C9, C3', C4', C6'	8
3'	-	159.5, C			
4'	6.23, t, 2.3	102.8, CH		C2'/6', C3'/5'	
5'	-	159.5, C			
6'	6.32, d, 2.3	105.7, CH		C9, C2', C4', C5'	8
3-OH	3.06, d, 9.7			C3	3
2'/6'-OH	6.99, s				

5. Experimental Section

Fermentation in Tryptophan-free Medium.

Saccharothrix sp. A1506 was isolated from a soil sample as described previously.[27] *Saccharothrix* sp. A1506 was cultured in 20×1 L Erlenmeyer flasks each containing 250 mL of a tryptophan-free medium (2% potato starch, 2% glucose, 2% soy bean powder, 0.5% yeast extract powder, 0.25% NaCl, 0.32% $CaCO_3$, 0.0005% $CuSO_4 \cdot 5H_2O$, 0.0005% $ZnSO_4 \cdot 7H_2O$, and 0.0005% $MnCl_2 \cdot 4H_2O$) and shaken at 220 rpm at 28 ºC for 4 days.

Precursor A (9): light yellow oil; $[\alpha]_D^{20}$ –42.67 (*c* = 0.28, MeCN); UV (MeCN) λ_{max} (log ε) 250 (4.3) nm; IR (neat) ν_{max} 3729, 3366, 2976, 1709, 1658, 1605, 1513, 1455, 1370, 1281, 1162, 1052, 970 and 686 cm^{-1}; ^1H and ^{13}C NMR data, see Table 4; HR-MS (ESI) $[M+H]^+$ *m/z* 349.1646 (calcd for $C_{19}H_{25}O_6$, 349.1651).

Chapter 3

Precursor-Directed *in situ* Synthesis of Saccharothriolide Analogs and their Structure-Activity Relationship Study

1. Introduction of Precursor-Directed *in situ* Synthesis

Generating analog libraries of natural products can be challenging; total synthesis is time consuming while even changing a specific functionality is often quite hard. Traditionally, the extraordinary structural complexity of natural products sometimes makes it challenging for traditional chemical synthesis. However, new strategies that combine chemical and biological approaches help to produce novel "unnatural" products, which substantially expand the structural diversity of natural products with potential pharmaceutical value.[44,46] One major strategy for combinatorial biosynthesis is precursor-directed biosynthesis. This approach offers an environmentally friendly way to produce natural product analogs, whereas chemical synthesis usually involves multiple protection/deprotection steps, harsh conditions, toxic organic solvents, and byproduct wastes.[46]

Based on this approach, we developed a precursor-directed *in situ* synthesis (PDSS) method for generating analogs. PDSS method combines biosynthesis, which routinely generates complex precursors, and semi-synthesis by Michael addition, which allows an unlimited range of simple nucleophilic regents.[47] The simplicity of precursor-directed *in situ* synthesis is attractive, as it does not necessarily require identification of the biosynthetic gene cluster and purification of precursors.

Our studies of *Saccharothrix* sp. A1506 have afforded saccharothriolides A-F (**1**-**6**) (Figure 2). Saccharothriolides possess unique phenyl-substituted 10-membered macrolide structures, and some exhibited moderate cytotoxicity to human fibrosarcoma HT1080 cells. Since they contain a variety of substituents at C-7, we expected the presence of precursors, with an α,β-unsaturated ketone that can function as a Michael acceptor.[27]

Saccharothriolides A (**1**) and B (**2**) are expected to be Michael addition products of precursor A and the amino aryl groups, anthranilic acid and 2-aminophenol, respectively. The biosynthetic origin of anthranilic acid and 2-aminophenol have been proposed to arise from the tryptophan which is abundant in the culture medium.[43-45] To avoid the effect of tryptophan on the production of main product **1**, we supplemented tryptophan-free media with the nucleophilic regents anthranilic acid (10 g L^{-1}) or 2-aminophenol (10 g L^{-1}). There were obvious changes in the LC-MS profile, suggesting the significant production of **1** or **2** (Figure 25).[48]

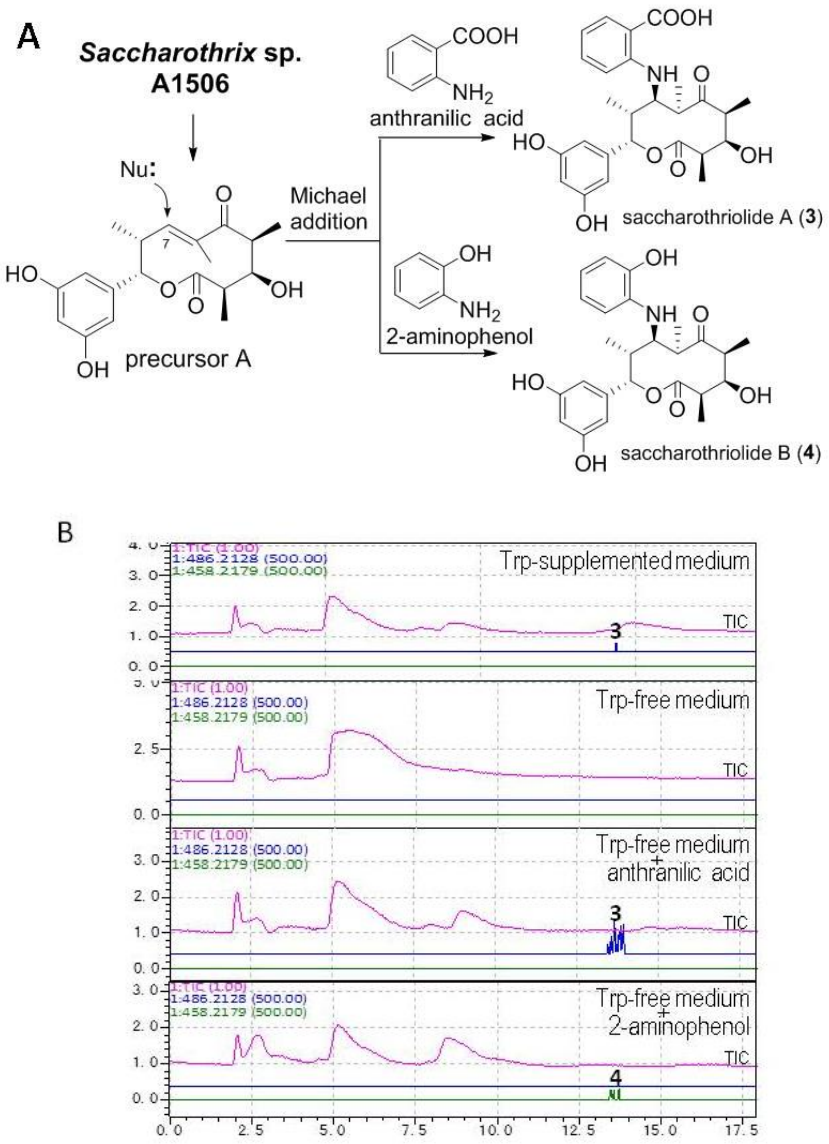

Figure 25. Structures of saccharothriolides A (**1**) and B (**2**) and their biosynthesis. (A) Plausible biosynthetic pathway of saccharothriolides. Precursor A is a Michael acceptor, to which anthranilic acid or 2-aminophenol attacks to yield saccharothriolide A (**1**) and B (**2**), respectively. (B) Production of saccharothriolides A (**1**) and B (**2**) in various culture conditions. LC-MS analyses were examined for crude extracts (PEGASIL ODS SP100, ϕ3 × 250 mm, 0.2 ml min/L, 40% aq. MeCN with 0.1% formic acid). Total ion chromatogram (TIC) and ion chromatograms for 486.2128 (up) and 458.2179 (down) (corresponding to [M+H]+ for **1** and **2**, respectively) are shown. [48]

As described above, these results supported that saccharothriolides were generated from precursors possessing α,β-unsaturated ketone *via* Michael-type addition. This reaction allowed us to explore **precursor-directed *in situ* synthesis (PDSS)** method to obtain further saccharothriolide analogs simply by adding nucleophilic substituents to the culture (Figure 26).

2. Precursor-Directed *in situ* Synthesis of Saccharothriolide Analogs

Previous structure-activity relationship (SAR) studies using saccharothriolides A-F had revealed the importance of the substituent at C-2" on their cytotoxicity (Figure 18); metabolites possessing an alcohol group showed activity, while those possessing a carboxylic acid were less potent. To investigate the necessity of the free hydroxy group, we planned to obtain 2- or 3-methoxyaniline-substituted saccharothriolide analogs G-J (**10**-**13**) by PDSS method (Figure 26).[48]

Saccharothrix sp. A1506 was cultivated in 3L of tryptophan-free medium for 4 days, followed by the addition of 2- or 3-methoxyaniline (10 g L^{-1}) as a nucleophile and acetone (1:1 *v/v*), then shaken at 4 °C for 1 day. The reaction mixture was extracted, and LC-MS-guided fractionation was carried out to yield four new analogs, saccharothriolides G (**10**), I (**12**) and their C-2 epimer saccharothriolides H (**11**) and J (**13**) (Figure 26).

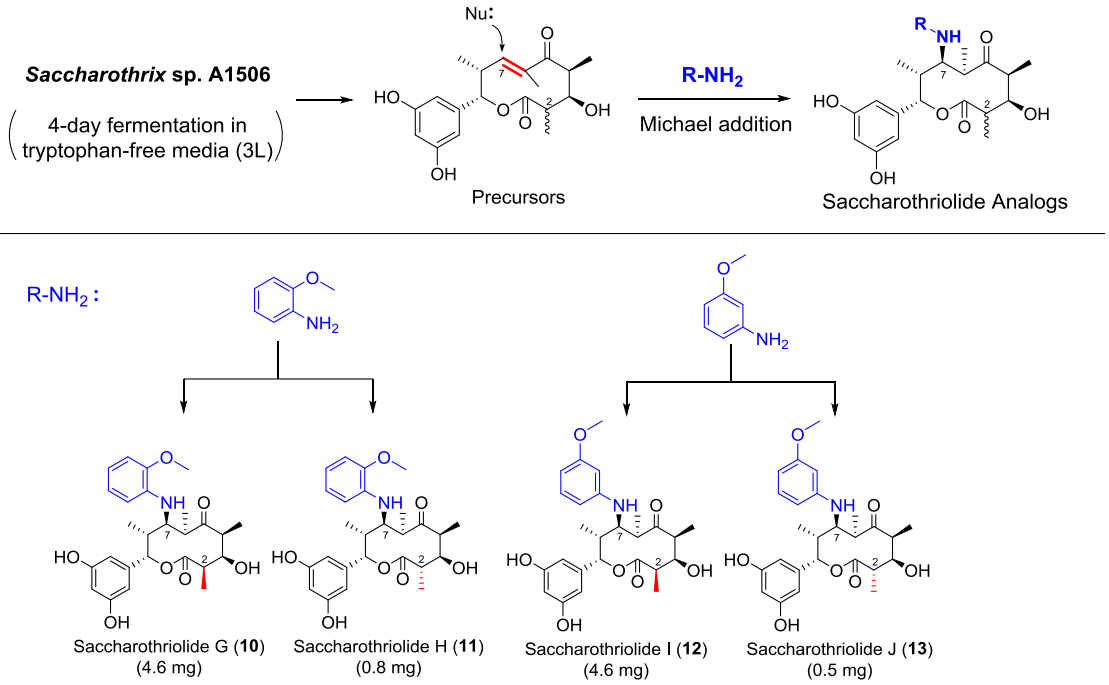

Figure 26. Precursor-directed in situ synthesis of saccharothriolides G-J (**10**-**13**) by addition of arylamines (2-methoxyaniline or 3-methoxyaniline).

3. Structure Elucidation of Saccharothriolides G-J

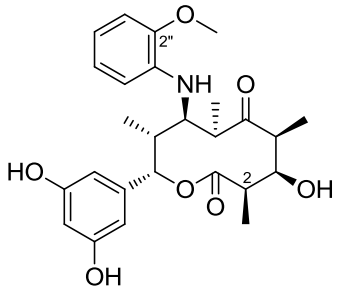

saccharothriolide G (**10**)

Saccharothriolide G (**10**) was obtained as a light-yellow oil with $[\alpha]_D^{20}$ –81.6 (*c* = 0.31, MeOH). The molecular formula was determined to be $C_{26}H_{33}NO_7$ by HR-ESI-MS (*m/z* 472.2321 $[M+H]^+$, calcd 472.2335), revealing that its molecular size was 14 Da larger than saccharothriolide B (**2**). ^1H and ^{13}C NMR data resembled those of **2** (Table 5 and 6, Figure S48), except for the presence of a methoxy group (δ_H 3.92, δ_C 56.5) and chemical shift differences in the amino aryl signals. The downfield shift of C-2" (δ_C 148.8 in **10**, δ_C 146.0 in **2**) and upfield shift of C-3" (δ_C 111.4 in **10**, δ_C 115.2 in **2**) suggested that **10** possessed a methoxy group instead of a phenolic hydroxy group at C-2". Installation of 2-methoxyaniline (*o*-anisidine) was unambiguously determined by HMBC correlations from H-6" to C-2", H-3" to C-1", and from the methoxy proton 2"-OCH_3 to C-2", along with the ^1H-^1H COSY correlations from H-3" to H-6". The planar structure of the molecule was deduced by the COSY, HMQC and HMBC data (Figure 27). The ^1H-^1H COSY data revealed the presence of three spin systems: CH_3-10/H-2/H-3/H-4/CH_3-11, CH_3-12/H-6/H-7/H-8/CH_3-13, and H-3"/H-4"/H-5"/H-6" (Figure 27). HMBC correlations from CH_3-11/CH_3-12 to C-5 connected C-4 and C-6 through a ketone group. HMBC correlations from CH_3-10 to carbonyl C-1, and from H-9 to CH_3-13/C-1, combined with the down-field shifted chemical shift of H-9 (δ_H 5.49), connected C-2 and C-9 through an ester bond, leading to the formation of the 10-membered lactone ring (Figure 27). The meta-disubstituted benzene ring was connected to C-9 based on the HMBC correlations from H-9 to the aromatic carbons C-2'/6' and C-1'.

The relative stereochemistry of **1** was determined by the NOESY and $^3J_{H\text{-}H}$ data (Figure 27). NOESY cross peaks between H-2 and H-4, and between H-3 and H-2/CH_3-10/H-4/CH_3-11, indicated that H-2, -3, and -4 are on the same α face. NOESY correlations between H-6 and CH_3-13/CH_3-11 indicated that H-6 and H-8 have α and β configurations, respectively. The NOESY correlations between H-7 and H-6/H-8/CH_3-12/CH_3-13 indicated that H-7 also has an α configuration, while the β-orientation of H-9 was revealed by the correlations between the aromatic proton H-6'

and H-8/CH_3-13. This result was also supported by the similar $^3J_{H\text{-}H}$ values between **10** and **2**. Thus, the relative configurations were deduced to be 2*R**, 3*R**, 4*S**, 6*R**, 7*R**, 8*R**, and 9*S**. The absolute stereochemistry of **10** was determined by comparing the ECD spectra of **10** and **2**. The ECD spectrum of **10** showed characteristic Cotton effects at 212 ($\Delta\varepsilon$, –29.3), 252 ($\Delta\varepsilon$, +15.9), and 296 ($\Delta\varepsilon$, –6.5) nm, which overlapped well with the spectrum of **2** (Figure 28). Thus, the absolute configuration of **10** was established to be 2*R*, 3*R*, 4*S*, 6*R*, 7*R*, 8*R*, and 9*S*.

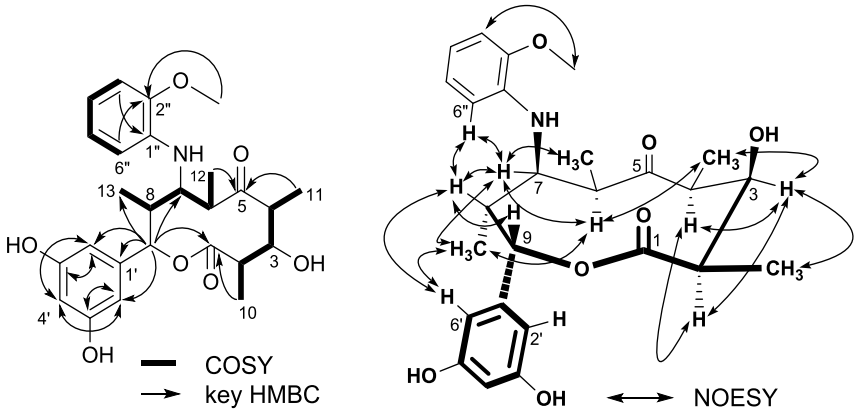

Figure 27. ^{1}H-^{1}H COSY (left, bold) correlations, and selected HMBC (left, arrow) and NOESY (right) correlations for saccharothriolide G (**10**).

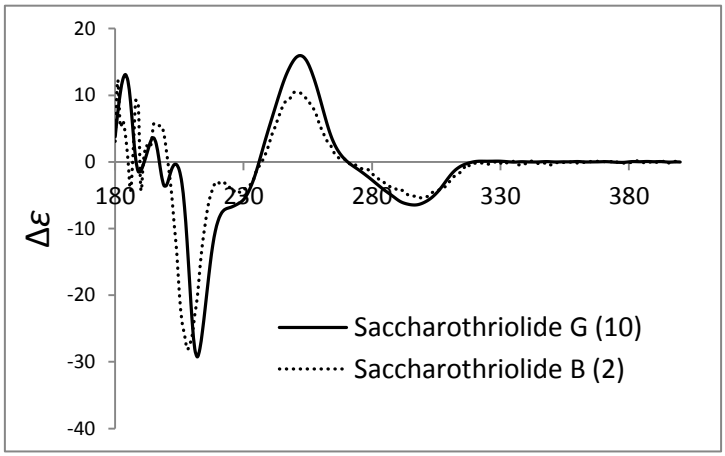

Figure 28. Experimental ECD spectra of saccharothriolide G (**10**) (solid line) and saccharothriolide B (**2**) (dotted line).

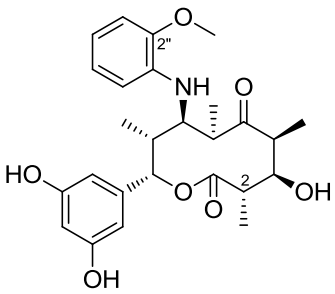

saccharothriolide H (**11**)

Saccharothriolide H (**11**) was obtained as a light yellow oil with $[\alpha]_D^{20}$ –81.2 (*c* = 0.05, MeOH). The molecular formula was determined to be $C_{26}H_{33}NO_7$ by HR-ESI-MS (*m/z* 472.2325 $[M+H]^+$, calcd 472.2335), being the same as that of saccharothriolide G (**10**). ^1H and ^{13}C NMR data of **11** resembled those of **10**, while differences were observed for the chemical shifts of H-2, H-3, CH_3-10, and CH_3-11 in the right half of the lactone ring (Table 5 and 6). Notably, the chemical shifts of the lactone ring were identical to those of saccharothriolide E (**5**), a C-2 epimer of **2**. From these results, **11** was deduced to be an epimer of **10** at C-2. The absolute stereochemistry of **11** was proven to be 2*S*, 3*R*, 4*S*, 6*R*, 7*R*, 8*R*, and 9*S*, the same as that of **5** on the basis of the coupling constants and optical rotation values.[28]

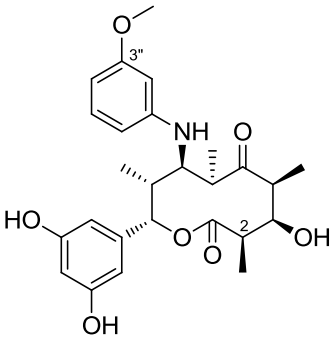

saccharothriolide I (**12**)

Saccharothriolide I (**12**) was obtained as a light yellow oil with $[\alpha]_D^{20}$-100.5 (*c* = 0.31, MeOH), and was given the same molecular formula, $C_{26}H_{33}NO_7$, as **10** by HRESIMS (*m/z* 472.2322 $[M+H]^+$, calcd 472.2335). The ^1H and ^{13}C NMR data of **12** resembled those of **10**. The chemical shifts of the lactone ring were very similar to those of **10**, while some differences of chemical shifts were observed between 3-methoxyaniline-substituent at C-7 in **12** and 2-methoxyaniline-substituent in **10** (Table 5 and 6). The proposed structure was confirmed by detailed analysis of the 2D NMR data of **12** (Figure 29). The relative configurations of **12** were proven to be same as that of **10** on the basis of the similar NOESY correlations and coupling constants. The ECD spectrum of **12** was identical to that of **10** (Figure 30), indicating the absolute stereochemistry was 2*R*, 3*R*, 4*S*, 6*R*, 7*R*, 8*R*, 9*S*.

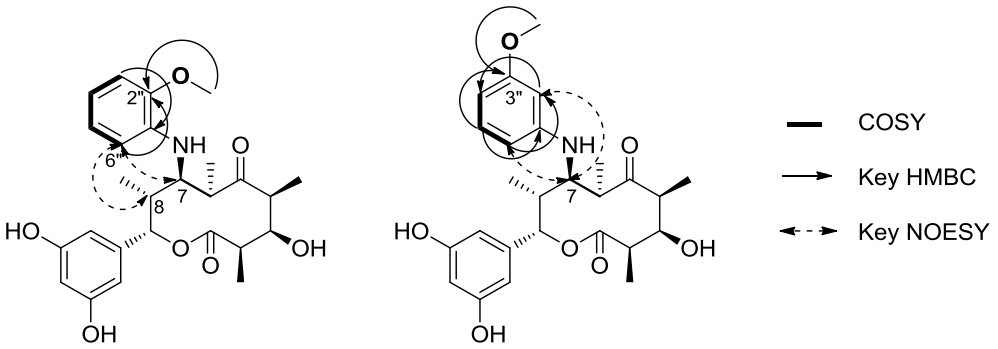

saccharothriolide G (**10**) saccharothriolide I (**12**)

Figure 29. Selected ^1H-^1H COSY (bold), HMBC (arrow) and NOESY (dotted arrow) correlations of 2-methoxyaniline-substituent in saccharothriolide G (**10**) and 3-methoxyaniline-substituent in saccharothriolide I (**12**).

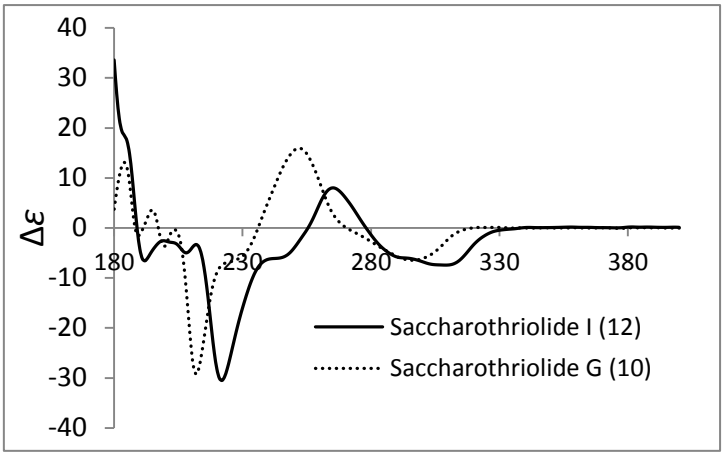

Figure 30. Experimental ECD spectra of saccharothriolide I (**12**) (solid line) and saccharothriolide G (**10**) (dotted line).

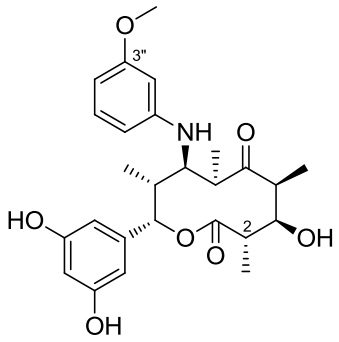

saccharothriolide J (**13**)

Saccharothriolide J (**13**) was obtained as a light yellow oil with $[\alpha]_D^{20}$-3.3 (*c* = 0.03, MeOH), and was given the same molecular formula, $C_{26}H_{33}NO_7$, as **12** by HRESIMS (*m/z* 472.2349 $[M+H]^+$, calcd 472.2335). ^1H and ^{13}C NMR data of 3-methoxyaniline-substituent revealed the same planar structure as **12**. The chemical shifts of the lactone ring were identical to those of **11**, a C-2 epimer of **10**. Therefore, **13** was deduced to be an epimer of **12** at C-2.

Table 5. ^{1}H NMR data for saccharothriolide analogs G-J (**10**-**13**) in methanol-d_4

position	δ_H, m, *J* (Hz)			
	10	**11**	**12**	**13**
2	2.89, qd, 6.9, 3.4	2.47, dq, 9.7, 6.9	2.89, qd, 6.9, 3.4	2.47, dq, 9.7, 6.9
3	3.81, brs	4.40, dd, 9.7, 3.4	3.81, brs	4.40, dd, 9.7, 3.4
4	3.30, q, 7.5	3.25, qd, 6.9, 3.4	3.30, q, 7.5	3.24, qd, 6.9, 3.4
6	3.43, qd, 6.9, 2.3	3.48, qd, 7.5, 1.7	3.41, qd, 7.5, 1.7	3.45, qd, 7.5, 1.7
7	3.53, brs	3.55, brs	3.52, brs	3.53, brs
8	2.24, m	2.15, qd, 7.5, 2.9	2.27, m	2.20, qd, 7.5, 3.4
9	5.49, brs	5.31, brs	5.51, brs	5.31, brs
10	1.20, d, 6.9	1.45, d, 6.9	1.20, d, 6.9	1.44, d, 6.9
11	1.46, d, 7.5	1.08, d, 6.9	1.45, d, 7.5	1.07, d, 6.9
12	1.36, d, 6.9	1.32, d, 7.5	1.36, d, 6.9	1.32, d, 7.5
13	1.04, d, 6.9	1.02, d, 6.9	1.04, d, 7.5	1.02, d, 7.5
2'/6'	5.83, d, 2.3	5.84, d, 1.7	5.89, d, 1.7	5.89, d, 1.7
4'	6.06, t, 2.3	6.05, t, 2.0	6.07, s	6.07, t, 1.7
2"	-	-	6.20, d, 1.7	6.16, t, 2.3
3"	6.87, d, 8.0	6.86, dd, 8.0, 1.2	-	-
4"	6.60, t, 6.9	6.58, td, 7.5, 1.2	6.21, dd, 8.6, 1.7	6.20, dd, 8.0, 2.3
5"	6.80, t, 7.5	6.79, td, 8.0, 1.2	7.04, t, 8.0	7.03, t, 8.0
6"	6.50, d, 7.5	6.46, d, 8.0	6.23, dd, 8.6, 1.7	6.21, dd, 8.0, 2.3
2"-OMe	3.92, s	3.93, s	-	-
3"-OMe	-		3.75, s	3.74, s

Table 6. ^{13}C NMR data for saccharothriolide analogs G-J (**10**-**13**) in methanol-d_4

position	δ_C			
	10	**11**	**12**	**13**
1	173.9, C	173.3, C	174.0, C	173.3, C
2	46.4, CH	44.3, CH	46.4, CH	44.2, CH
3	81.2, CH	73.7, CH	81.0, CH	73.7, CH
4	51.0, CH	52.4, CH	51.0, CH	52.5, CH
5	225.9, C	217.4, C	226.3, C	217.1, C
6	43.7, CH	41.9, CH	43.5, CH	41.8, CH
7	63.2, CH	62.4, CH	63.0, CH	62.4, CH
8	42.6, CH	43.1, CH	42.8, CH	43.2, CH
9	74.0, CH	74.4, CH	74.0, CH	74.4, CH
10	14.0, CH_3	16.7, CH3	14.0, CH_3	16.7, CH3
11	18.3, CH_3	8.8, CH3	18.3, CH_3	8.8, CH3
12	20.4, CH_3	19.3, CH3	20.5, CH_3	19.4, CH3
13	10.8, CH_3	11.2, CH3	10.8, CH_3	11.1, CH3
1'	144.9, C	144.4, C	144.7, C	144.3, C
2'	104.7, CH	104.6, CH	104.7, CH	104.6, CH
3'	159.5, C	159.5, C	159.6, C	159.6, C
4'	102.2, CH	102.3, CH	102.3, CH	102.4, CH
5'	159.5, C	159.5, C	159.6, C	159.6, C
6'	104.7, CH	104.6, CH	104.7, CH	104.6, CH
1"	138.9, C	139.0, C	150.4, C	150.4, C
2"	148.8, C	148.9, C	99.5, C	99.5, C
3"	111.4, CH	111.3, CH	162.8, CH	162.8, CH
4"	117.3, CH	117.0, CH	103.4, CH	103.1, CH
5"	122.6, CH	122.6, CH	131.4, CH	131.4, CH
6"	110.4, CH	110.1, CH	106.5, CH	106.4, CH
2"-OMe	56.5, CH_3	56.4, CH_3	-	-
3"-OMe	-	-	55.6, CH_3	55.6, CH_3

4. Structure-Activity Relationship (SAR) Study

We previously investigated the SAR of saccharothriolides A–F (**1**-**6**) which revealed that substitution at C-7 affects the cytotoxicity against human fibrosarcoma HT1080 cells.[27,28] Saccharothriolides B (**2**) and E (**5**), both of which have a 2-aminophenol group at C-7, exhibited moderate cytotoxicity (IC_{50} values, 13.9 μM and 29.2 μM, respectively). When the C-7 substituent was anthranilic acid, i.e. saccharothriolides A (**1**), D (**4**), compounds were inactive even at 100 μM (Table 7).

To further analyze the structure-activity relationship of these 10-membered macrolides, we examined the cytotoxicity of precursor A and saccharothriolide analogs G-J (**10**-**13**) against HT1080 cells. Precursor A showed equivalent activity (IC_{50} value, 12.3 μM) to saccharothriolide B (**2**), while its H_2O Michael addition product, saccharothriolide C (**3**) was inactive. 2- or 3-methoxyaniline-substituted saccharothriolide analogs G (**10**), I (**12**) and J (**13**) exhibited weak activity (IC_{50} values: 53.5, 37.2 and 70.2 μM, respectively), making them less potent than the C-2 epimer of **10**, saccharothriolide H (**11**) (IC_{50} value, 24.8 μM) (Table 7).

These results not only confirmed the importance of the phenolic hydroxyl group at C-2" in the observed cytotoxicity, but also suggested that the stereochemistry of C-2 also plays an important role for cytotoxicity (Figure 30).

Table 7. IC_{50} values of saccharothriolides A-F, precursor A and saccharothriolide analogs G-J against HT1080 cells.

Natural products	Saccharothriolide A	> 100 μM
	Saccharothriolide B	**13.9** μM
	Saccharothriolide C	> 100 μM
	Saccharothriolide D	> 100 μM
	Saccharothriolide E	29.2 μM
	Saccharothriolide F	66.4 μM
	Precursor A	**12.3** μM
Analogs	Saccharothriolide G	53.5 μM
	Saccharothriolide H	24.8 μM
	Saccharothriolide I	37.2 μM
	Saccharothriolide J	70.2 μM

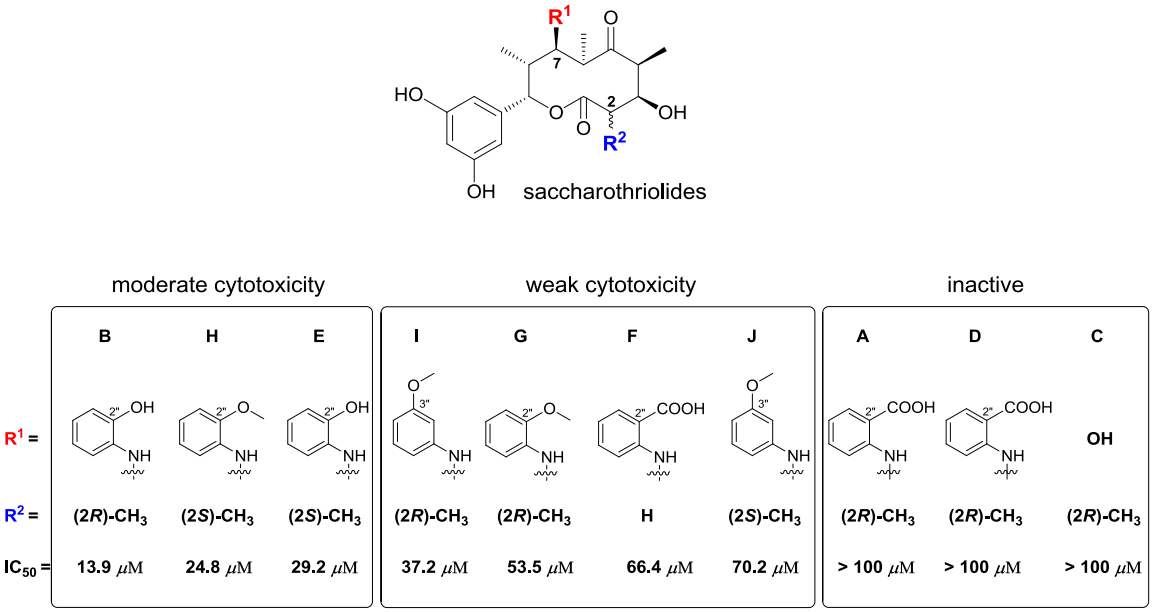

Figure 30. SAR study of saccharothriolides A–J.

5. Experimental Section

General Procedure for Precursor-Directed *in situ* Synthesis (PDSS).

After 4 days-cultivation of *Saccharothrix* sp. A1506, nucleophilic reagent (10 g/L) and acetone (1:1 v/v) were added into the culture broth, and shaken at 140 rpm at 4 ^{o}C for 1 day. After the mixtures were centrifuged (20 min, rt, 8,000 rpm), the supernatant was concentrated and extracted with ethyl acetate. The ethyl acetate soluble fraction was concentrated *in vacuo*.

Extraction and Isolation of Saccharothriolides G (10) and H (11).

2-methoxyaniline (10 g/L) and acetone (1:1 v/v) were added into culture broth, and shaken at 140 rpm at 4 °C for 1 day. Following the above extraction procedure, 1.06 g of the obtained extract was subjected to column chromatography on silica gel and eluted with $CHCl_3$/MeOH (20:1, 10:1, 5:1, and 1:1 v/v) to give 16 fractions. Fraction 2 were subjected to RP-HPLC (PEGASIL ODS SP100, ϕ10×250 mm, 50% MeCN, 2.0 mL/min) to yield product **1** (4.64 mg, t_R = 29.3 min). The fraction 3 was subjected to RP-HPLC (PEGASIL ODS SP100, ϕ10×250 mm, 43% MeCN, 2.0 mL/min) to yield product **2** (0.82 mg, t_R = 34.5 min).

Extraction and isolation of Saccharothriolides I (12) and J (13).

3-methoxyaniline (10 g/L) and acetone (1:1 v/v) were added into culture broth, and shaken at 140 rpm at 4 °C for 1 day. Following the above extraction procedure, 3.96 g of the obtained extract was subjected to column chromatography on silica gel and eluted with $CHCl_3$/MeOH (20:1, 10:1, 5:1, and 1:1 v/v) to give 23 fractions. Fractions 5 and 6 (350 mg) were subjected to column chromatography on silica gel again and eluted with hexane/EtOAc (1:1, 1:3 v/v), 100% EtOAc to give 36 subfractions. Subfractions 16-25 (19 mg) were subjected to RP-HPLC (PEGASIL ODS SP100, ϕ10×250 mm, 48% MeCN, 2.0 mL/min) to yield product **12** (4.6 mg, t_R = 32 min). The fraction 7-9 (156 mg) subjected to column chromatography on silica gel and eluted with hexane/EtOAc (1:2 v/v) and 100% EtOAc to give 20 subfractions. Subfractions 4-6 were subjected to RP-HPLC (PEGASIL ODS SP100, ϕ10×250 mm, 45% MeCN, 2.0 mL/min) to yield product **13** (0.5 mg, t_R = 27 min).

Saccharothriolide G (10): light yellow oil; $[\alpha]_D^{20}$ –81.6 (*c* = 0.31, MeOH); UV (MeOH) λ_{max} (log ε) 250 (4.31), and 283 (3.85) nm; CD (*c* 6.56×10^{-4} M, MeOH) $\lambda_{max}(\Delta\varepsilon)$ 212 (–29.3), 252 (+15.9), and 296 (–6.5) nm; IR (neat) ν_{max} 3728, 3701, 3625, 3598, 3408, 2977, 3940, 1743, 1603, 1514, 1457, 1244, 1168, 742, and 679 cm^{-1}; ^{1}H and ^{13}C NMR data, see Tables 5 and 6; HR-MS (ESI) $[M+H]^+$ *m/z* 472.2321 (calcd for $C_{26}H_{34}NO_7$, 472.2335).

Saccharothriolide H (11): light yellow oil; $[\alpha]_D^{20}$ –81.2 (*c* = 0.05, MeOH); UV (MeOH) λ_{max} (log ε) 250 (3.99) and 283 (3.78) nm; IR (neat) ν_{max} 3728, 3597, 3406, 2972, 2937, 1602, 1513, 1456, 1244, 1165, 1051, 1031, 996, 742, 679, and 653 cm^{-1}; ^{1}H and ^{13}C NMR data, see Tables 5 and 6; HR-MS (ESI) $[M+H]^+$ *m/z* 472.2325 (calcd for $C_{26}H_{34}NO_7$, 472.2335).

Saccharothriolide J (12): light pink oil; $[\alpha]_D^{20}$ -100.5 (*c* = 0.31, MeOH); UV (MeOH) λ_{max} (log ε) 250 (4.73) and 284 (4.28) nm; IR (neat) ν_{max} 3729, 3625, 3598, 3394, 2978, 1745, 1606, 1512, 1456, 1164, 681 and 650 cm^{-1}; ^{1}H and ^{13}C NMR data, see Tables 5 and 6; HR-MS (ESI) $[M+H]^+$ *m/z* 472.2322 (calcd for $C_{26}H_{34}NO_7$, 472.2335).

Saccharothriolide I (13): light yellow oil; $[\alpha]_D^{20}$ -3.3 (*c* = 0.03, MeOH); UV (MeOH) λ_{max} (log ε) 250 (4.13) nm; IR (neat) ν_{max} 3728, 3597, 3400, 2975, 2939, 1607, 1508, 1455, 1254, 1209, 1161, 1036, 997, 687 and 650 cm^{-1}; ^{1}H and ^{13}C NMR data, see Tables 5 and 6; HR-MS (ESI) $[M+H]^+$ *m/z* 472.2349 (calcd for $C_{26}H_{34}NO_7$, 472.2335).

CONCLUSIONS

This thesis represents a systematic work on the isolation, structure elucidation, cytotoxicity evaluation of new metabolites saccharothriolides A-F and a key precursor "precursor A". Precursor-directed *in situ* synthesis (PDSS) of saccharothriolide analogs G-J, and the SAR study of these saccharothriolides represent a powerful approach to expand chemical diversity of natural products as potential anticancer drug-leads from this rare actinomycete source.

In **Chapter 1**, we discovered six novel 10-membered macrolides from a rare actinomycete *Saccharothrix* sp. A1506, and determined their chemical structures by extensive spectroscopic analyses including advanced universal NMR database method and HR-ESI-MS data. All of the sp^3 carbons in the 10-membered ring had chirality, which were determined by the modified Mosher's method and TDDFT-calculation of ECD spectra. Saccharothriolides A, B, D and E had an aryl amine substituent in the lactone ring through a C-N bond, while saccharothriolide C possessed a hydroxy group at C-7. Saccharothriolides D and E were determined to be C-2 epimers of saccharothriolides A and B, respectively. Saccharothriolide F was identified to be a demethylated congener of saccharothriolides A and D at the C-2 position. It should be noted that only saccharothriolide B showed moderate biological activities.

In **Chapter 2**, structural analysis implied their common biosynthetic origin, whereas we predicted the presence of precursors possessing α,β-unsaturated ketone that can function as Michael acceptors. We successfully isolated the key precursor metabolite "precursor A" by improving the culture media, extraction and isolation conditions.

In **Chapter 3**, saccharothriolides were generated from precursors possessing α,β-unsaturated ketone via Michael-type addition. This reaction allowed us to explore precursor-directed *in situ* synthesis (PDSS) to obtain further saccharothriolide analogs simply by adding nucleophilic substituents to the culture. The structure-activity relationship (SAR) study using saccharothriolides A–F had revealed the importance of the OH substituent at C-2" on their cytotoxicity. To investigate the necessity of the free hydroxy group, we prepared 2- or 3-methoxyaniline-substituted saccharothriolide analogs G-J by PDSS method, and examined their effect on the cytotoxicity against human fibrosarcoma HT1080 cells, which confirmed the importance of the OH group at C-2", while the stereochemistry of C-2 also plays an important role.

The novel chemical scaffolds and bioactivities of saccharothriolides would promote us

to discover more potent analogs and investigate their mode of action. This effective PDSS method can provide functional modified analogs which can be obtained difficultly from total synthesis method.

REFERENCES AND NOTES

1 J. Bérdy, *J Antibiot*. 2005, **58**, 1-26.

2 K. Tiwari, R. K. Gupta, *Crit. Rev. Biotechnol*. 2012, **32**, 108-132.

3 P. A. Jose, S. R. D. Jebakumar, *Front. Microbiol*. 2013, **4**, 240.

4 D. P. Labeda, R. T. Testa, M. P Lechaevalier, H. A. Lechevalier, *Int.J. Syst. Bacteriol*. 1984, **34**, 426-431.

5 K. Nakae, I. Kurata, F. Kojima, M. Igarashi, M. Hatano, R. Sawa, Y. Kubota, H. Adachi, A. Nomoto, *J. Nat. Prod*. 2013, **76**, 720-722.

6 X. L. Wang, J. Tabudravu, M. Jaspars , H. Deng, *Tetrahedron*. 2013, **69**, 6060-6064.

7 R. Murakami, T. Tomikawa, K. Shin-ya, J. Shinozaki, T. Kajiura, T. Kinoshita, A. Miyajima, H. Seto, Y. Hayakawa, *J. Antibiot*. 2001, **54**, 710-713.

8 R. Murakami, J. Shinozaki, T. Kajiura, I. Kozone, M. Takagi, K. Shin-Ya, H. Seto, Y. Hayakawa, *J. Antibiot*. 2009, **62**, 123-127.

9 M. Takeuchi, S. Takahashi, R. Enokita, Y. Sakaida, H. Haruyama, T. Nakamura, T. Katayama, M. Inukai, *J. Antibiot*. 1992, **45**, 297-305.

10 D. E. Nettleton, T. W. Doyle, B. Krishnan, G. K. Matsumoto, J. Clardy, *Tetrahedron Lett*. 1985, **26**, 4011-4014.

11 R. Merrouche, N. Bouras, Y. Coppel, F. Mathieu, M. C. Monje, N. Sabaou, A. Lebrihi, *J. Nat. Prod.* 2010, **73**, 1164-1166.

12 N. I. Kalinovskaya, A. I. Kalinovsky, L. A. Romanenko, P. S. Dmitrenok, T. A. Kuznetsova, *Nat. Prod. Commun.* 2010, **5**, 597-602.

13 D. Boubetra, N. Sabaou, A. Zitouni, C. Bijani, A. Lebrihi, F. Mathieu, *Microbiol. Res*. 2013, **168**, 223-230.

14 M. Gan, B. Liu, Y. Tan, Q. Wang, H Zhou, H. He, Y. Ping, Z. Yang, Y. Wang, C. Xiao, *J. Nat. Prod.* 2015, **78**, 2260-2265.

15 D. J. Newman, G. M. Cragg, *J. Nat. Prod.* 2012, **75**, 311-335.

16 H. Kakeya, *Nat. Prod. Rep*. 2016, **33**, 648-654.

17 J. Solecka, J. Zajko, M. Postek, A. Rajnisz, *Cent. Eur. J. Biol.* 2012, **7**, 373-390.

18 M. N. Thaker, N. Waglechner, G. D. Wright, *Nat. Protoc*. 2014, **9**, 1469-1479.

19 D. I. Kurtböke, *Appl. Microbiol. Biotechnol*. 2012, **93**, 1843-1852.

20 G. Drager, A. Kirschning, R. Thiericke, M. Zerlin, *Nat. Prod. Rep.* 1996, **13**, 365-375.

21 S. Kanoh, B. K. Rubin, *Clin. Microbiol. Rev*. 2010, **23**, 590-615.

22 P. Sun, S. Lu, T.V. Ree, K. Krohn, L. Li, W. Zhang, *Curr. Med. Chem.* 2012, **19**, 3417-3455.

23 K. Hostettmann, J. L. Wolfender, *Pestic. Sci*. 1997, **51**, 471-482.

24 F. Berrue, S.T. Withers, B. Haltli, J. Withers, R. G. Kerr, *Mar. Drugs*. 2011, **9**, 369-381.

25 D. Krug, R. Müller, *Nat. Prod. Rep*. 2014, **31**, 768-783.

26 K. R. Duncan, M. Crüsemann, A. Lechner, A. Sarkar, J. Li, N. Ziemert, M. Wang, N. Bandeira, B. S. Moore, P. C. Dorrestein, P. R. Jensen, *Chem. Biol*. 2015, **22**, 460-471.

27 S. Lu, S. Nishimura, G. Hirai, M. Ito, T. Kawahara, M. Izumikawa, M. Sodeoka, K. Shin-ya, T. Tsuchida, H. Kakeya, *Chem. Commun*. 2015, **51**, 8074-8077.

28 S. Lu, S. Nishimura, M. Ito, T. Tsuchida, H. Kakeya, *J. Nat. Prod.* 2016, **79**, 1891-1895.

29 T. Stalin, N. Rajendiran, *J. Photoch. Photobio. A*. 2006, **182**, 137-150.

30 E. Fleury, M. I. Lannou, O. Bistri, F. Sautel, G. Massiot, A. Pancrazi, J. Ardisson, *Eur. J. Org. Chem*. 2009, **29**, 4992-5001.

31 Y. Kobayashi, J. Lee, K. Tezuka, Y.Kishi, *Org. Lett*. 1999, **1**, 2177-2180.

32 J. Lee, Y. Kobayashi, K. Tezuka, Y. Kishi, *Org.Lett*. 1999, **1**, 2181-2184.

33 I. Ohtani, T. Kusumi, Y. Kashman, H. Kakisawa. *J. Am. Chem. Soc*. 1991, **113**, 4092-4096.

34 J. M. Seco, E. Quinoá, R. Riguera, *Chem. Rev*. 2004, **104**, 17-117.

35 The difference of the stereochemistry of C-2 had a negligible effect on the conformation of the chromophores. This was supported by NOESY correlations and $^{3}J_{H\text{-}H}$ values. Metabolites **5** and **2** exhibited similar NOESY correlations and coupling constants for atoms in the left half portion of the macrolide.

36 D. Tillett, E. Dittmann, M. Erhard, H. Von Dohren, T. Borner, B. A. Neilan. *Chem. Biol*. 2000, **7**, 753-764.

37 L. Katz, G. W. Ashley, *Chem. Rev*. 2005, **105**, 499-527.

38 S. Ōmura, *Macrolide Antibiotics: Chemistry, Biology, and Practice*. Academic Press, 2002,1-637

39 J. Ligon, S. Hill, J. Beck, R. Zirkle, I. Molnár,J. Zawodny, S. Money, T. Schupp, *Gene*. 2002, **285**, 257-267.

40 P. R. August, L. Tang, Y. J. Yoon, S. Ning, R. Müller, T. W.Yu, M. Taylor, D. Hoffmann, C. G. Kim, X. H. Zhang, C. R.Hutchinson, H. G. Floss, *Chem. Biol*. 1998, **5**, 69-79.

41 J. Piel, C. Hertweck, P. R. Shipley, D. M.Hunt, M. S.Newman, B. S.Moore, *Chem. Biol*. 2000, **7**, 943-955.

42 Anthranilic acid and 2-hydroxyacetanilide were purified froma part of the 6 L-culture.

43 C. E. Dalgliesh, W. E. Knox, A. Neuberger, *Nature*. 1951, **168**, 20-22.

44 E. Pan, N. W. Oswald, A. G. Legako, J. M. Life, B. A. Posner, J. B. MacMillan, *Chem. Sci*. 2013, **4**, 482-488.

45 Husted, R. R. Biosynthesis and reactions of cyclic hydroxamates in maize. Lib.dr.iastate.edu .1968.

46 H. Sun, Z. Liu, H. Zhao, E. L. Ang, *Drug Des. Devel. Ther*. 2015, **9**, 823-833.

47 S. Lu, S. Nishimura, M. Ito, T. Kato, H. Kakeya, *J. Antibiot*. In press, 2017. doi: 10.1038/ja.2016.153.

SUPPORTING INFORMATION

Supplementary tables:

Supplementary figures:

Table S1. Predicted and adjusted ^{13}C NMR chemical shifts for **7** (**C3-C6** tetrad)

No. in **7**	δ_C of **7** predicted by Chemdraw 2001	No. in Kishi's model	δ_C of Kishi's model predicted by Chemdraw 2001	$\Delta\delta$ (δ_7- δ_{model})	observed δ_C for **7**(methanol-d_4)	Adjusted δ_C for **7** ($\delta_{observed}$-$\Delta\delta$)
3	71.2	5	70.6	0.6	81.41	80.81
4	37.6	6	40.1	-2.5	39.69	42.19
5	70.7	7	74.6	-3.9	81.47	85.37
6	36.8	8	37.3	-0.5	40.80	41.30
11	8.3	11	8.0	0.3	16.21	15.91
12	9.7	12	13.9	-4.2	16.04	20.24

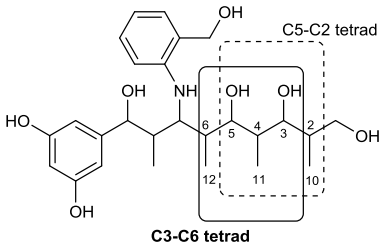

7

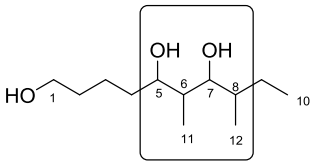

Kishi's model

Table S2. Differences between adjusted carbon chemical shifts (ppm) of **7** (**C3-C6** tetrad) and those of **1a-h** (methanol-d_4).

No.in **7**	No. in Kishi's model	Chemical shift difference $\Delta\delta$= $\delta_{adjusted7}$- $\delta_{1a\text{-}h}$							
		1a (*s*-*a*-*s*)	**1b** (*s*-*s*-*s*)	**1c** (*s*-*a*-*a*)	**1d** (*s*-*s*-*a*)	**1e** (*a*-*a*-*s*)	**1f** (*a*-*s*-*s*)	**1g** (*a*-*a*-*a*)	**1h** (*a*-*s*-*a*)
3	5	8.15	5.61	8.21	4.11	5.83	5.77	5.80	5.34
4	6	1.05	1.73	2.48	2.26	-0.53	1.15	-0.42	1.66
5	7	8.95	6.41	5.24	5.19	7.72	9.39	4.78	9.64
6	8	3.27	3.13	2.69	2.55	3.22	2.75	2.89	2.51
11	11	5.37	8.14	4.88	9.34	4.17	5.41	3.70	5.82
12	12	7.58	5.68	3.68	4.72	8.10	4.86	3.09	4.86
$\Sigma\|\Delta\delta\|$		34.37	30.7	27.18	28.17	29.57	29.33	**20.68**	29.83
$\Sigma\|\Delta\delta\|$-|4|		33.32	28.97	24.70	25.91	29.04	28.18	**20.26**	28.17
$\Sigma\|\Delta\delta\|$-|5|		25.42	24.29	21.94	22.98	21.85	19.94	**15.90**	20.19
$\Sigma\|\Delta\delta\|$-|4|-|5|		24.37	22.56	19.46	20.72	21.32	18.79	**15.48**	18.53
$\Sigma\|\Delta\delta\|$-|5|-|11|		20.05	16.15	17.06	13.64	17.68	14.53	**12.20**	14.37

Table S3. Predicted and adjusted ^{13}C NMR chemical shifts for **7** (**C5-C2** tetrad)

No. in **7**	δ_C of **7** predicted by chemdraw 2001	No. in Kishi's model	δ_C of Kishi's model predicted by Chemdraw 2001	$\Delta\delta$ (δ_7- δ_{model})	Observed δ_C for **7** (methanol-d_4)	Adjusted δ_C for **7** ($\delta_{observed}$-$\Delta\delta$)
5	70.7	5	70.6	0.1	81.47	81.37
4	37.6	6	40.1	-2.5	39.69	42.19
3	71.2	7	74.6	-3.4	81.41	84.81
2	38.0	8	37.3	0.7	38.95	38.25
11	8.3	11	8.0	0.3	16.21	15.91
10	10.2	12	13.9	-3.7	16.00	19.70

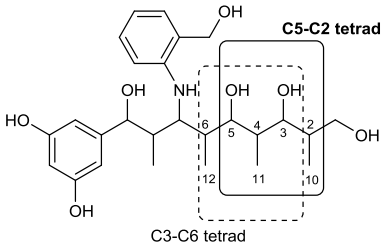

7

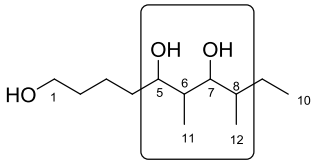

Kishi's model

Table S4. Differences between adjusted carbon chemical shifts (ppm) of **7** (**C5-C2** tetrad) and those of **1a-h** (methanol-d_4).

No. in **7**	No. in Kishi's model	Chemical shift difference $\Delta\delta$= $\delta_{adjusted7}$- $\delta_{1a\text{-}h}$							
		1a (*s*-*a*-*s*)	**1b** (*s*-*s*-*s*)	**1c** (*s*-*a*-*a*)	**1d** (*s*-*s*-*a*)	**1e** (*a*-*a*-*s*)	**1f** (*a*-*s*-*s*)	**1g** (*a*-*a*-*a*)	**1h** (*a*-*s*-*a*)
5	5	8.71	6.17	8.77	4.67	6.39	6.33	6.36	5.90
4	6	1.05	1.73	2.48	2.26	-0.53	1.15	-0.42	1.66
3	7	8.39	5.85	4.68	4.63	7.16	8.83	4.22	9.08
2	8	0.22	0.08	-0.36	-0.50	0.17	-0.30	-0.16	-0.54
11	11	5.37	8.14	4.88	9.34	4.17	5.41	3.70	5.82
10	12	7.04	5.14	3.14	4.18	7.56	4.32	2.55	4.32
$\Sigma\|\Delta\delta\|$		30.78	27.11	24.31	25.58	25.98	26.34	**17.41**	27.32
$\Sigma\|\Delta\delta\|$-$\|4\|$		29.73	25.38	21.83	23.32	25.45	25.19	**16.99**	25.66
$\Sigma\|\Delta\delta\|$-$\|3\|$		22.39	21.26	19.63	20.95	18.82	17.51	**13.19**	18.24
$\Sigma\|\Delta\delta\|$-$\|4\|$-$\|3\|$		21.34	19.53	17.15	18.69	18.29	16.36	**12.77**	16.58
$\Sigma\|\Delta\delta\|$-$\|3\|$-$\|11\|$		17.02	13.12	14.75	11.61	14.65	12.10	**9.49**	12.42

Table S5. Experimental and DFT-calculated $^{3}J_{H\text{-}H}$ coupling constants for saccharothriolides A (**1**) and B (**2**).

No.	**1**		**2**	
	experimental ^{3}J (Hz)	DFT-calculated ^{3}J (Hz)	experimental ^{3}J (Hz)	DFT-calculated ^{3}J (Hz)
H_2-H_3	3.4	4.1	3.4	4.2
H_3-H_4	very small*	1.3	1.2	1.3
H_6-H_7	very small*	3.2	2.3	2.8
H_7-H_8	5.2	5.5	4.0	5.6
H_8-H_9	very small*	1.7	very small*	1.8

*^{1}H NMR signals were broad, which hampered calculation of the exact coupling constants.

Figure S1. Comparison of ^{1}H and ^{13}C NMR chemical shifts of saccharothriolides.

(a) Differences between ^{1}H and ^{13}C NMR chemical shifts of saccharothriolides A (**1**) and D (**4**).

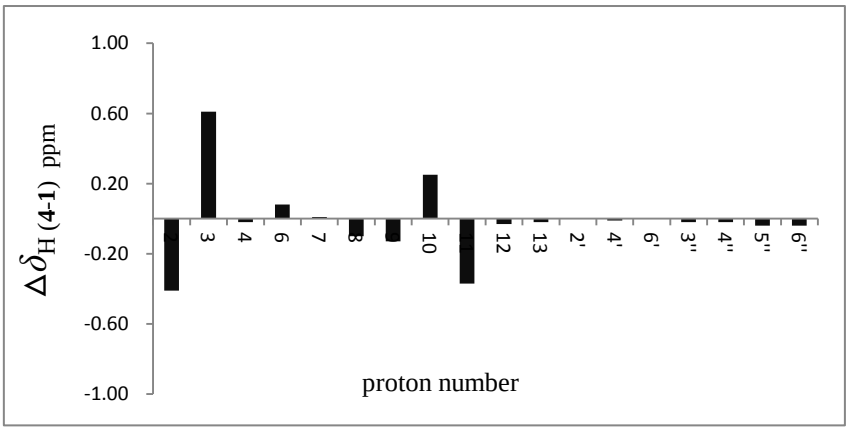

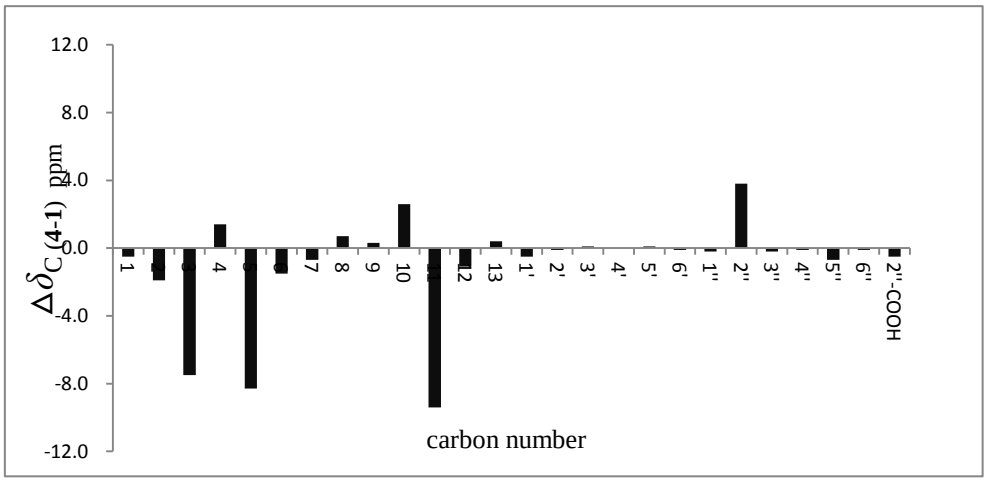

(b) Differences between ^{1}H and ^{13}C NMR chemical shifts of saccharothriolides B (**2**) and E (**5**).

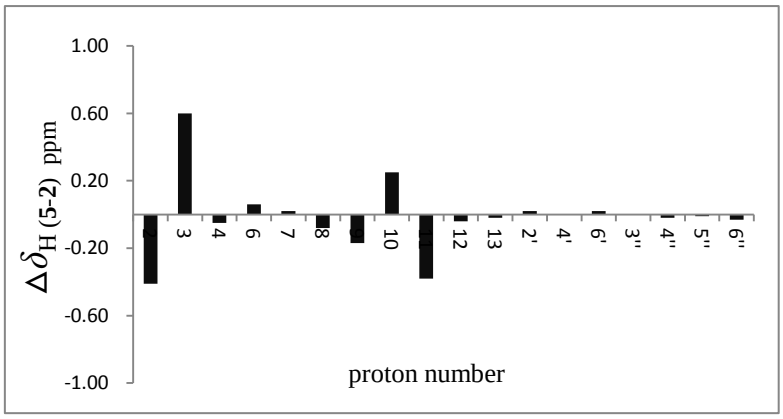

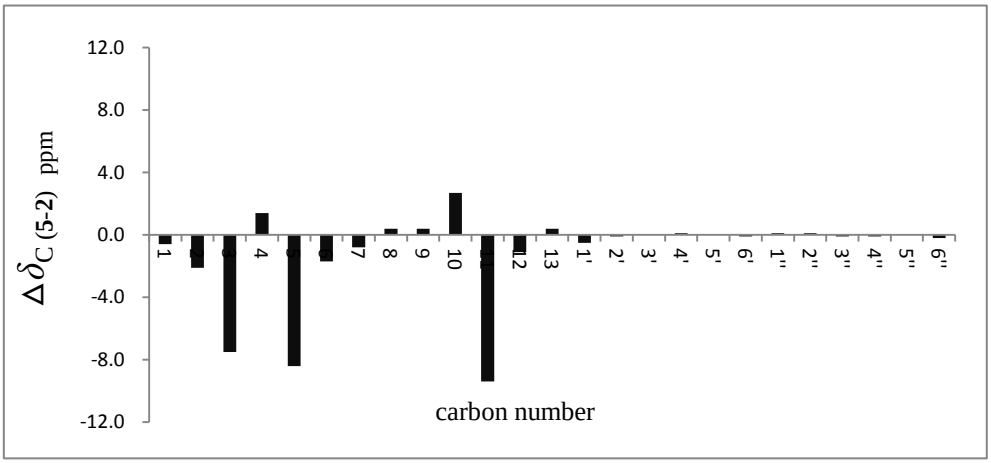

(c) Differences between ^{1}H and ^{13}C NMR chemical shifts of saccharothriolides D (**4**) and F (**6**).

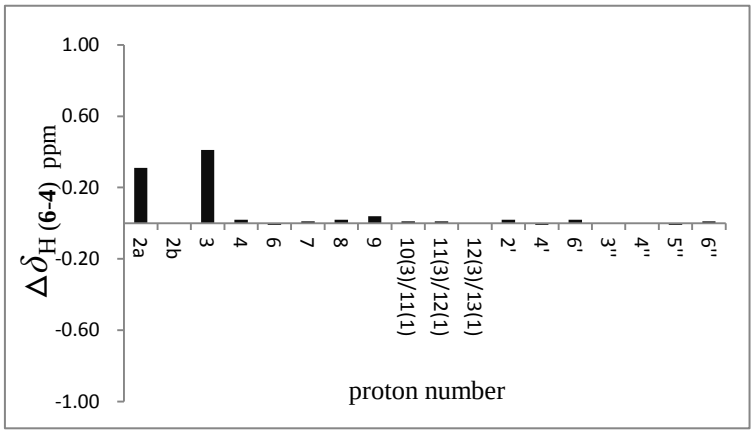

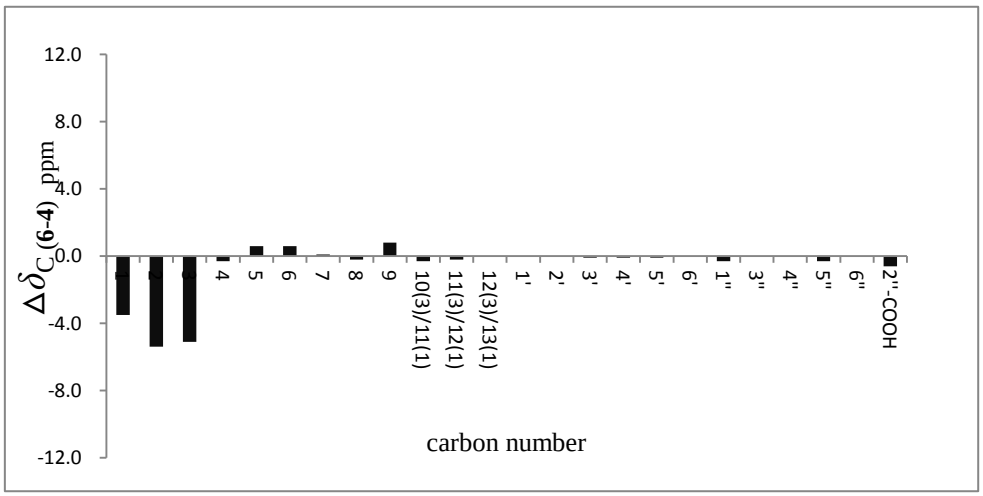

Figure S2. HR-ESI-MS spectra of saccharothriolides A-F (**1**-**6**).

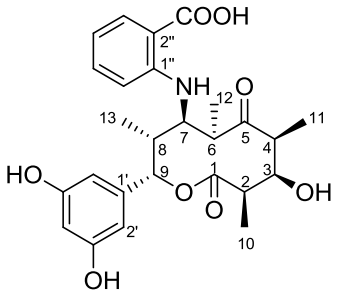

saccharothriolide A (**1**)

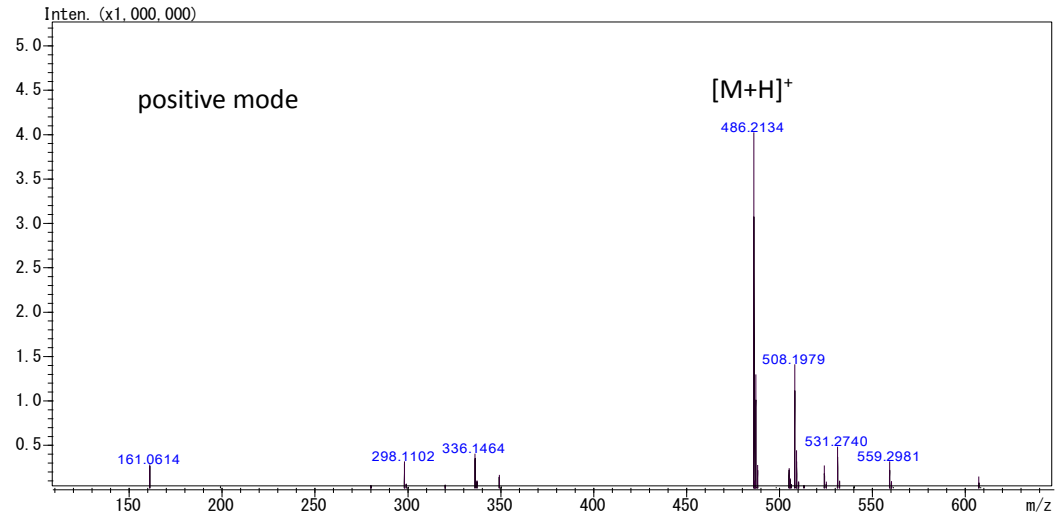

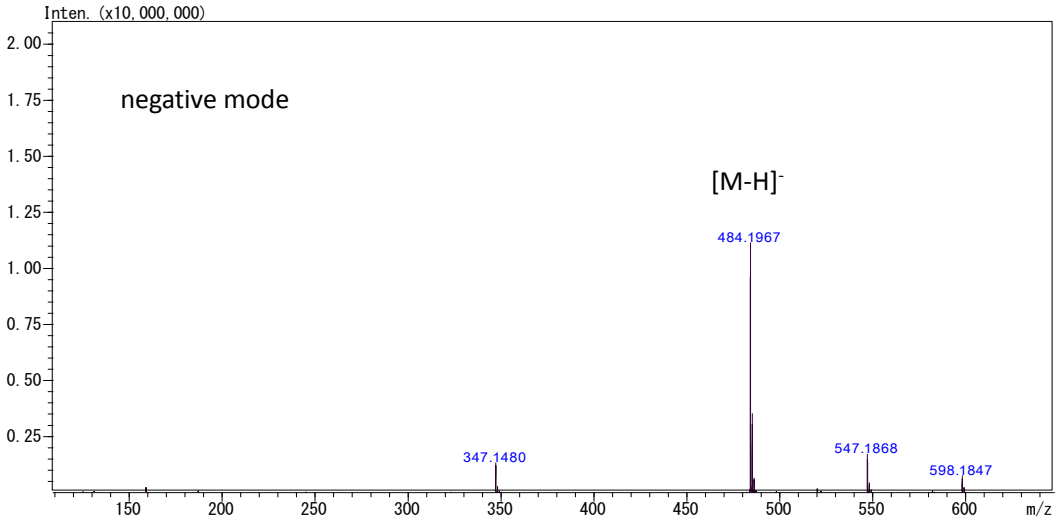

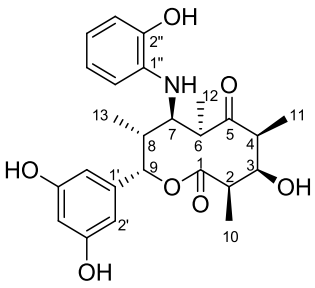

saccharothriolide B (**2**)

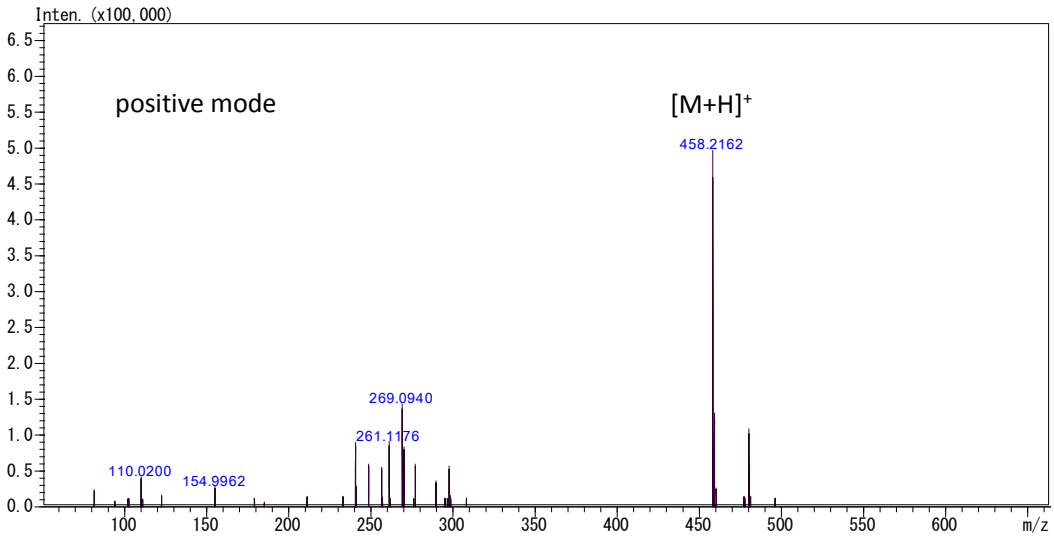

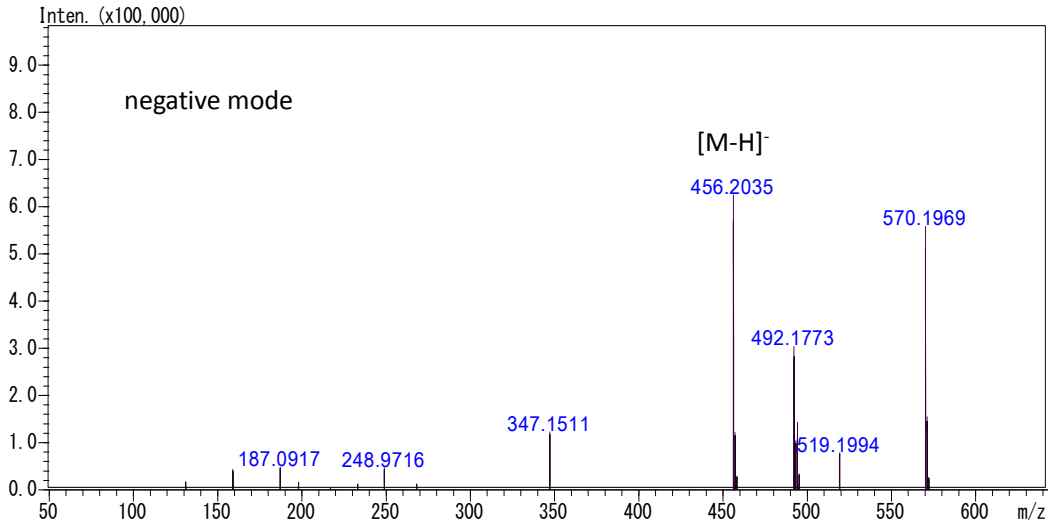

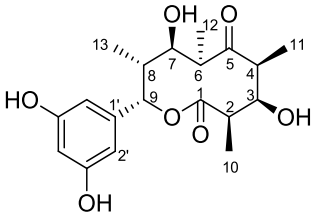

saccharothriolide C (**3**)

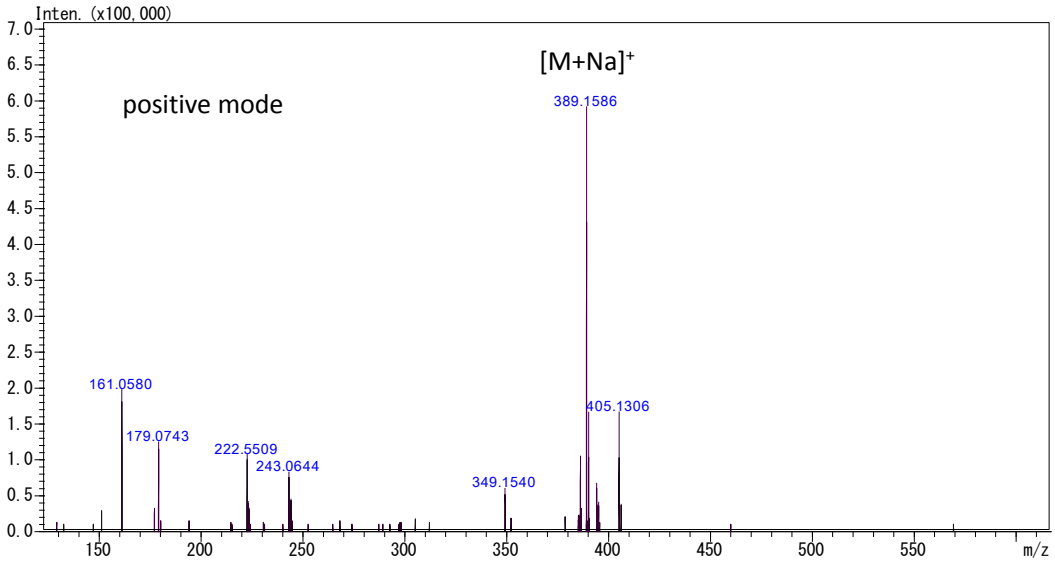

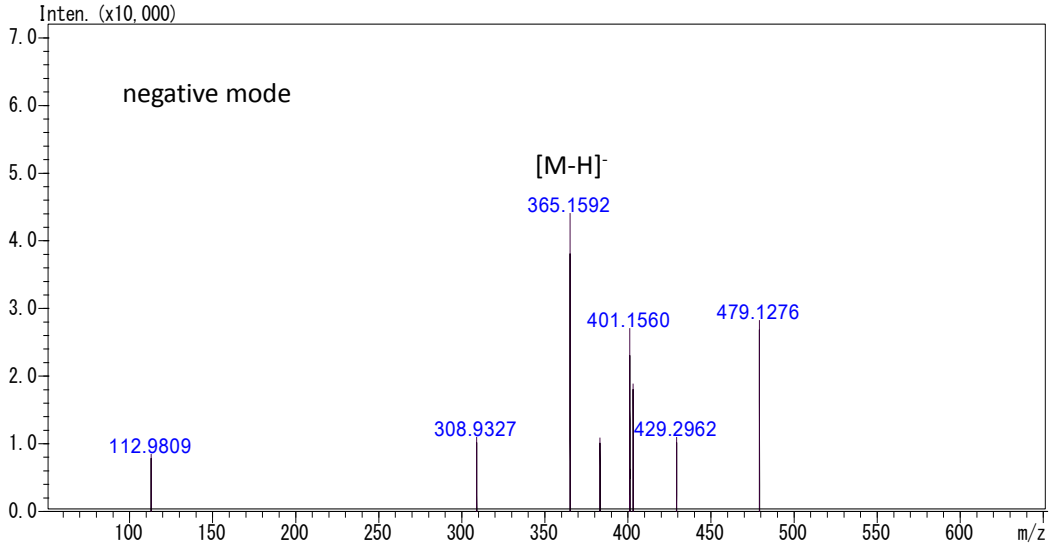

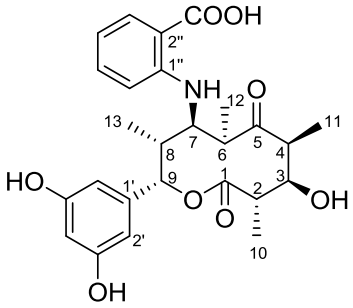

saccharothriolide D (**4**)

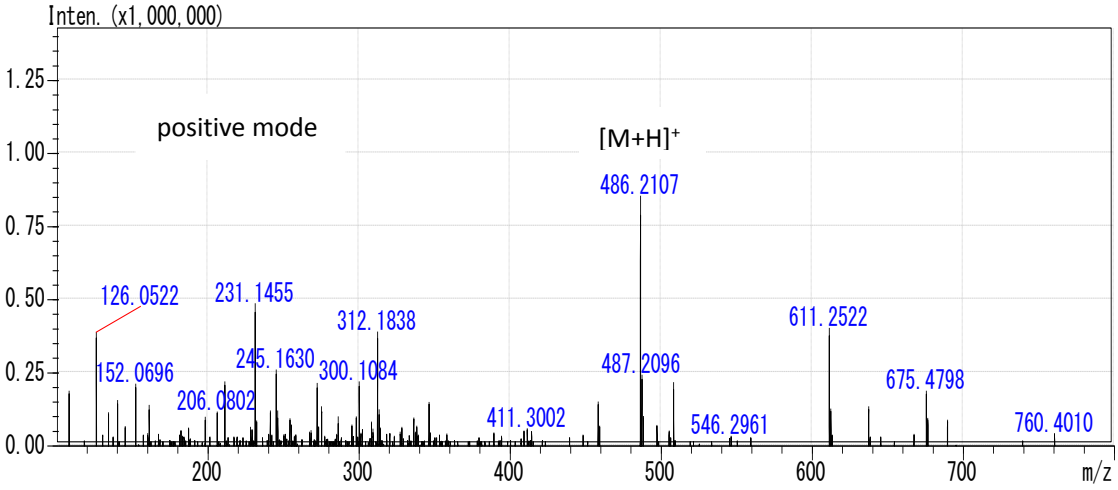

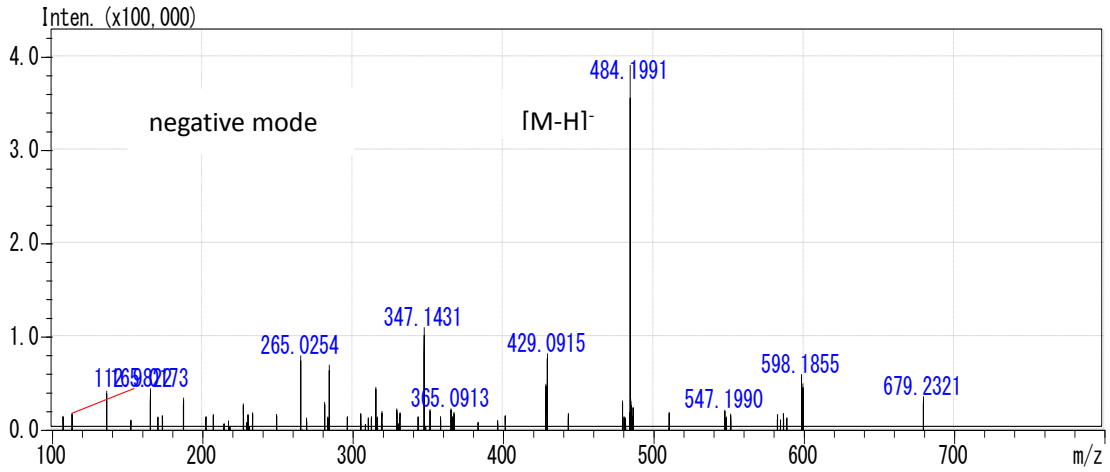

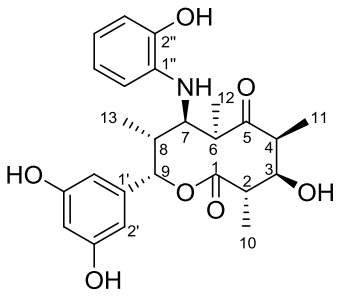

saccharothriolide E (**5**)

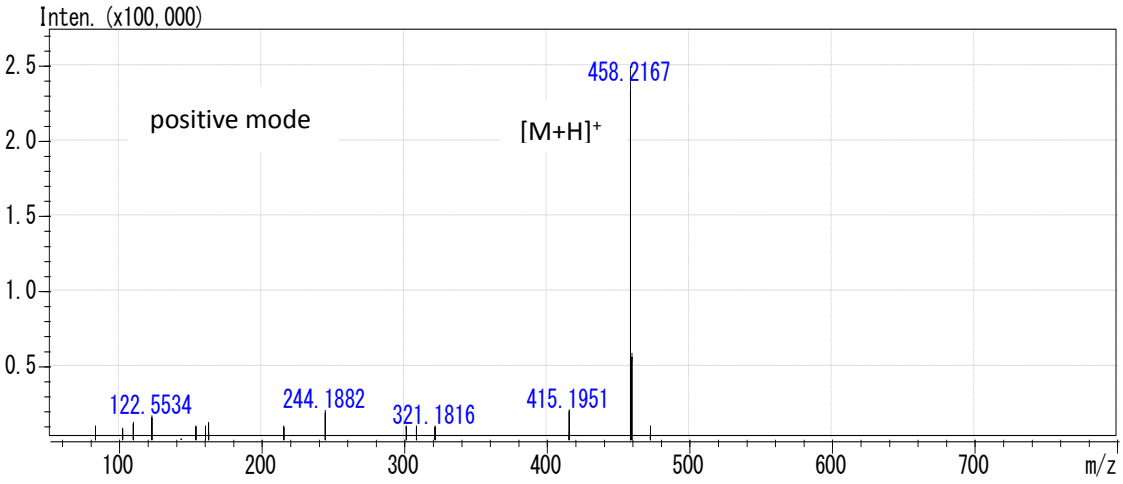

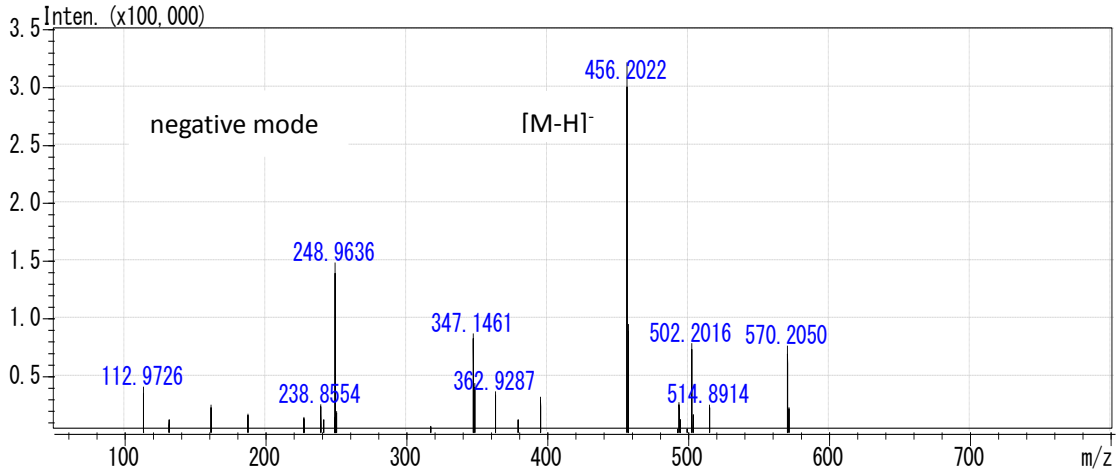

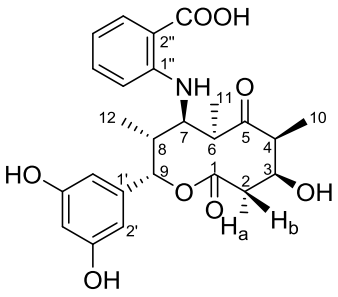

saccharothriolide F (**6**)

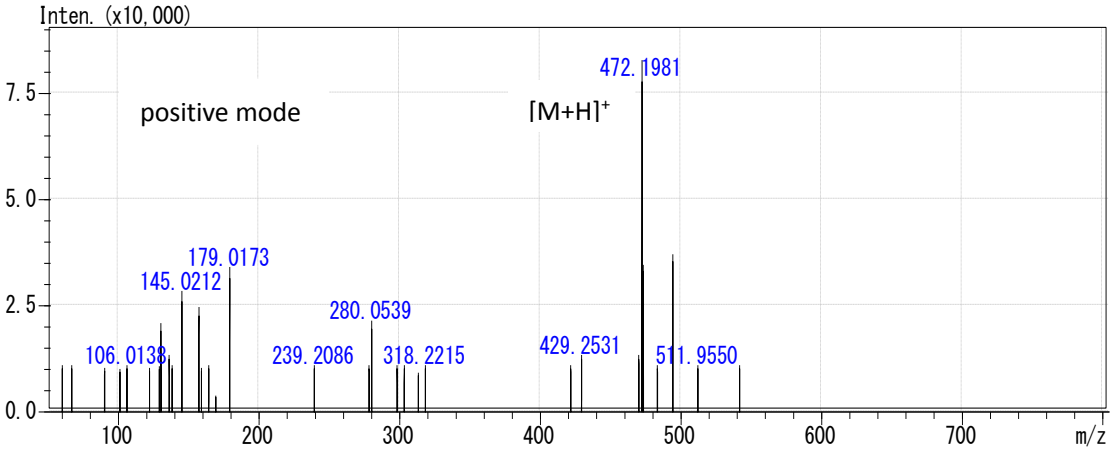

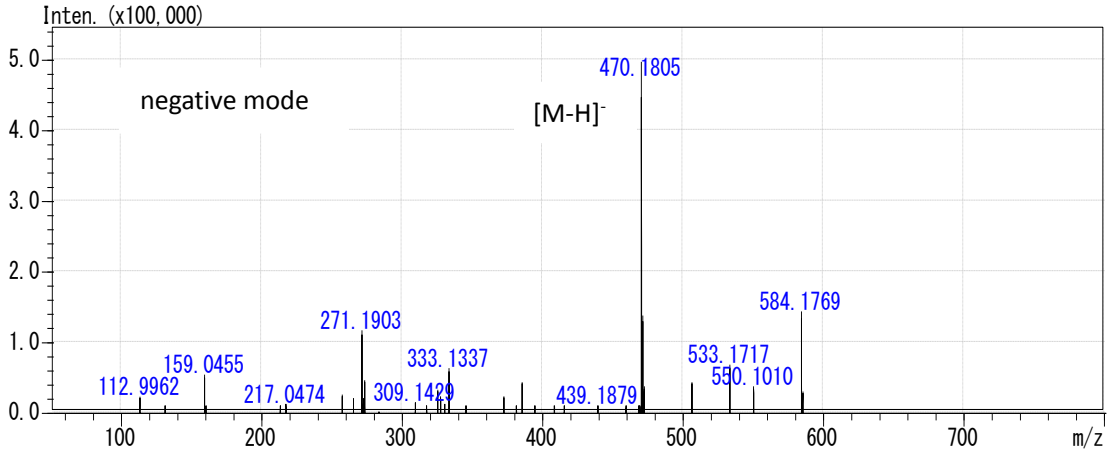

Figure S3. UV spectra of saccharothriolides A-F (**1-6**) in methanol.

2-Aminobenzoic acid in metabolite **1** is known to show a characteristic absorption around 336 nm, which is caused by forming a six-membered intramolecular H-bonded ring through the carboxylic acid and the amino group.[29]

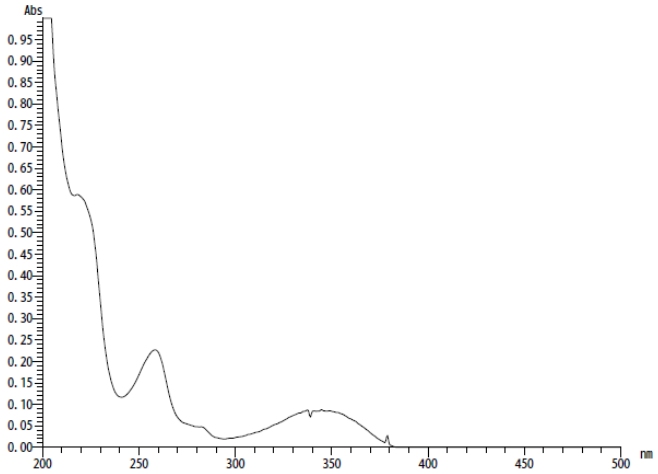

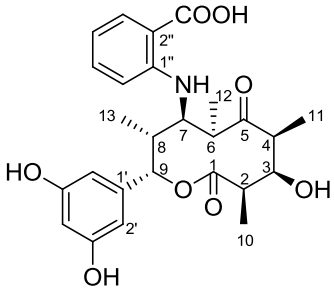

saccharothriolide A (**1**)

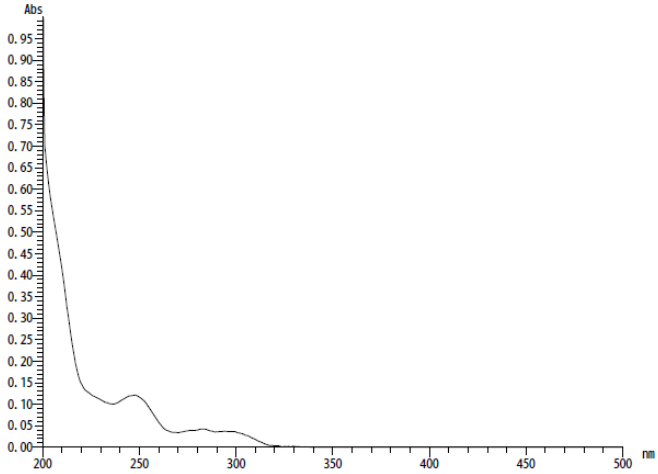

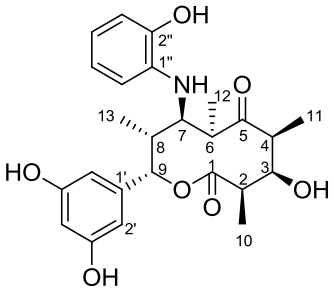

saccharothriolide B (**2**)

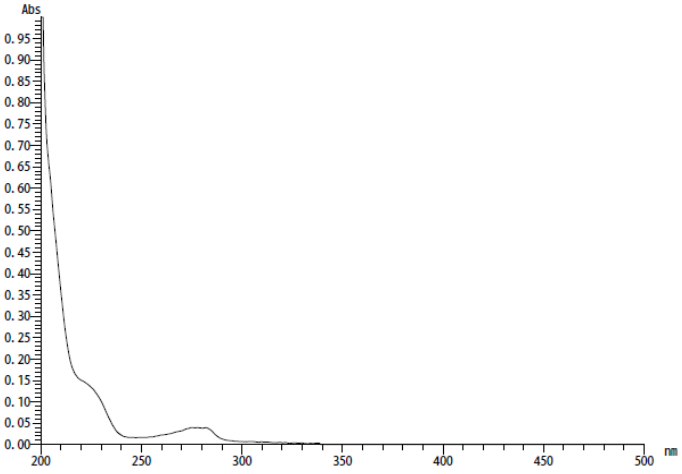

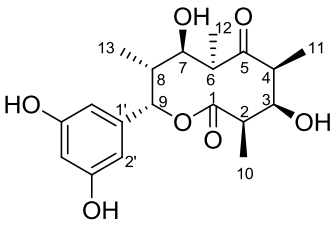

saccharothriolide C (**3**)

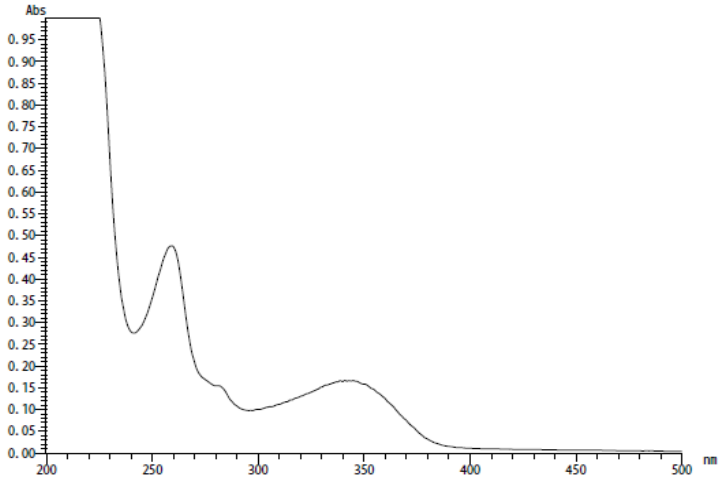

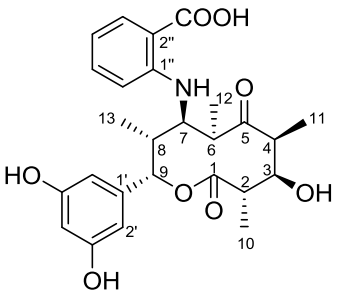

saccharothriolide D (**4**)

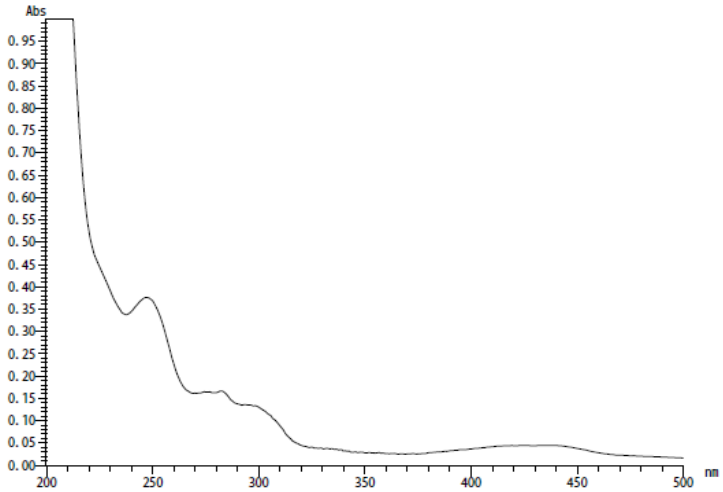

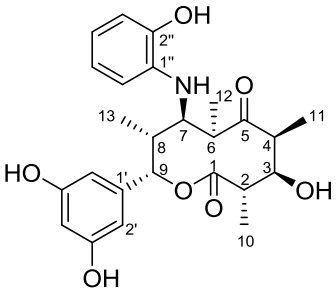

saccharothriolide E (**5**)

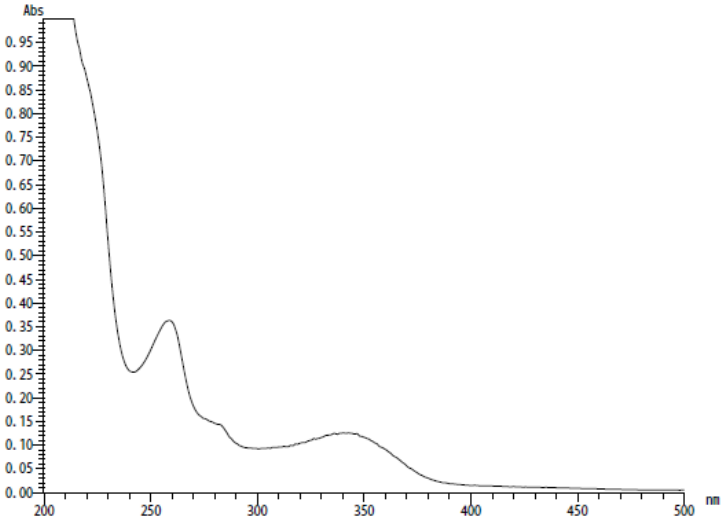

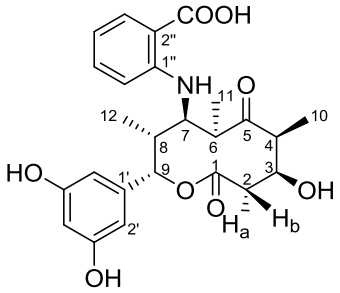

saccharothriolide F (**6**)

Figure S4. ^{1}H NMR spectrum of saccharothriolide A (**1**) in methanol-d_4.

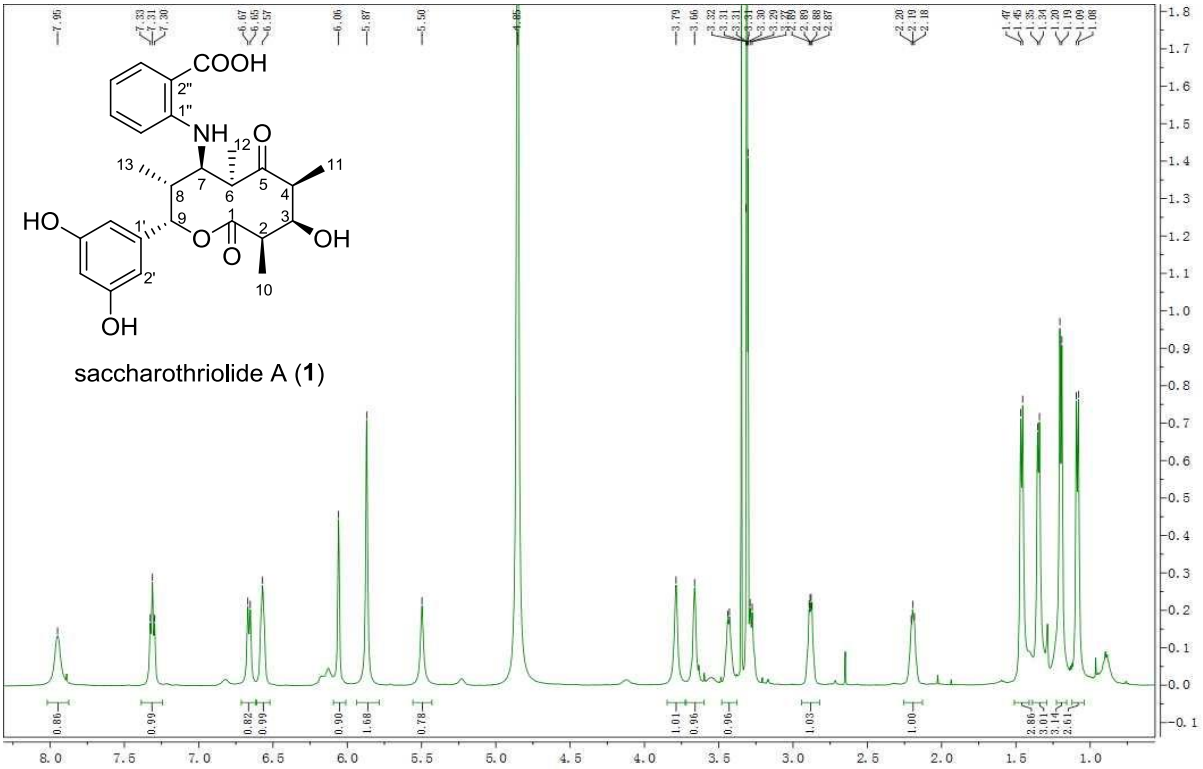

Figure S5. ^{13}C NMR spectrum of saccharothriolide A (**1**) in methanol-d_4.

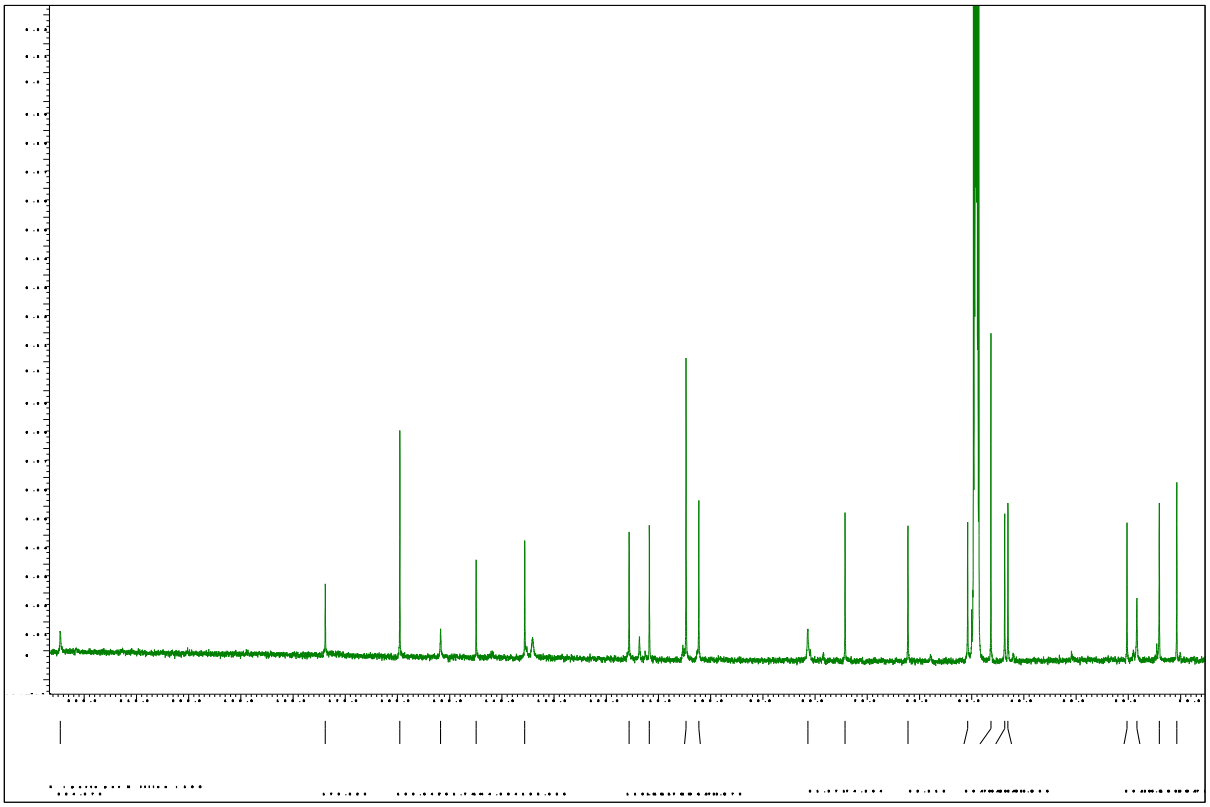

Figure S6. ^{1}H-^{1}H COSY spectrum of saccharothriolide A (**1**) in methanol-d_4.

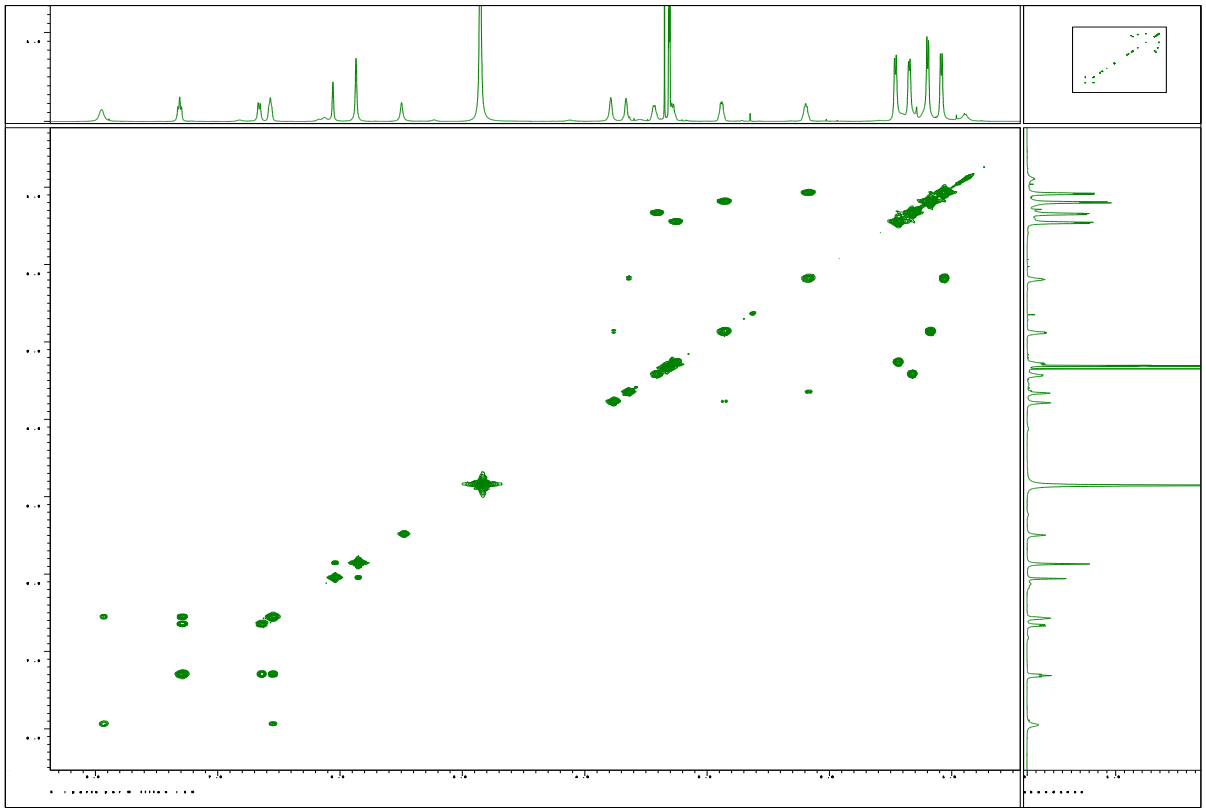

Figure S7. HMQC spectrum of saccharothriolide A (**1**) in methanol-d_4.

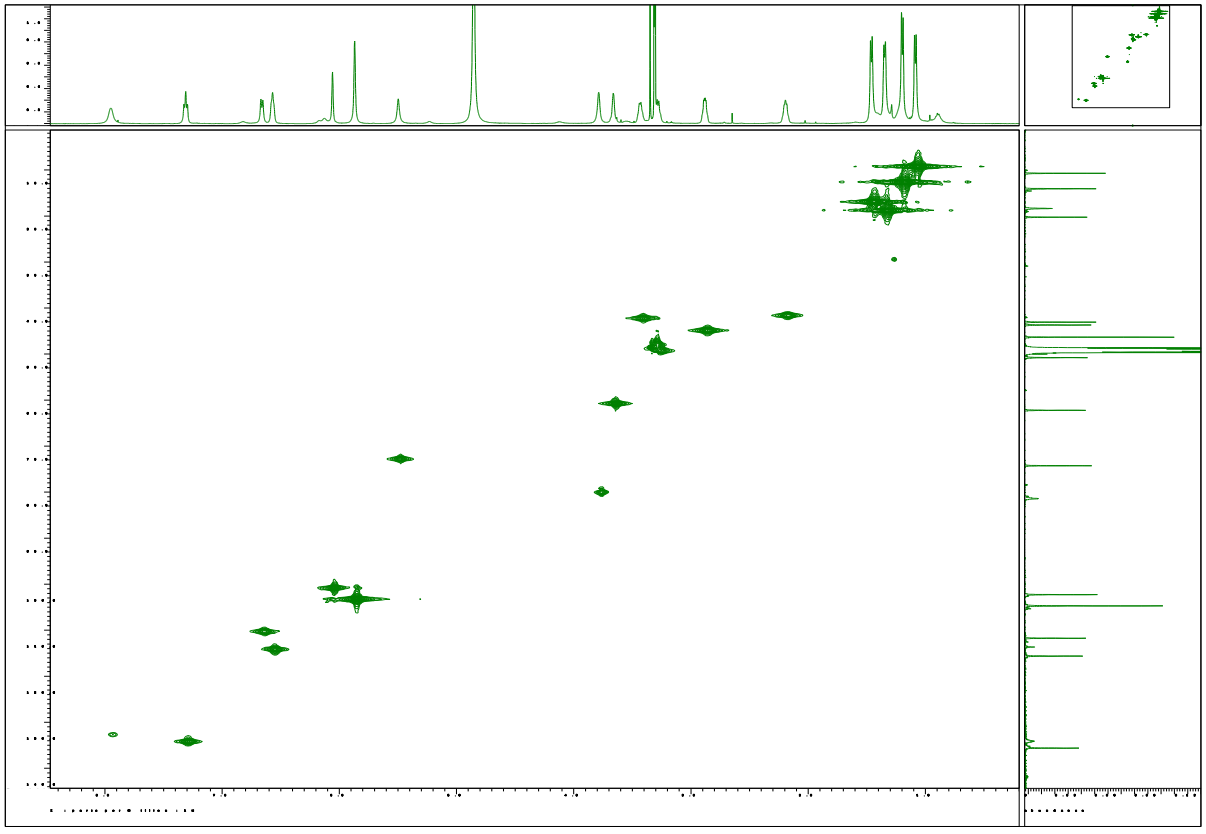

Figure S8. HMBC spectrum of saccharothriolide A (**1**) in methanol-d_4.

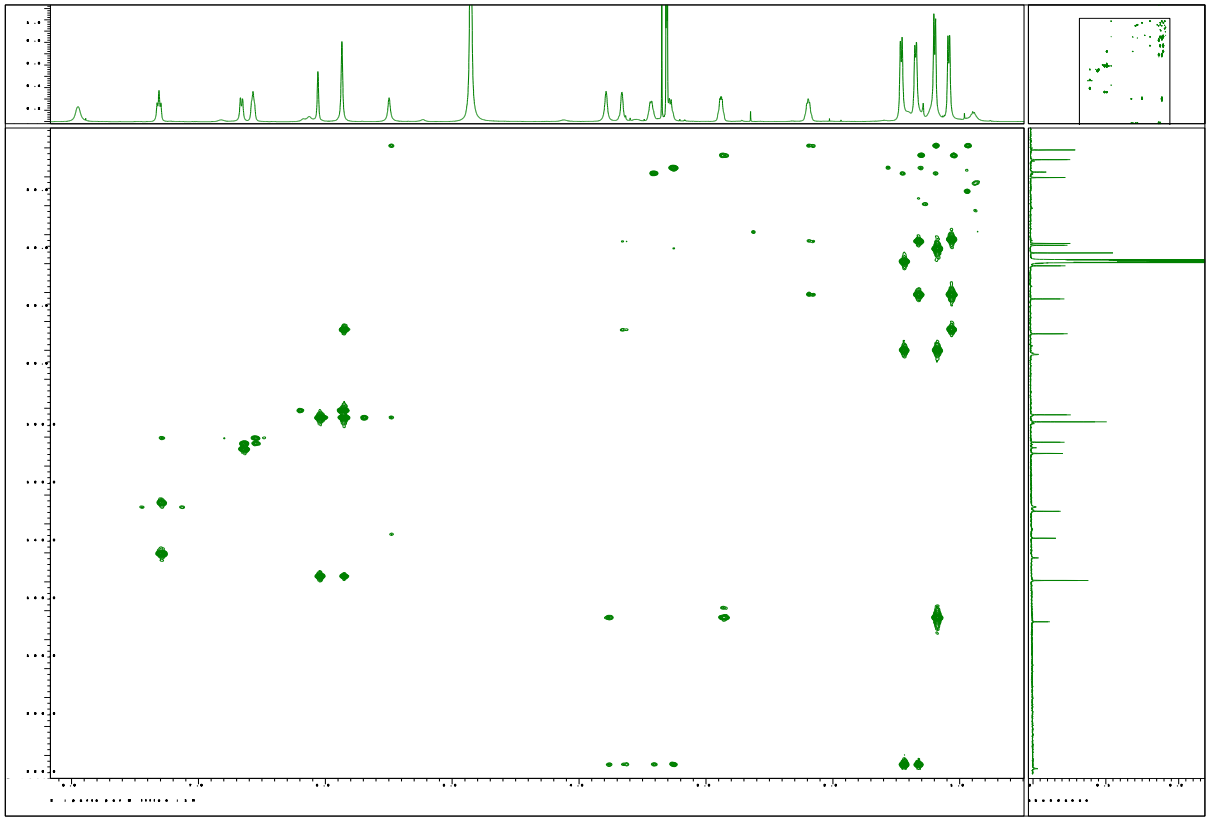

Figure S9. NOESY spectrum of saccharothriolide A (**1**) in methanol-d_4.

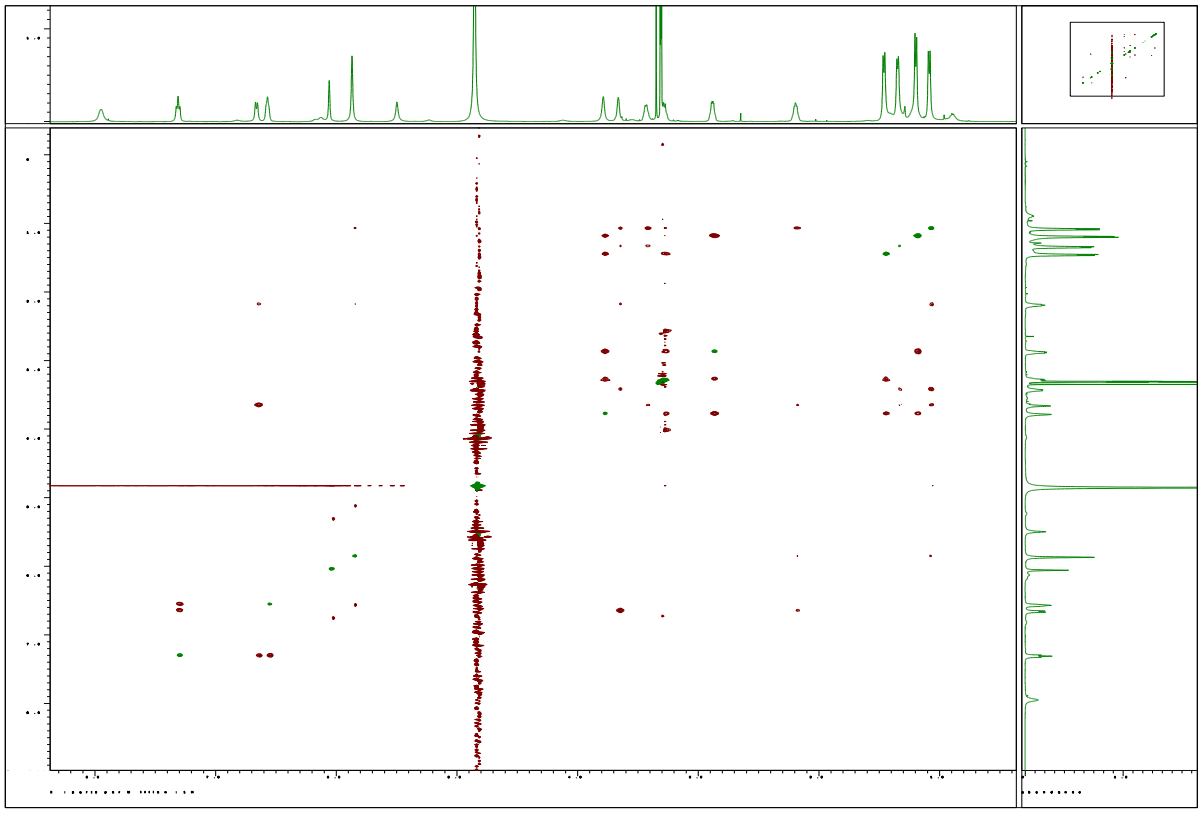

Figure S10. [1]H NMR spectrum of saccharothriolide B (**2**) in methanol-d_4.

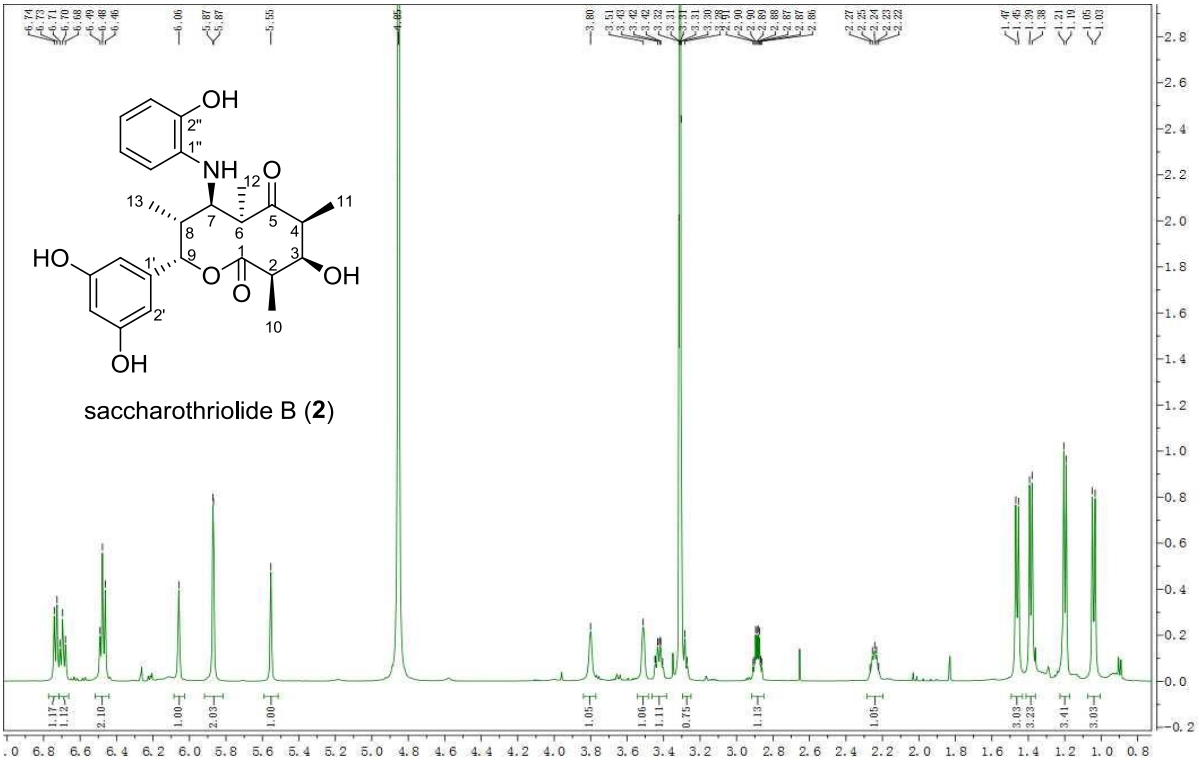

Figure S11. [13]C NMR spectrum of saccharothriolide B (**2**) in methanol-d_4.

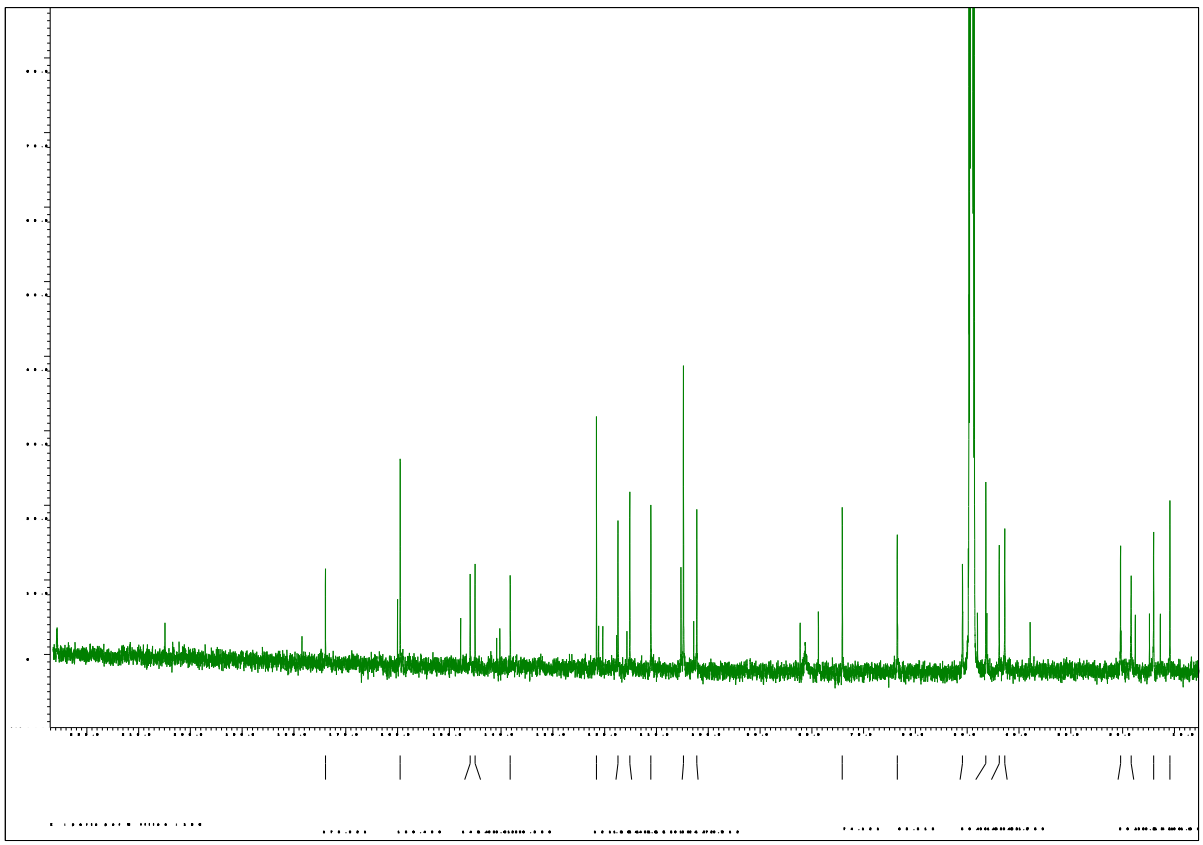

Figure S12. ^{1}H-^{1}H COSY spectrum of saccharothriolide B (**2**) in methanol-d_4.

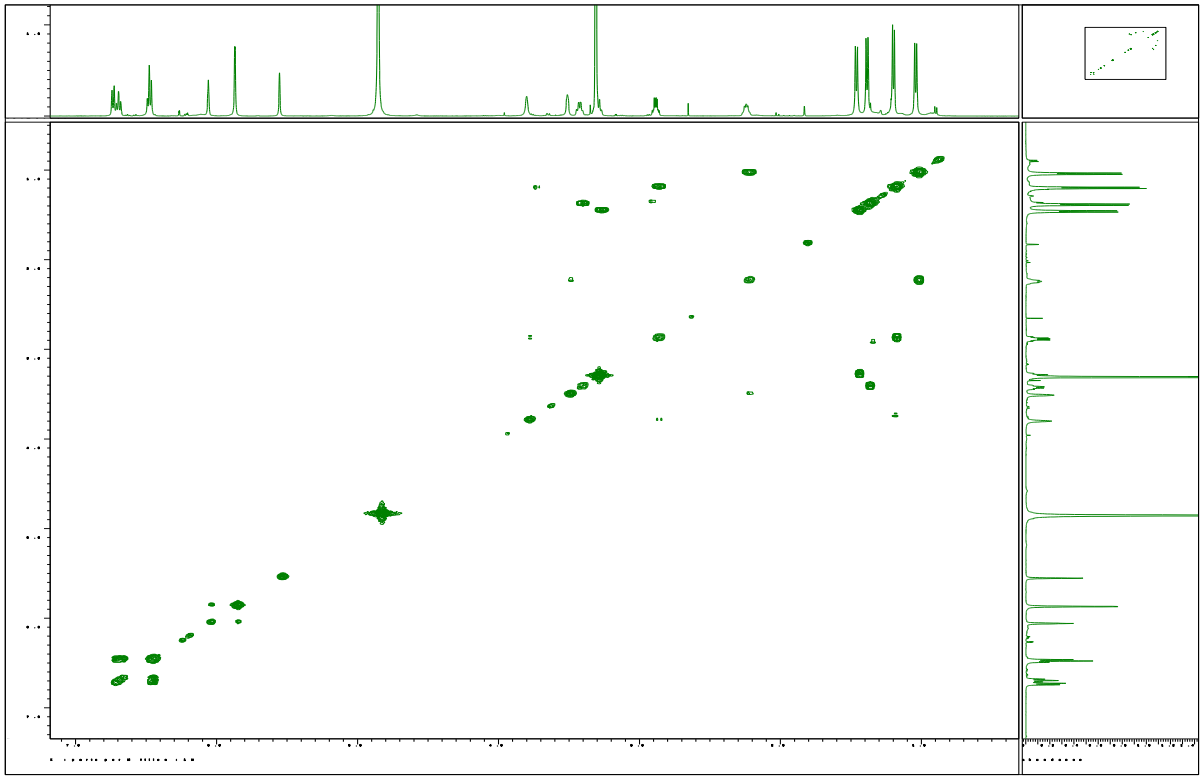

Figure S13. HMQC spectrum of saccharothriolide B (**2**) in methanol-d_4.

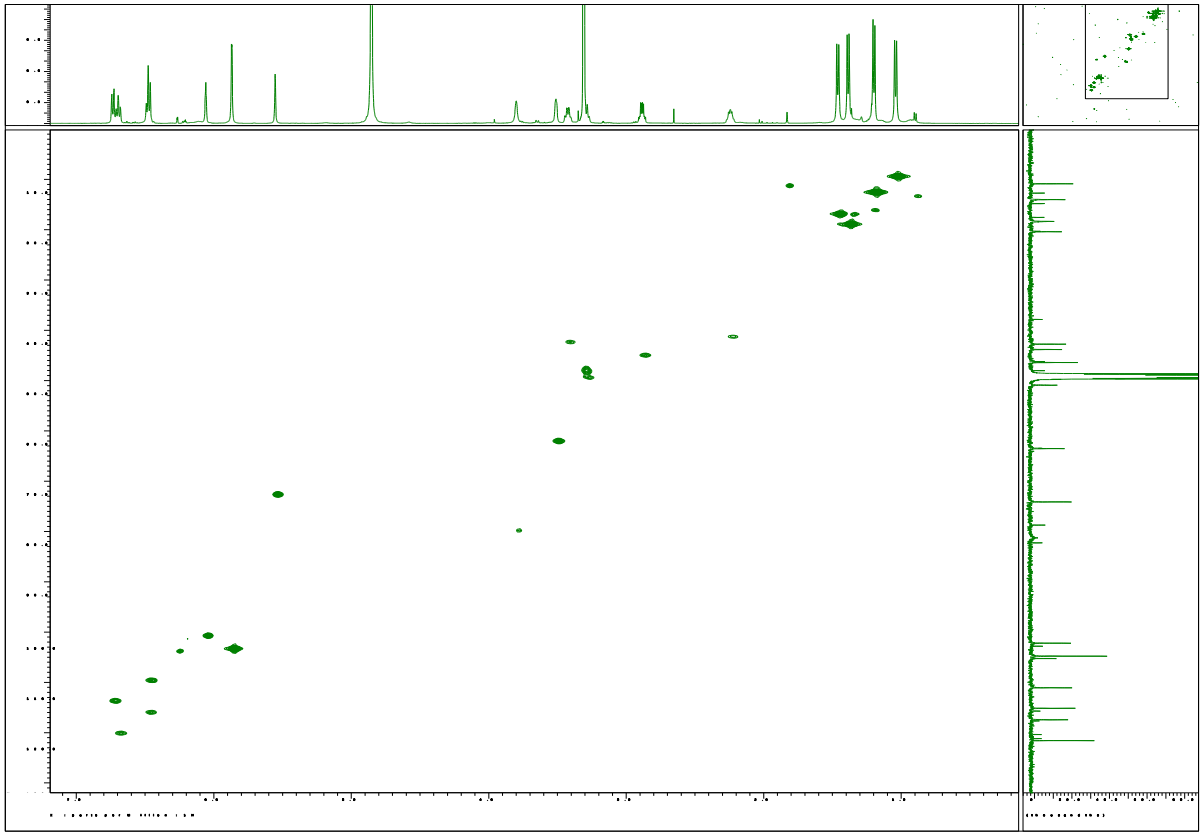

Figure S14. HMBC spectrum of saccharothriolide B (**2**) in methanol-d_4.

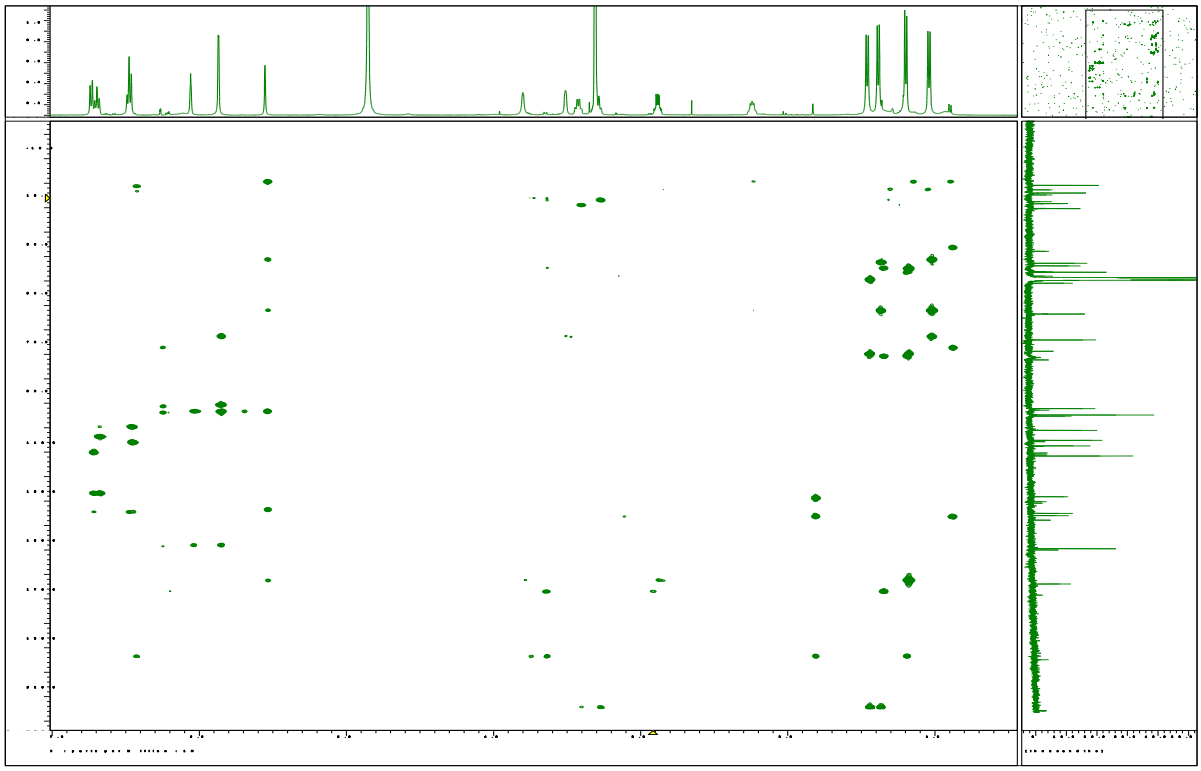

Figure S15. NOESY spectrum of saccharothriolide B (**2**) in methanol-d_4.

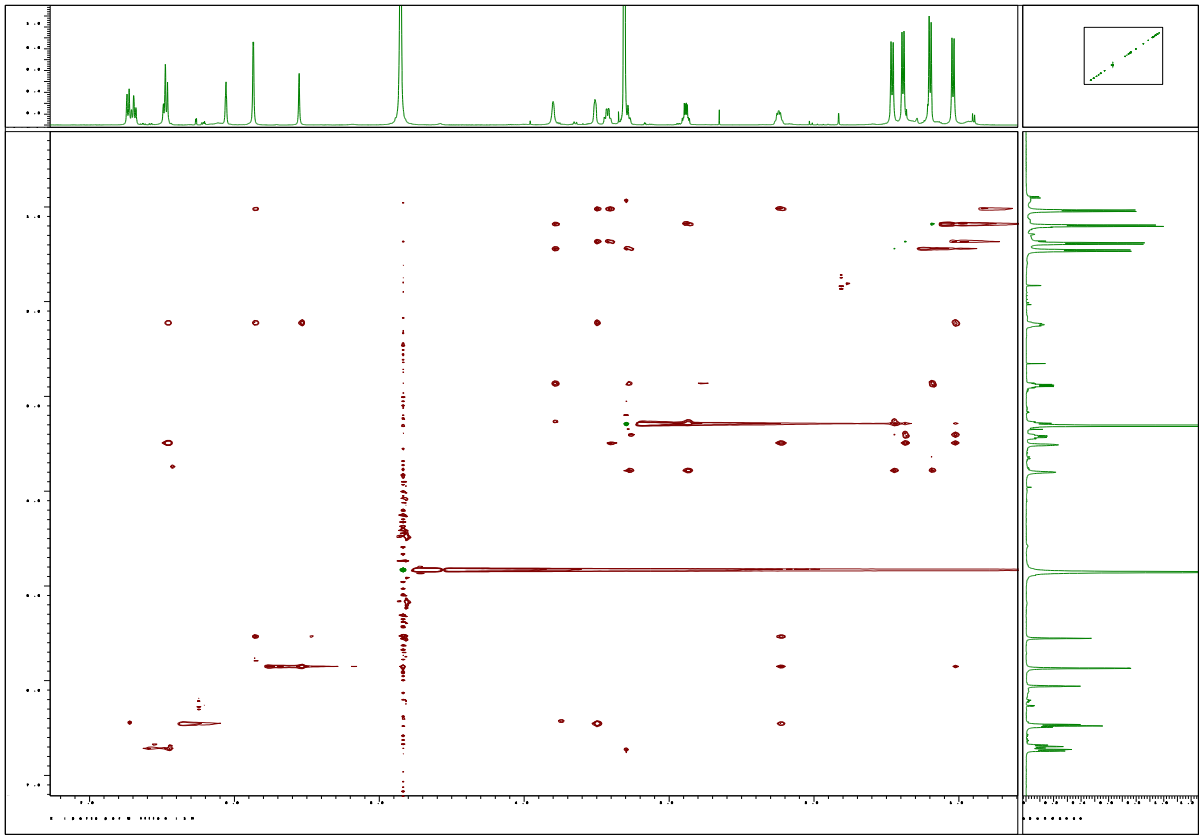

Figure S16. [1]H NMR spectrum of saccharothriolide C (**3**) in methanol-d_4.

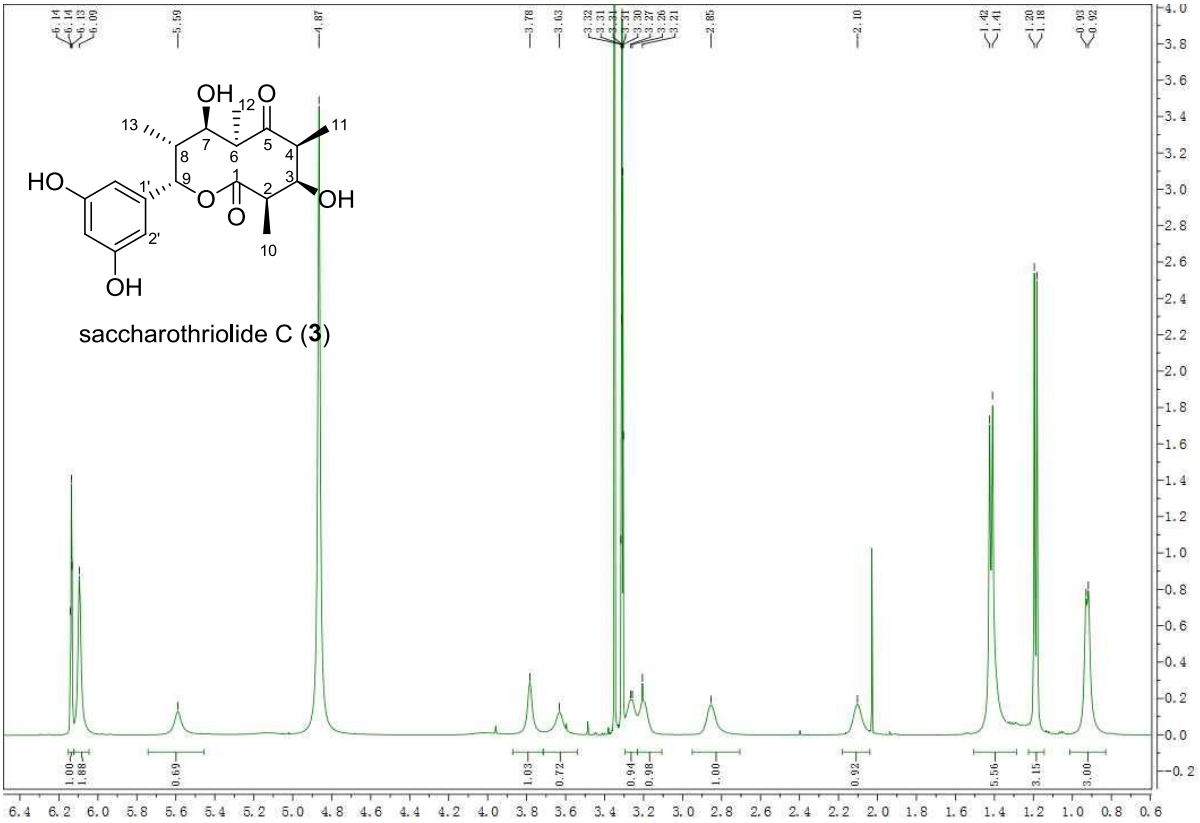

Figure S17. [13]C NMR spectrum of saccharothriolide C (**3**) in methanol-d_4.

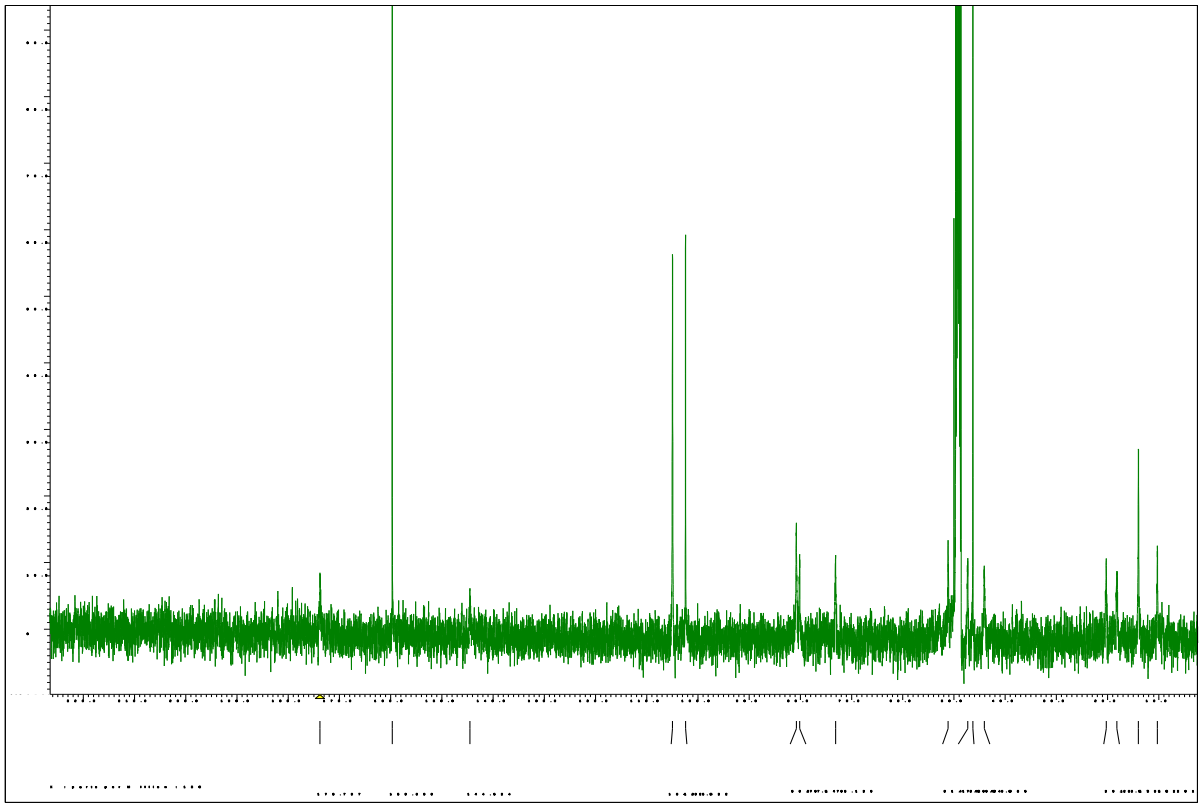

Figure S18. ^{1}H-^{1}H COSY spectrum of saccharothriolide C (**3**) in methanol-d_4.

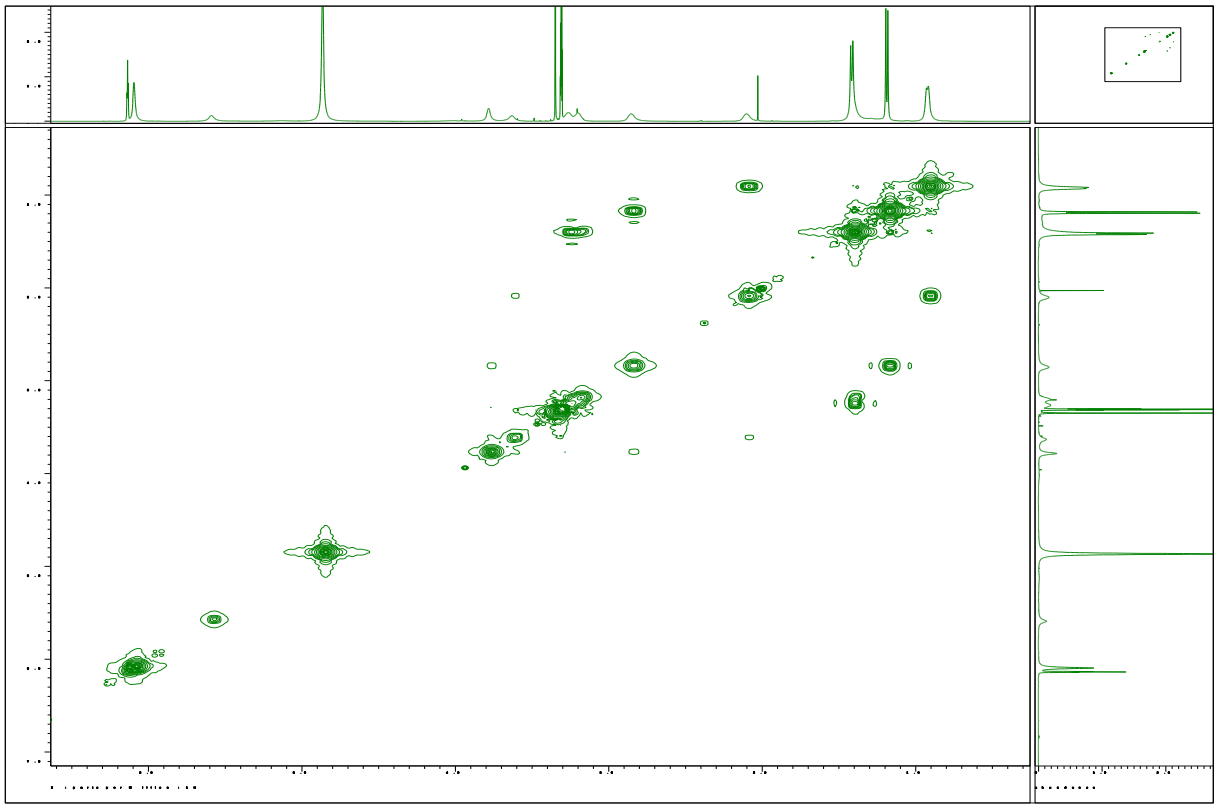

Figure S19. HMQC spectrum of saccharothriolide C (**3**) in methanol-d_4.

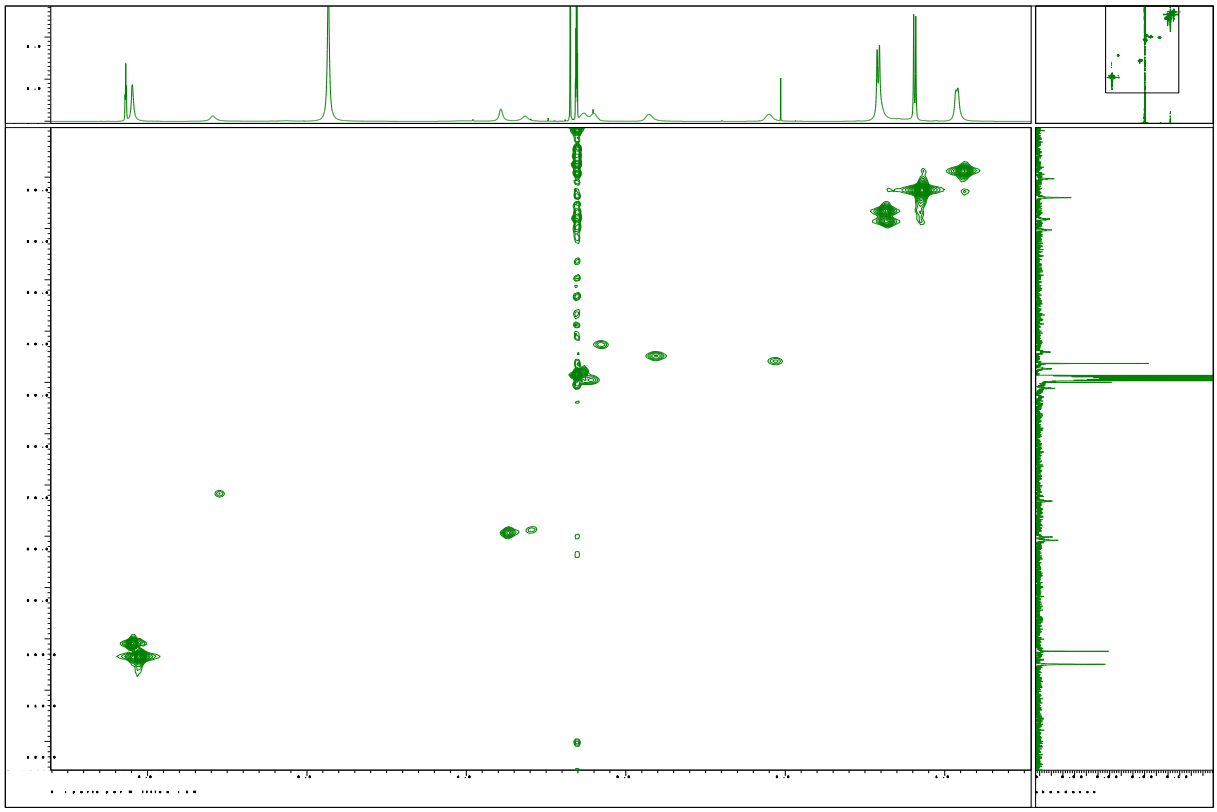

Figure S20. NOESY spectrum of saccharothriolide C (**3**) in methanol-d_4.

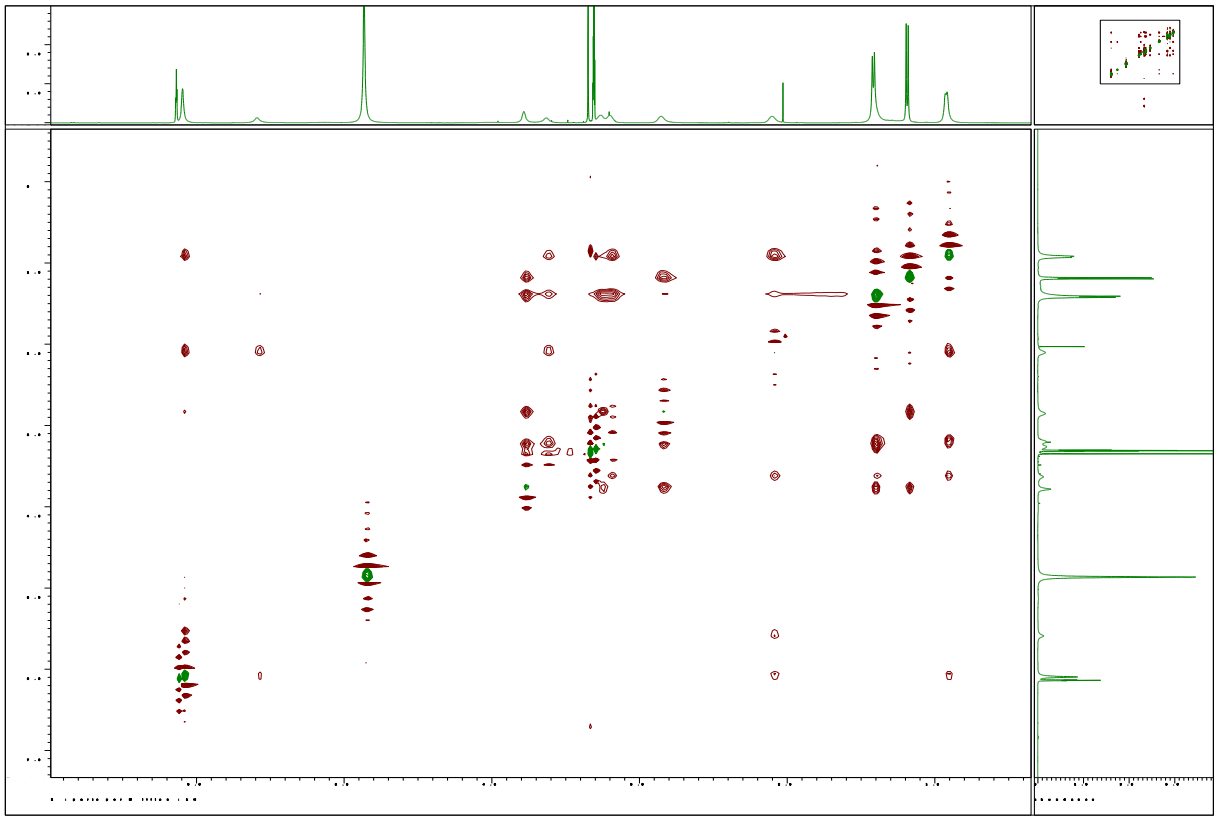

Figure S21. ^{1}H NMR spectrum of saccharothriolide D (**4**) in methanol-d_4.

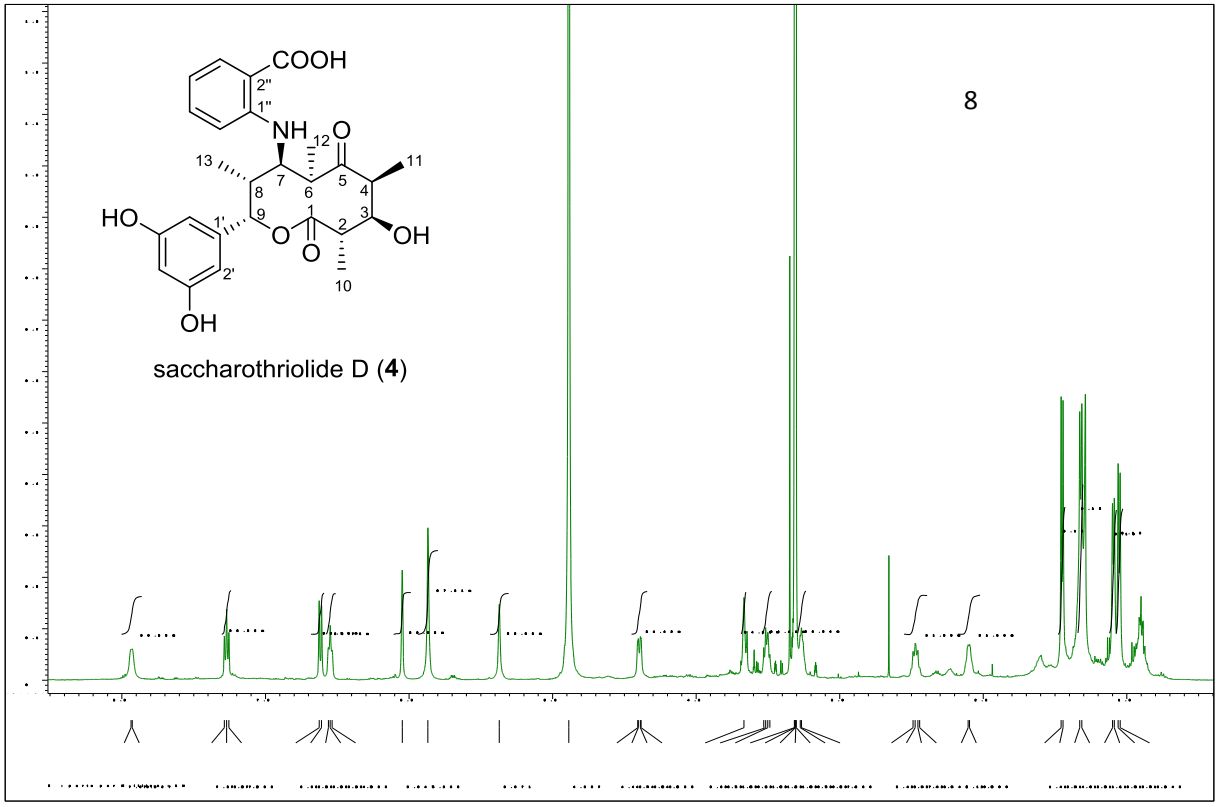

Figure S22. ^{13}C NMR spectrum of saccharothriolide D (**4**) in methanol-d_4.

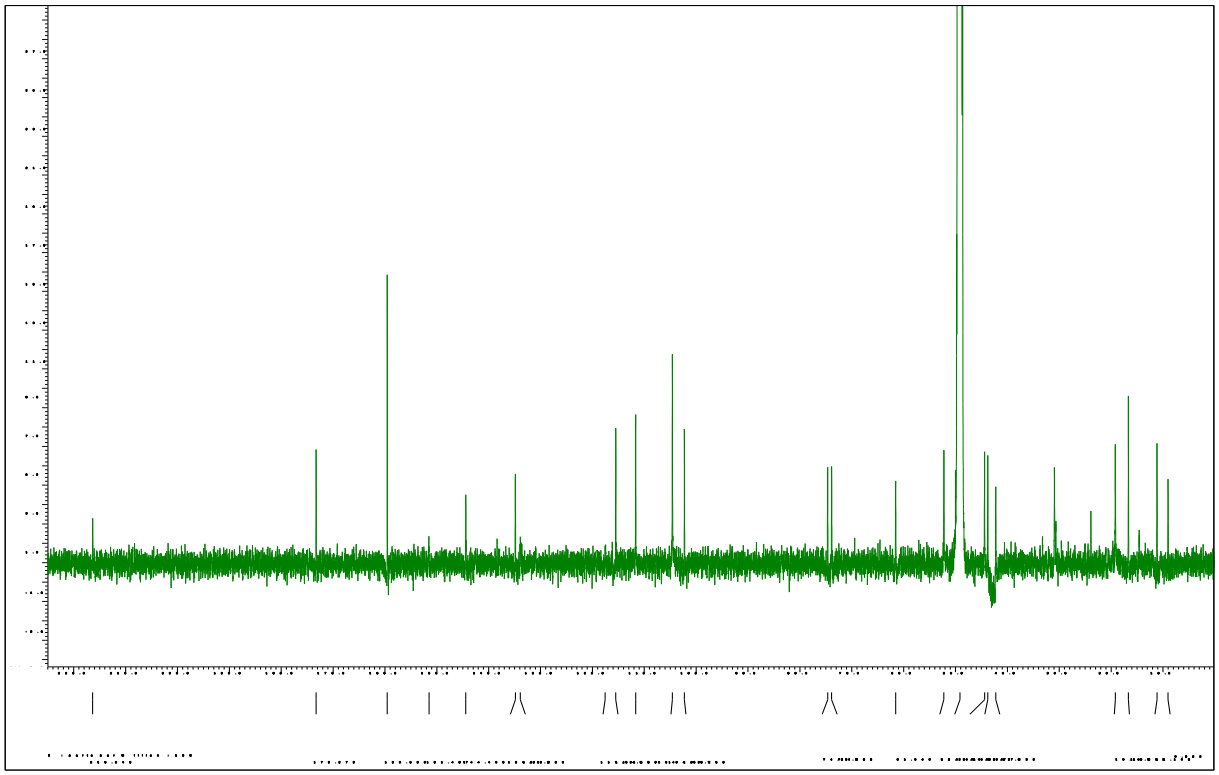

Figure S23. ^{1}H-^{1}H COSY spectrum of saccharothriolide D (**4**) in methanol-d_4.

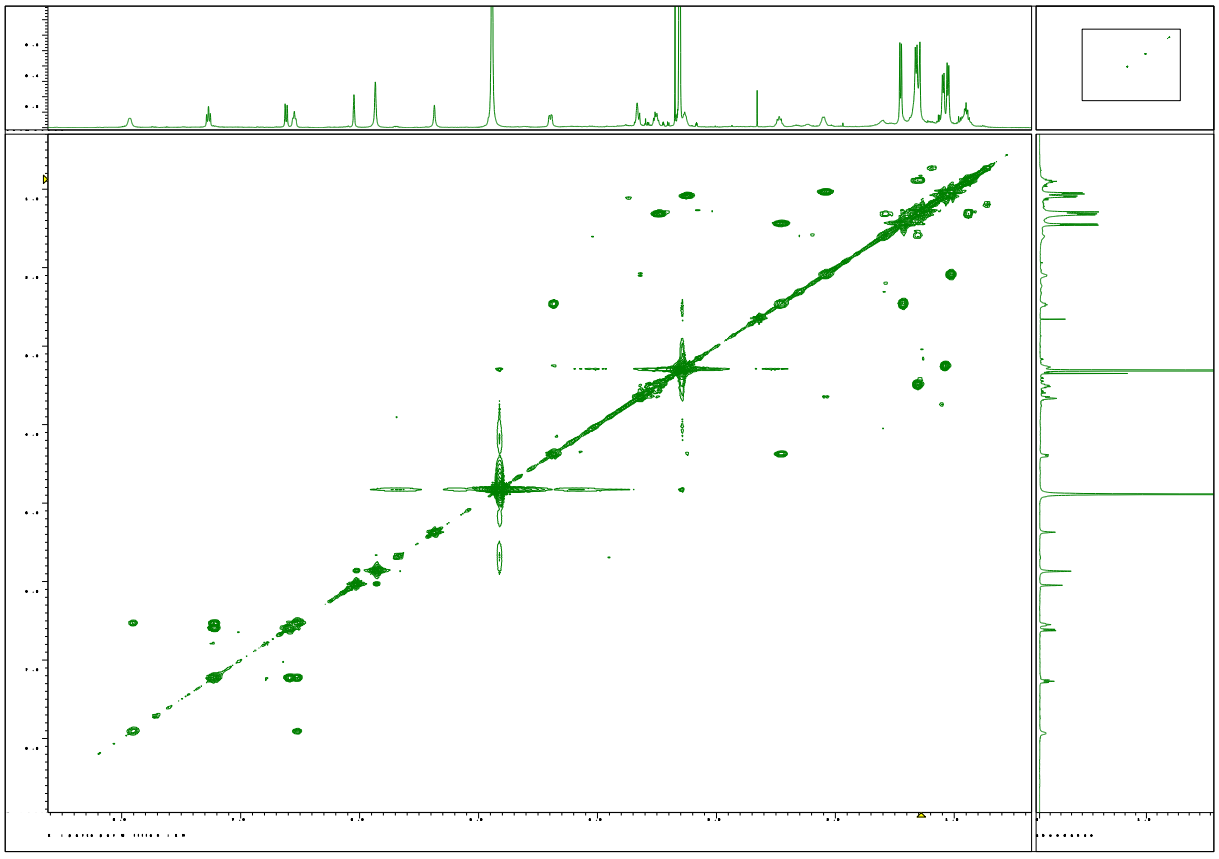

Figure S24. HMQC spectrum of saccharothriolide D (**4**) in methanol-d_4.

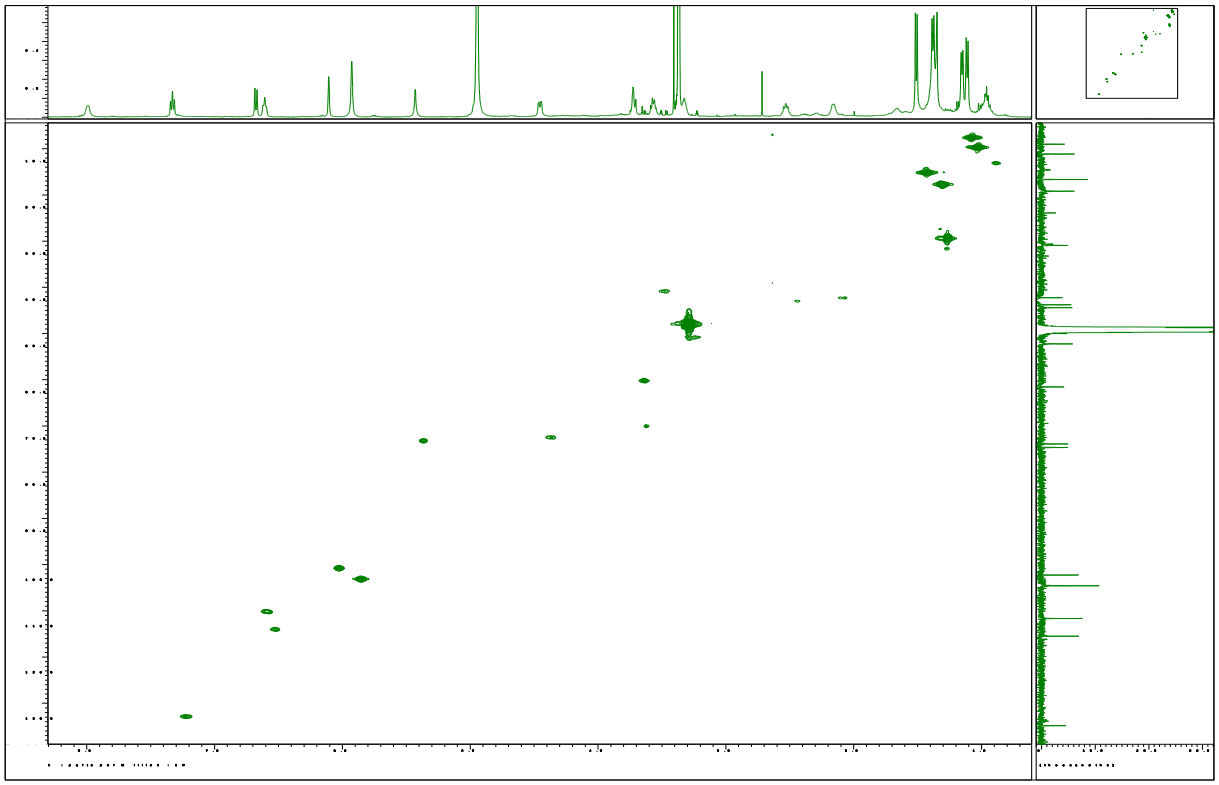

Figure S25. HMBC spectrum of saccharothriolide D (**4**) in methanol-d_4.

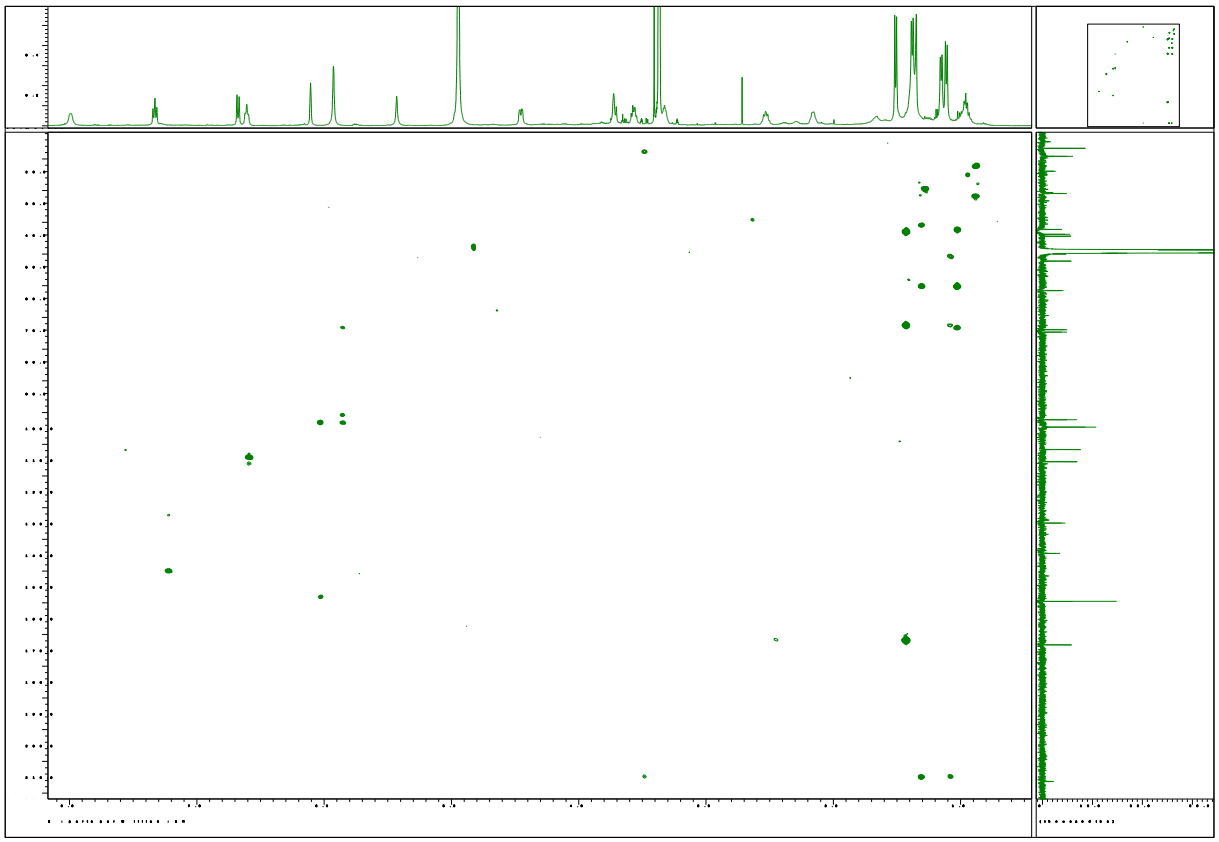

Figure S26. NOESY spectrum of saccharothriolide D (**4**) in methanol-d_4.

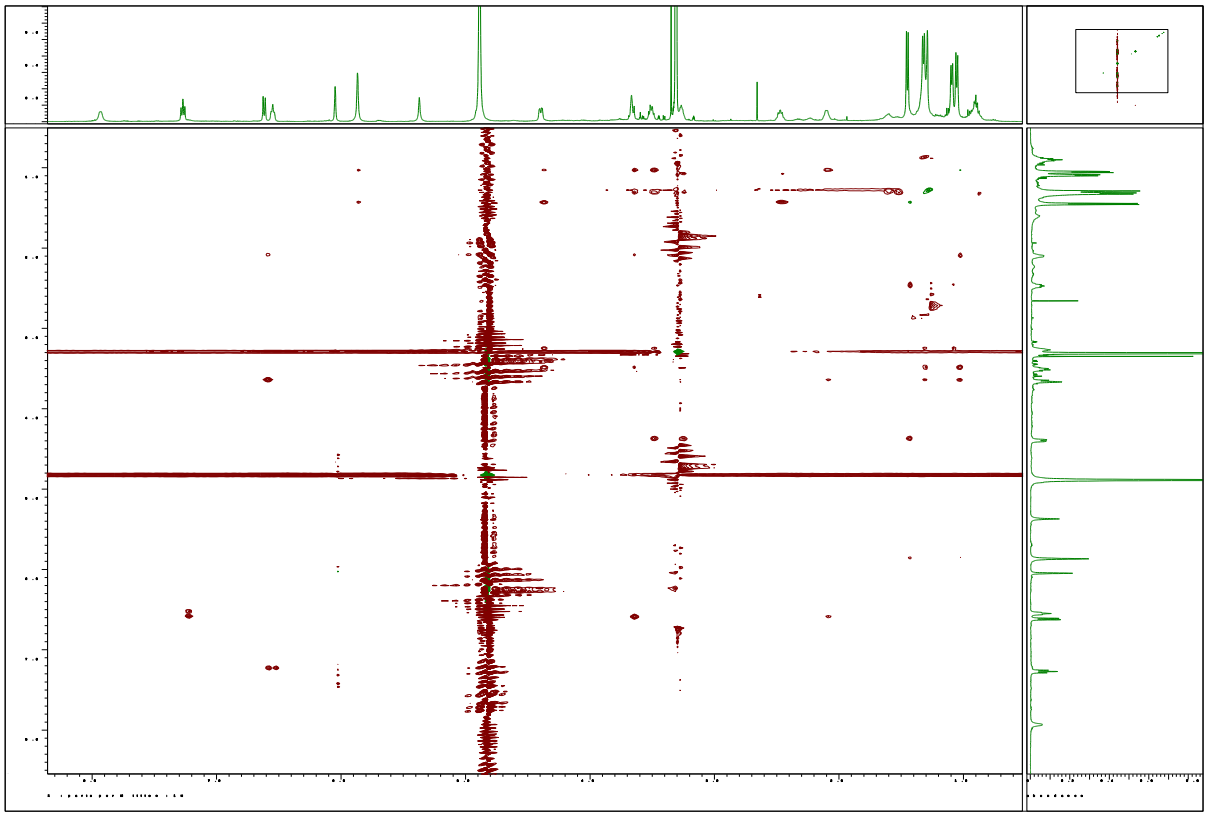

Figure S27. ^{1}H NMR spectrum of saccharothriolide E (**5**) in methanol-d_4.

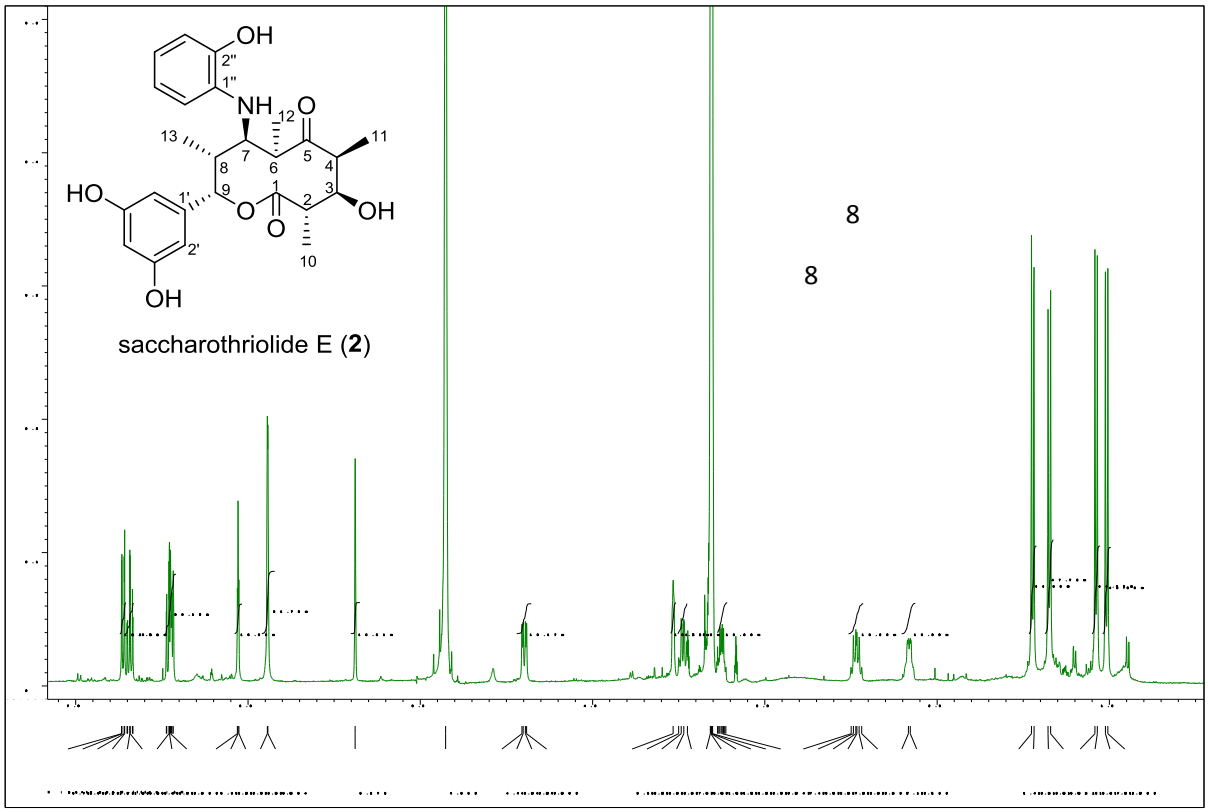

Figure S28. ^{13}C NMR spectrum of saccharothriolide E (**5**) in methanol-d_4.

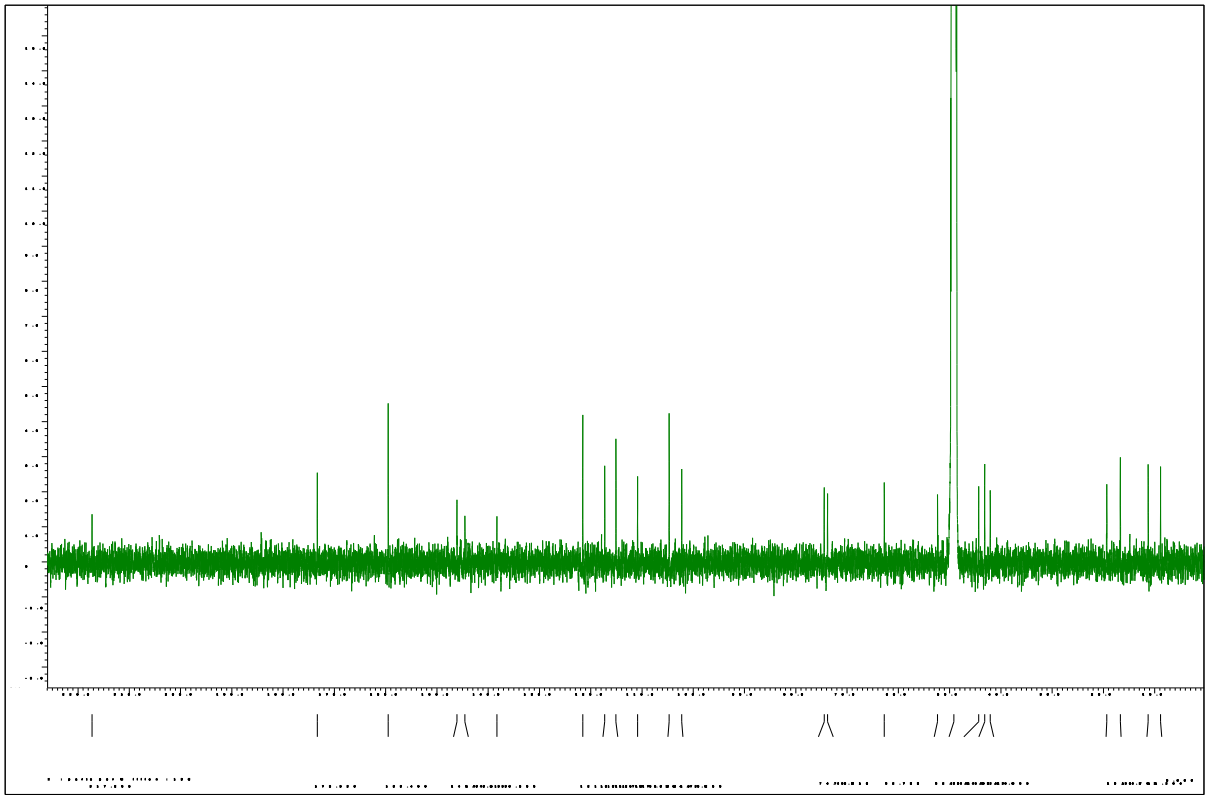

Figure S29. ^{1}H-^{1}H COSY spectrum of saccharothriolide E (**5**) in methanol-d_4.

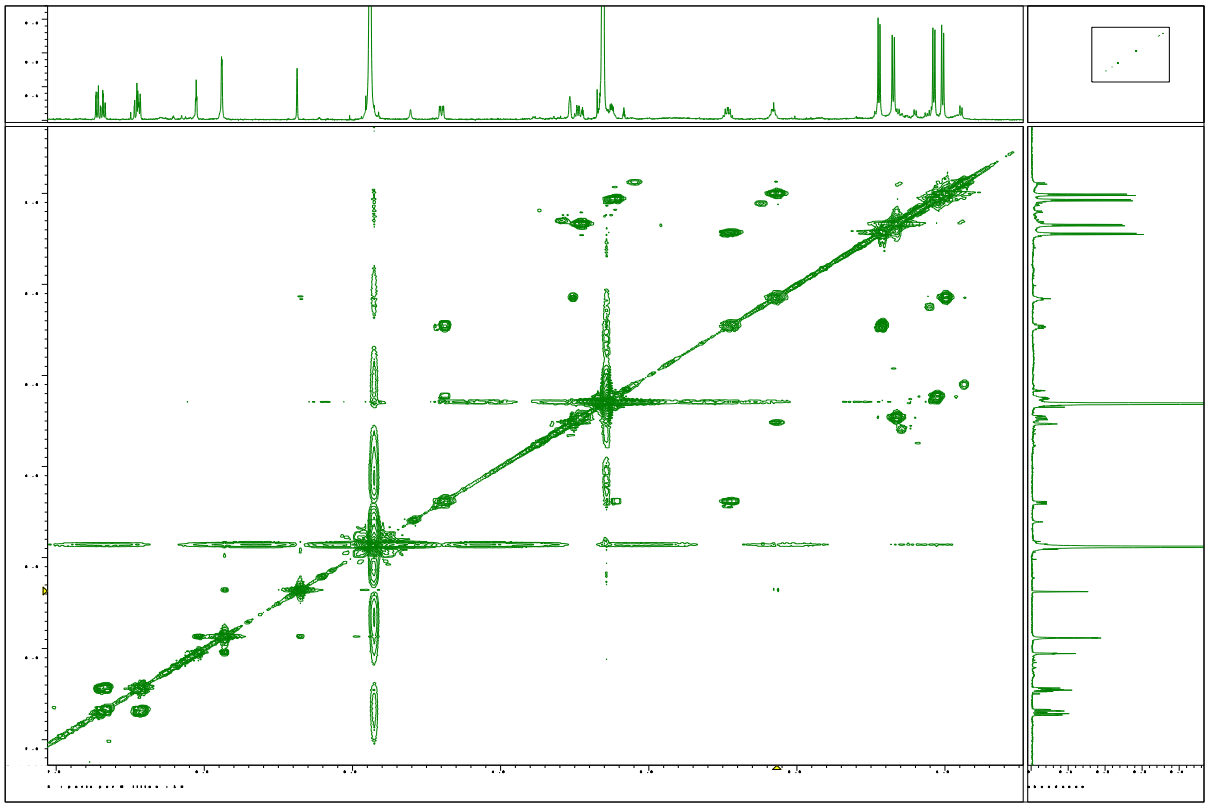

Figure S30. HMQC spectrum of saccharothriolide E (**5**) in methanol-d_4.

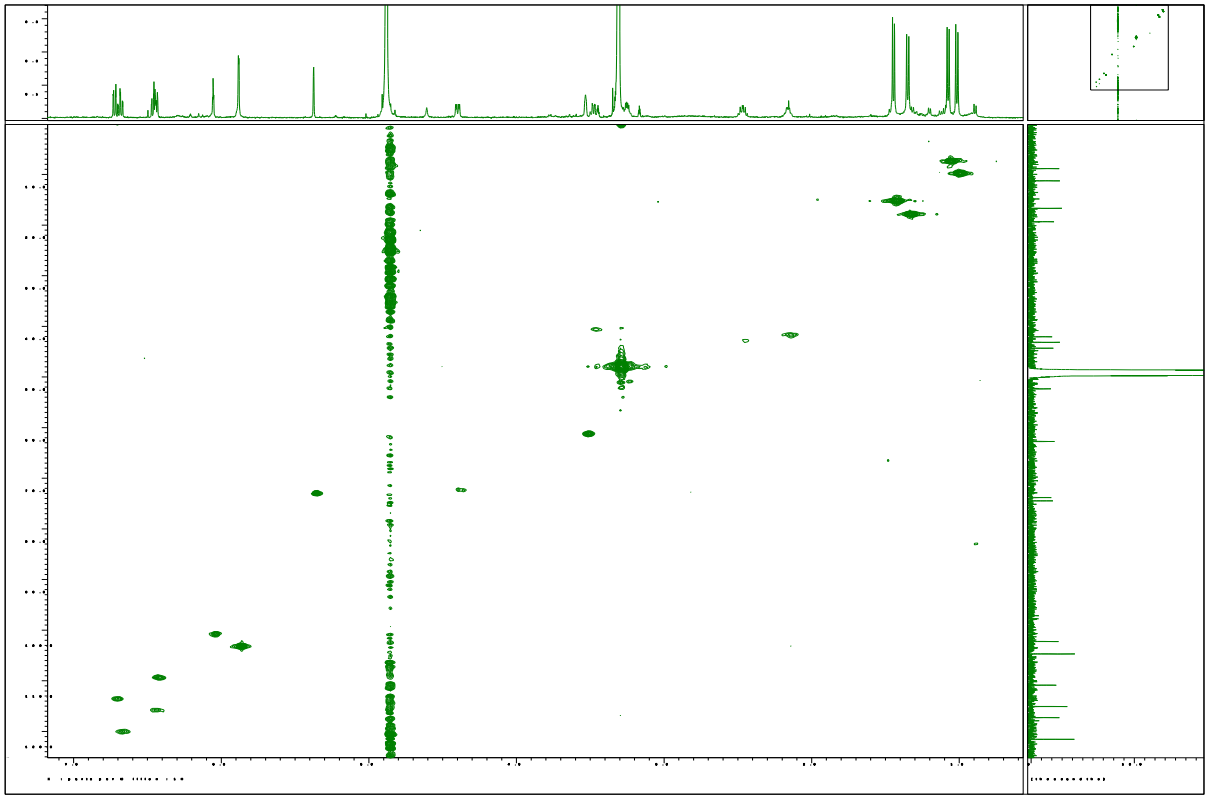

Figure S31. HMBC spectrum of saccharothriolide E (**5**) in methanol-d_4.

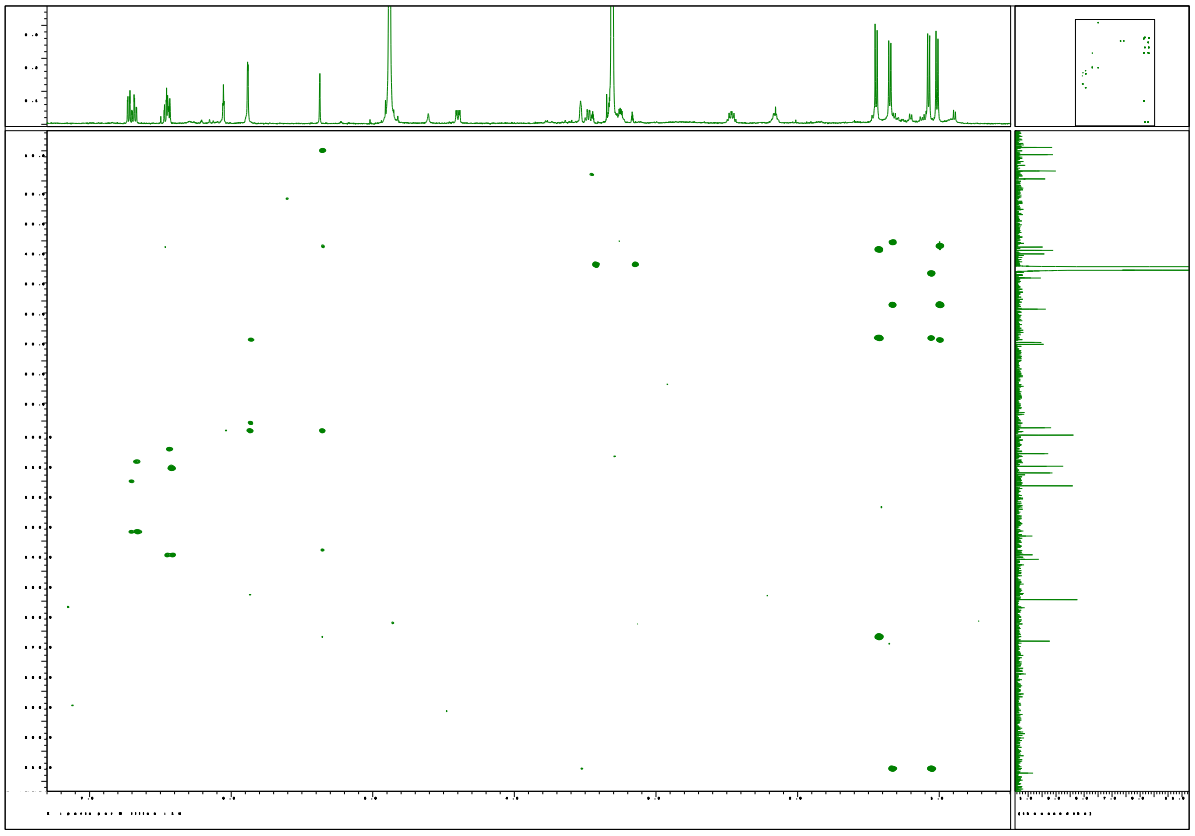

Figure S32. NOESY spectrum of saccharothriolide E (**5**) in methanol-d_4.

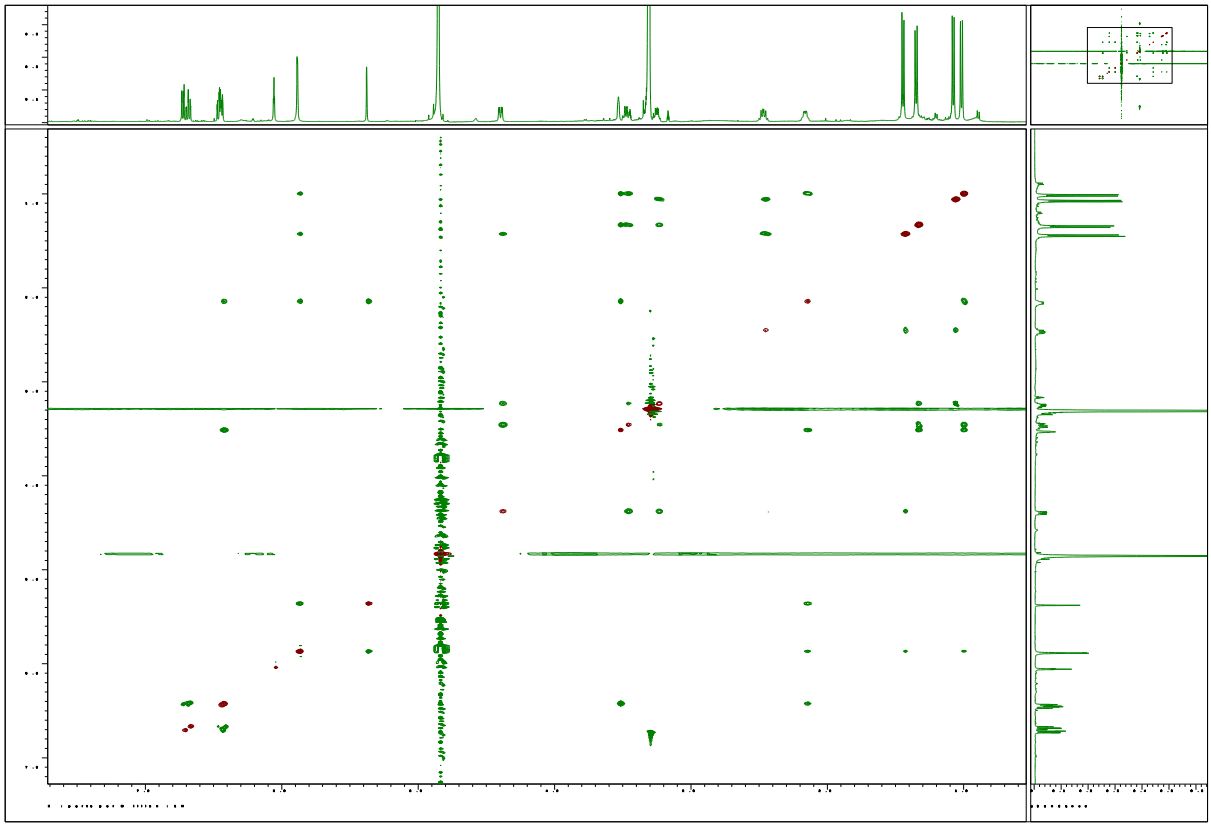

Figure S33. ^{1}H NMR spectrum of saccharothriolide F (**6**) in methanol-d_4.

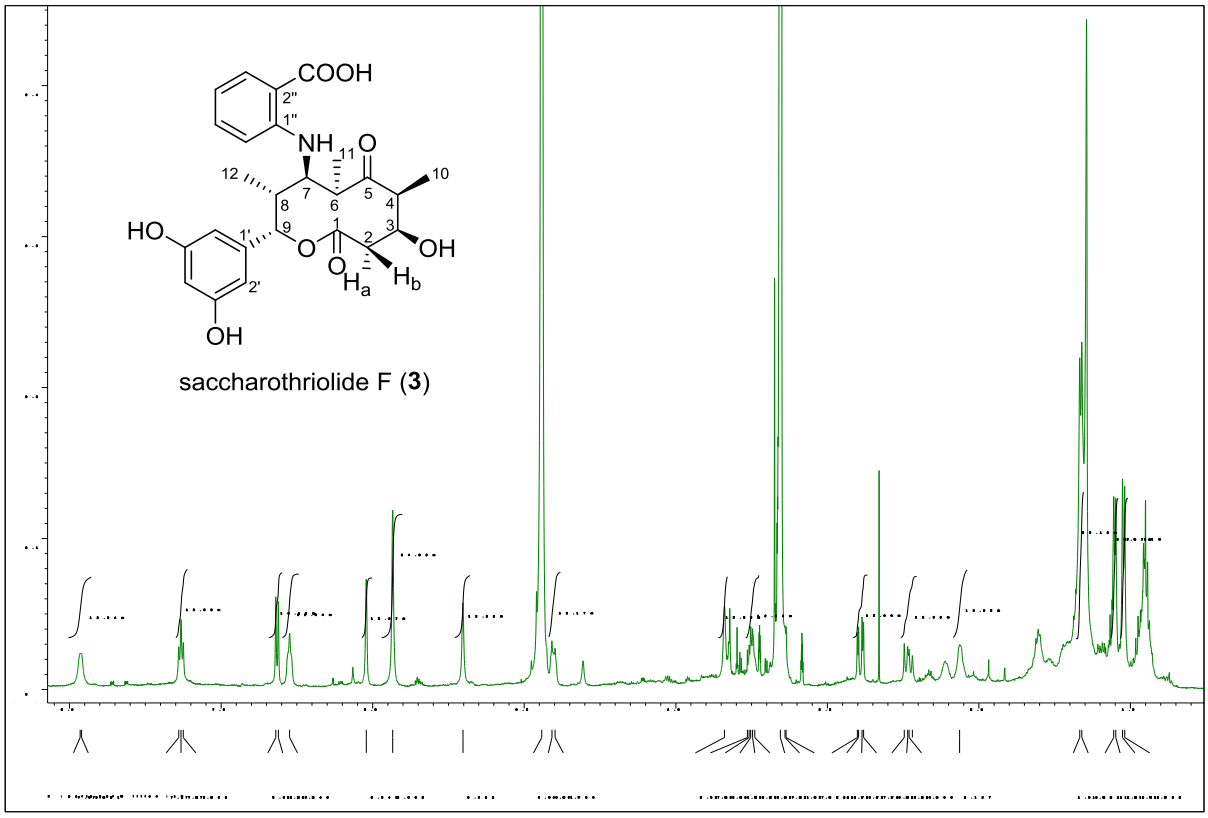

Figure S34. ^{13}C NMR spectrum of saccharothriolide F (**6**) in methanol-d_4.

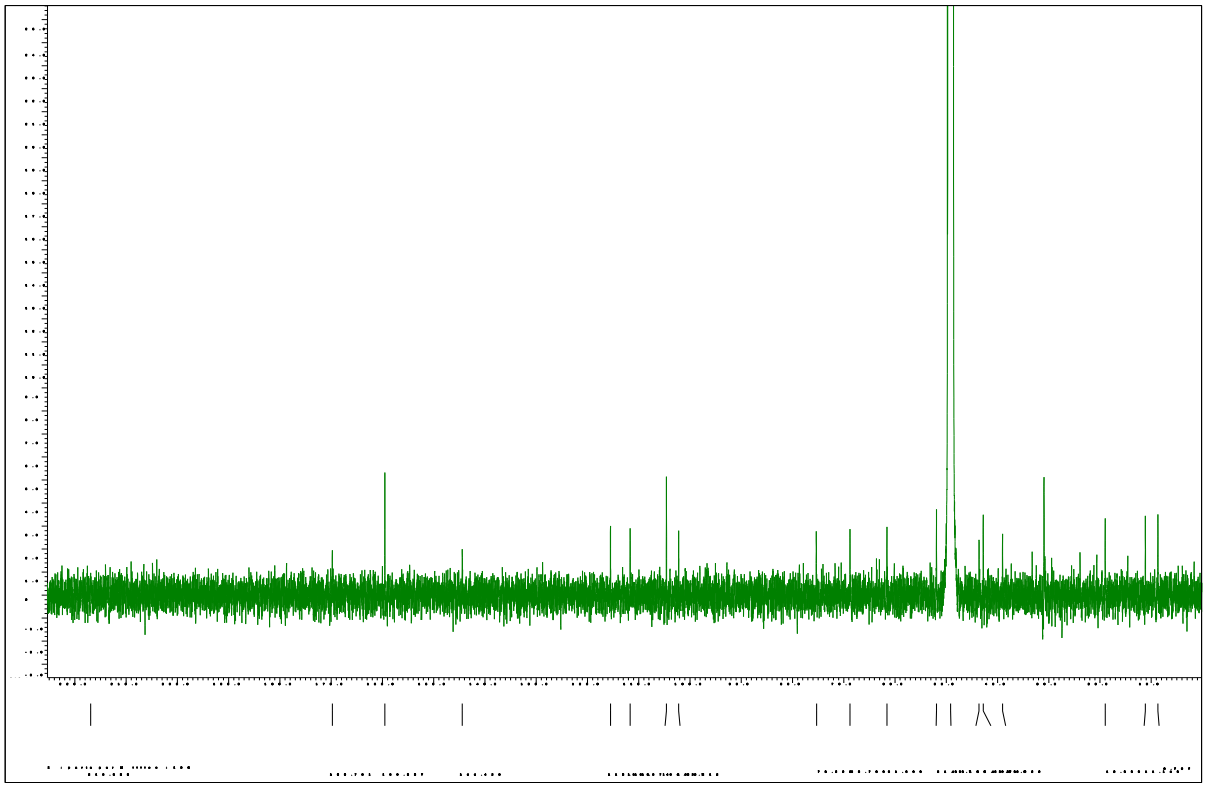

Figure S35. ^{1}H-^{1}H COSY spectrum of saccharothriolide F (**6**) in methanol-d_4.

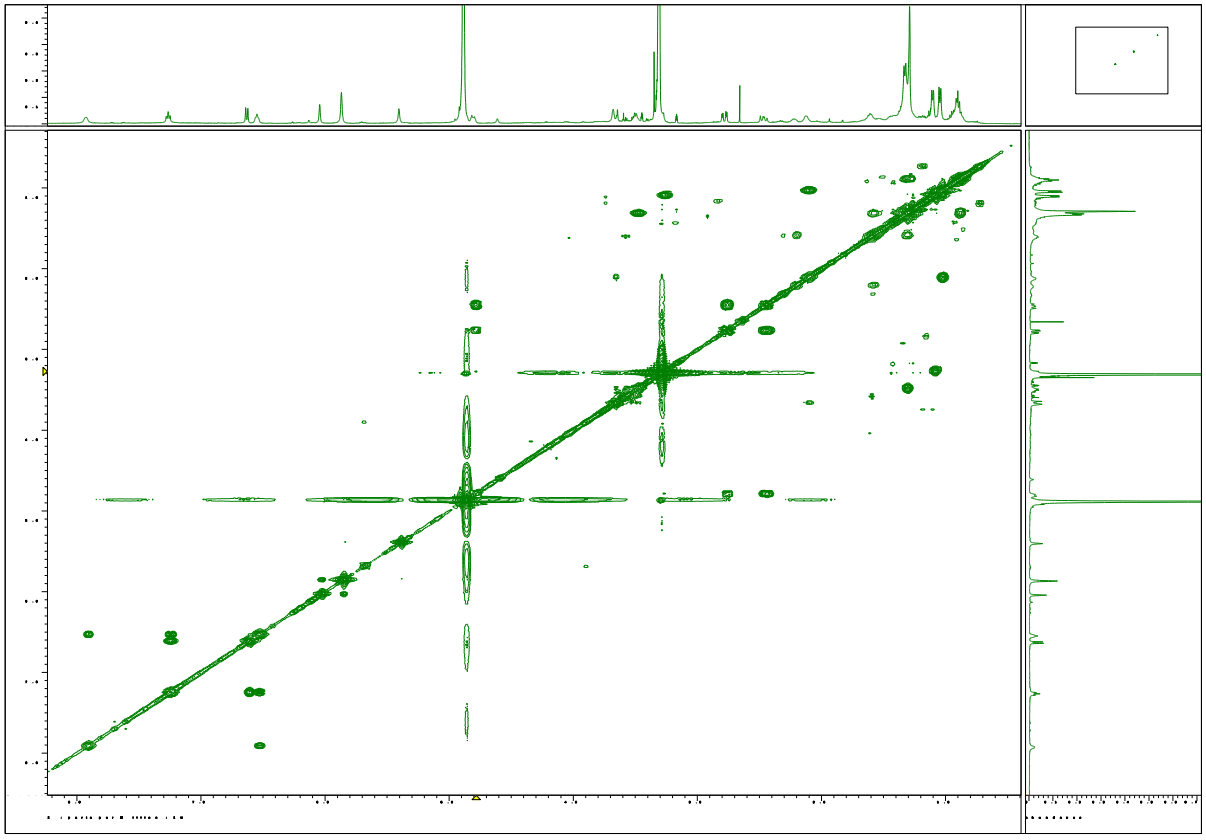

Figure S36. HMQC spectrum of saccharothriolide F (**6**) in methanol-d_4.

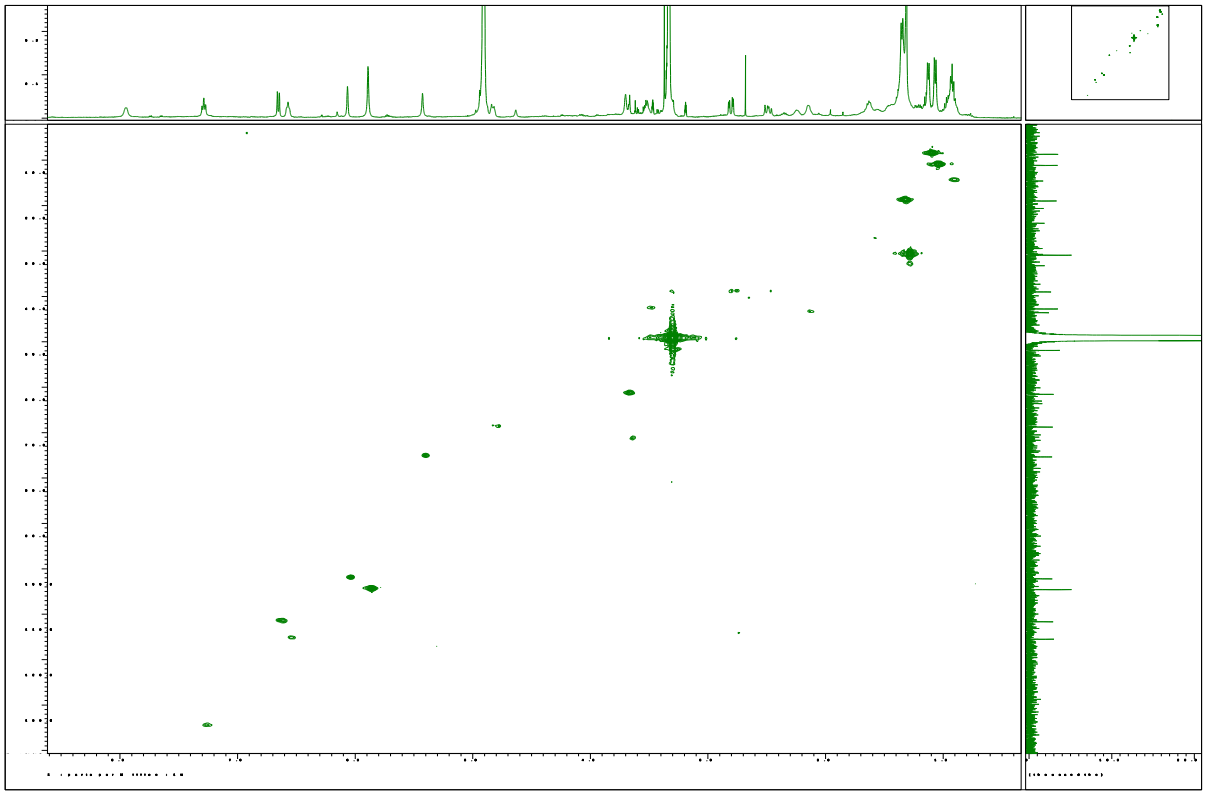

Figure S37. HMBC spectrum of saccharothriolide F (**6**) in methanol-d_4.

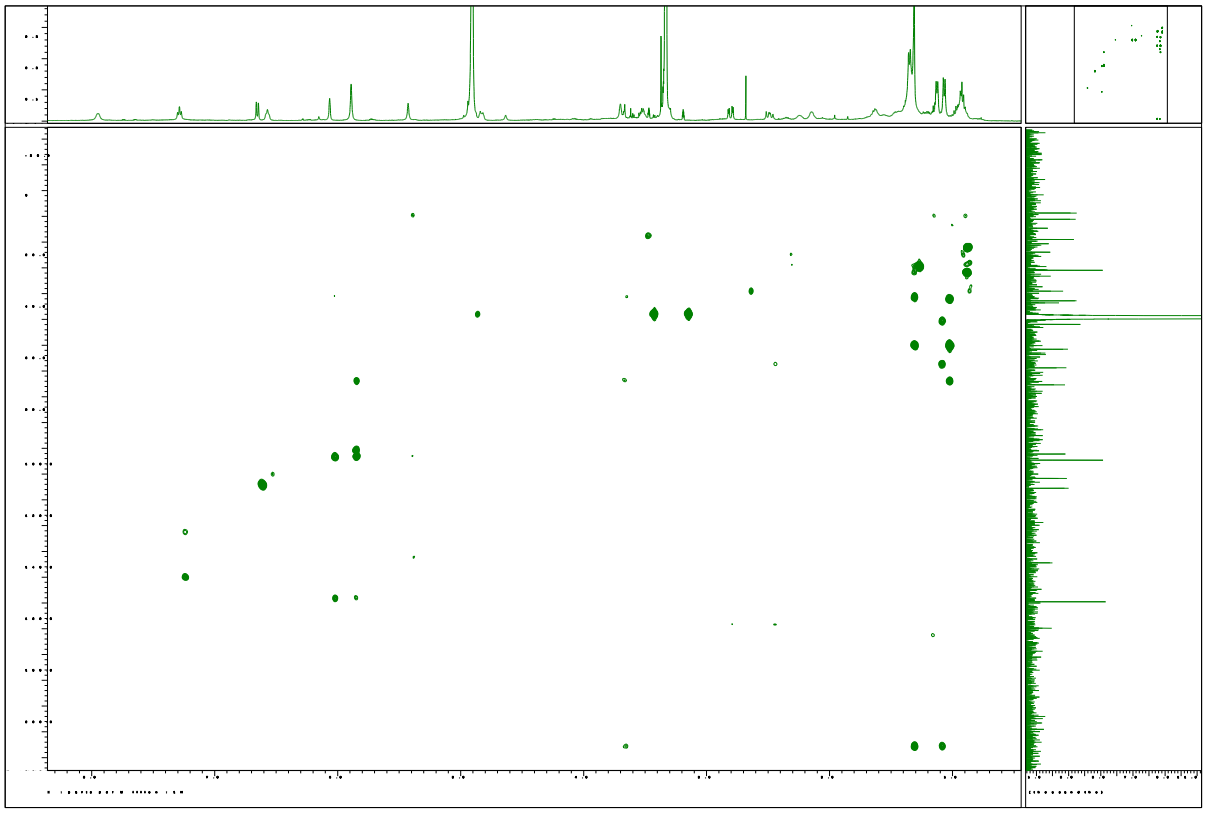

Figure S38. NOESY spectrum of saccharothriolide F (**6**) in methanol-d_4.

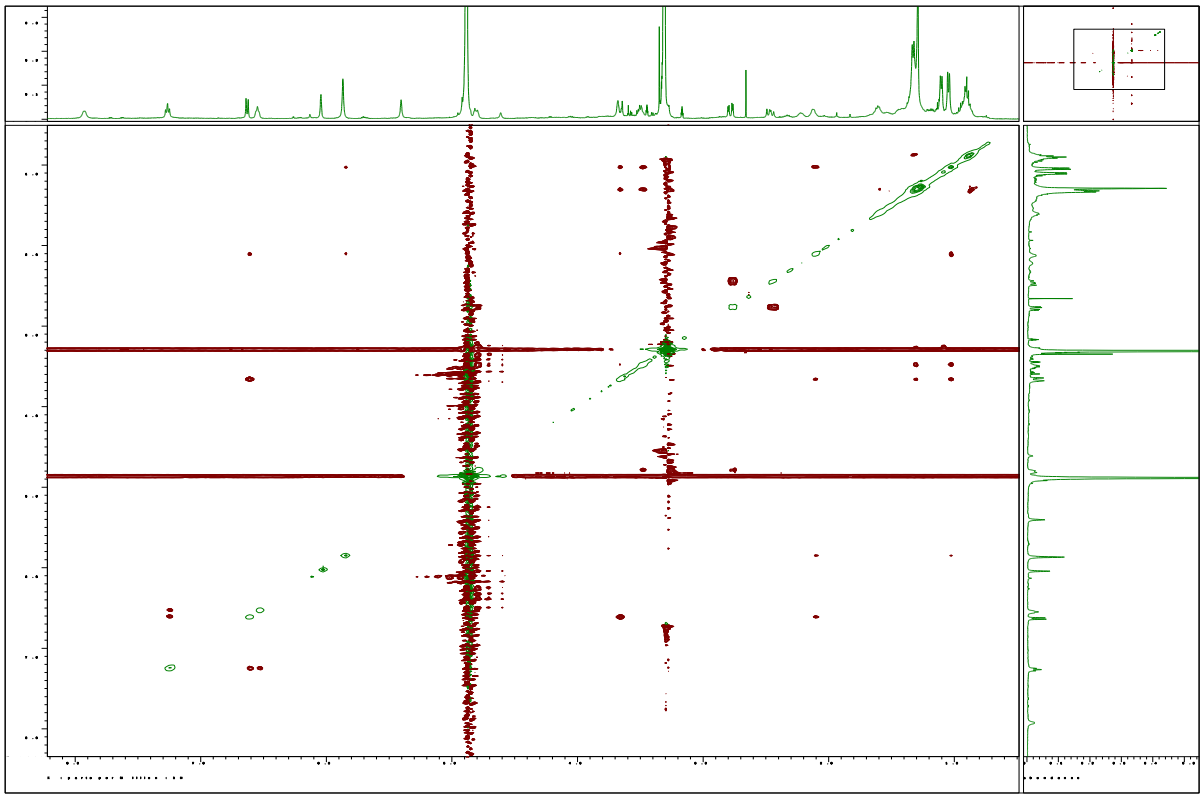

Figure S39. Optimized structures of saccharothriolides A (**1**), B (**2**), and C (**3**).

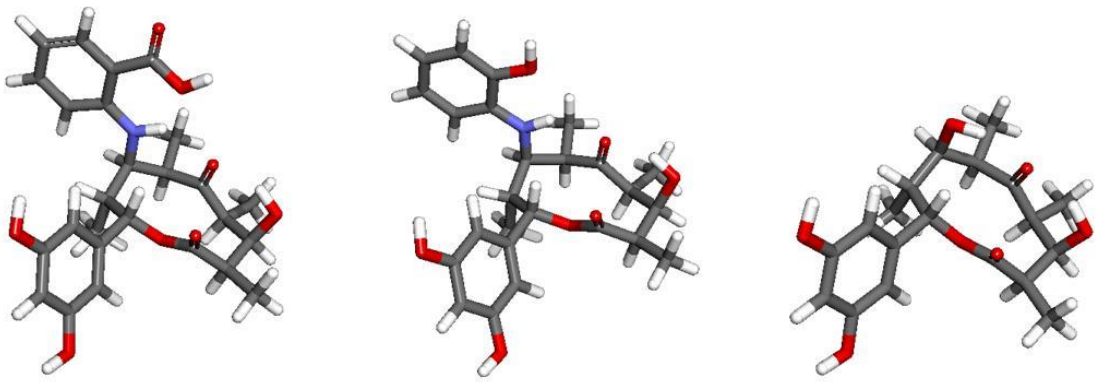

Figure S40. HR-ESI-MS spectra of precursor A (**9**).

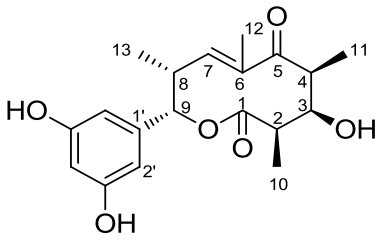

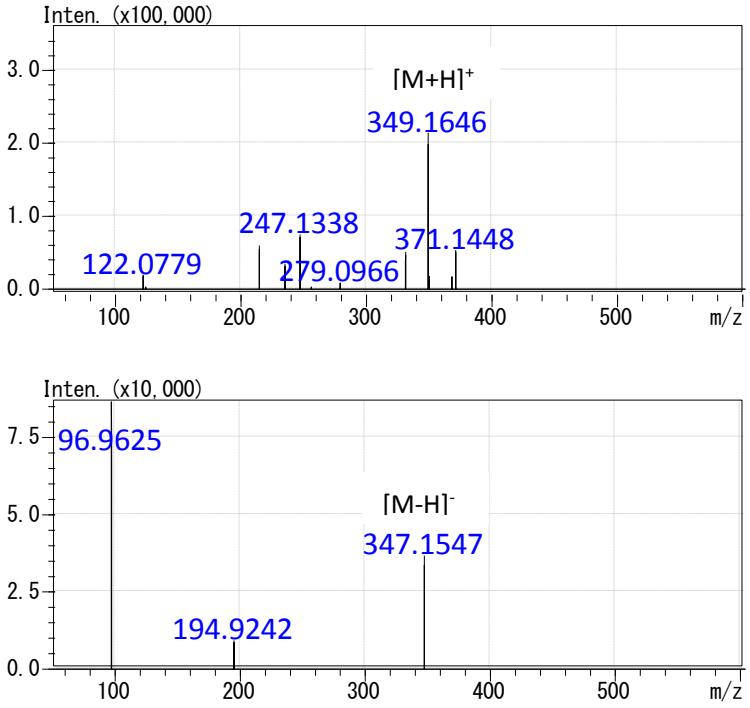

Figure S41. UV spectrum of precursor A (**9**). in acetonitrile.

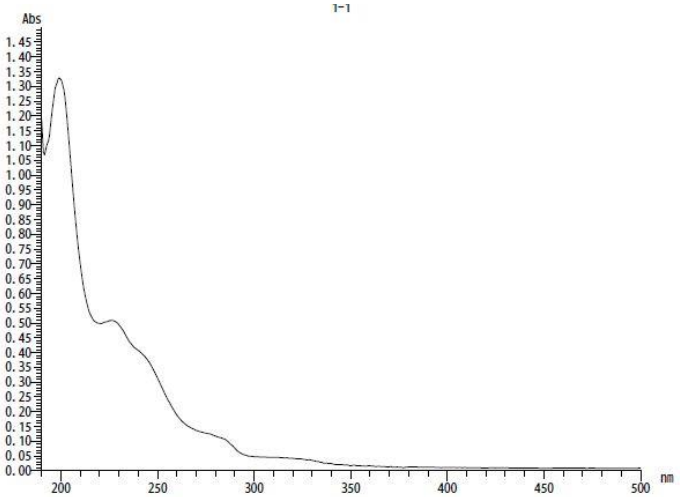

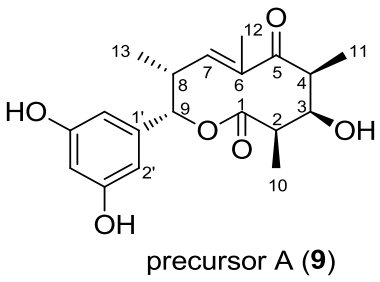

Figure S42. ^{1}H NMR spectrum of precursor A (**9**) in acetonitrile-d_3.

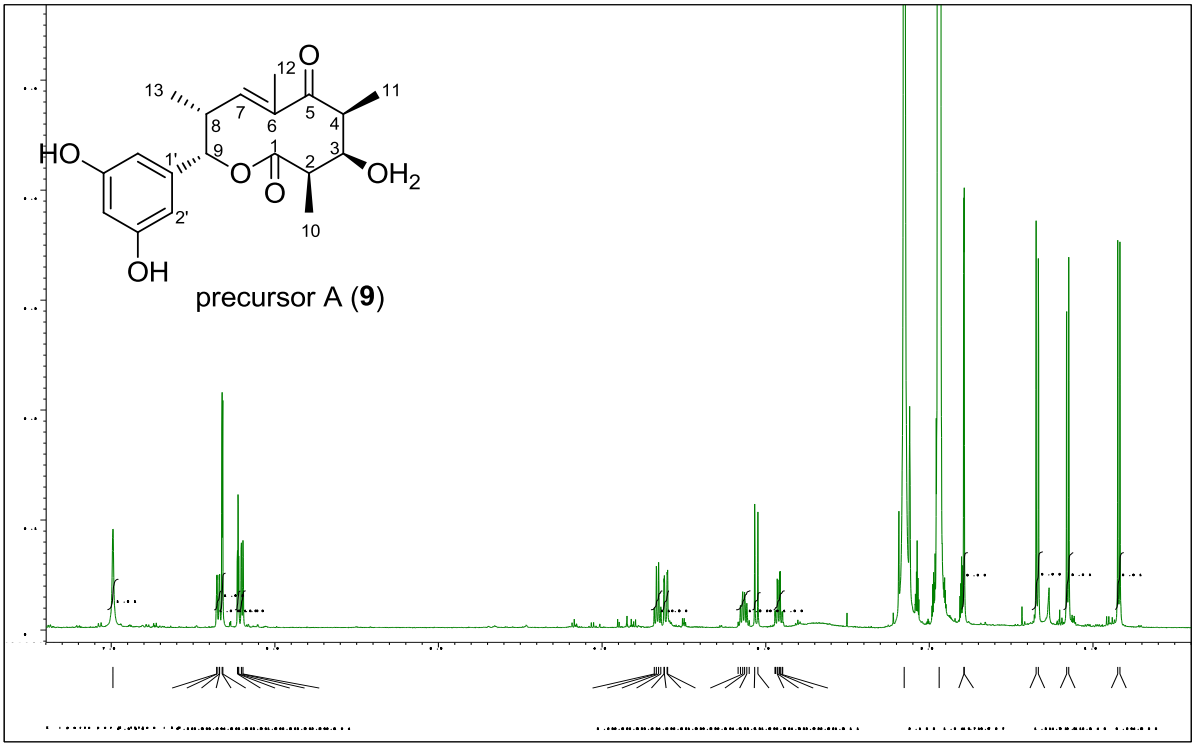

Figure S43. ^{13}C NMR spectrum of precursor A (**9**) in acetonitrile-d_3.

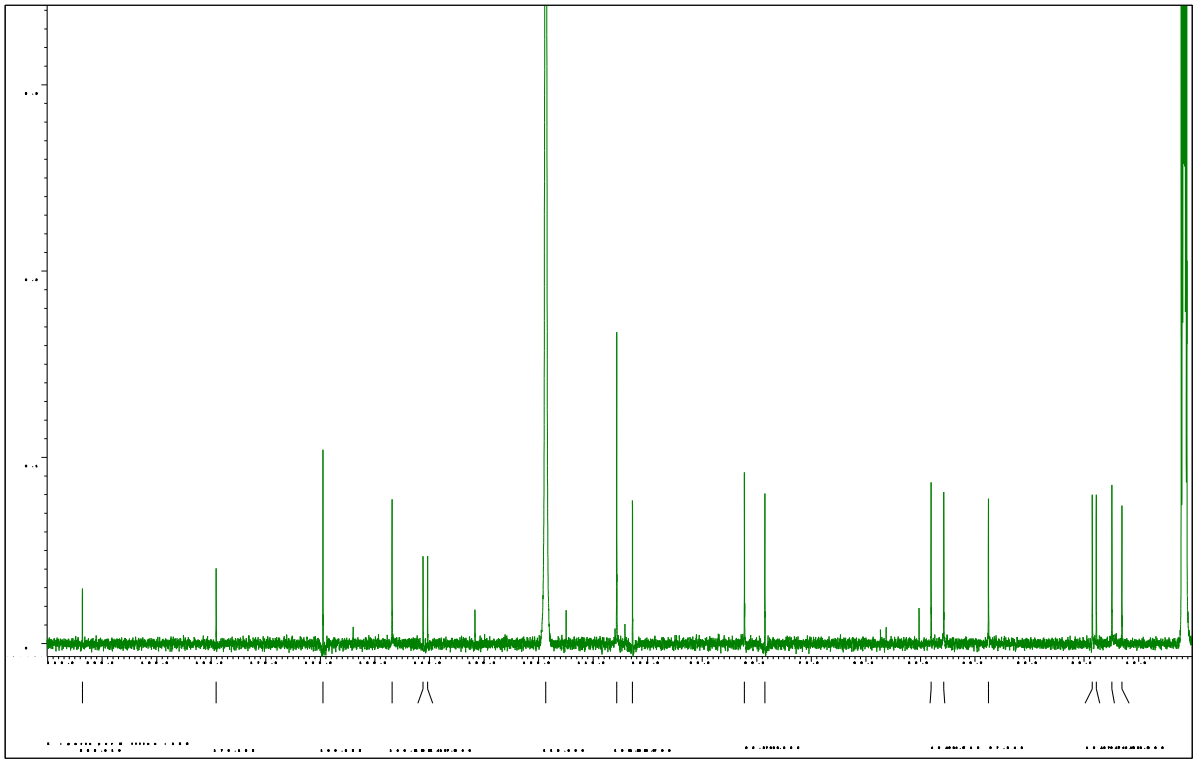

Figure S44. ^{1}H-^{1}H COSY spectrum of precursor A (**9**) in acetonitrile-d_3.

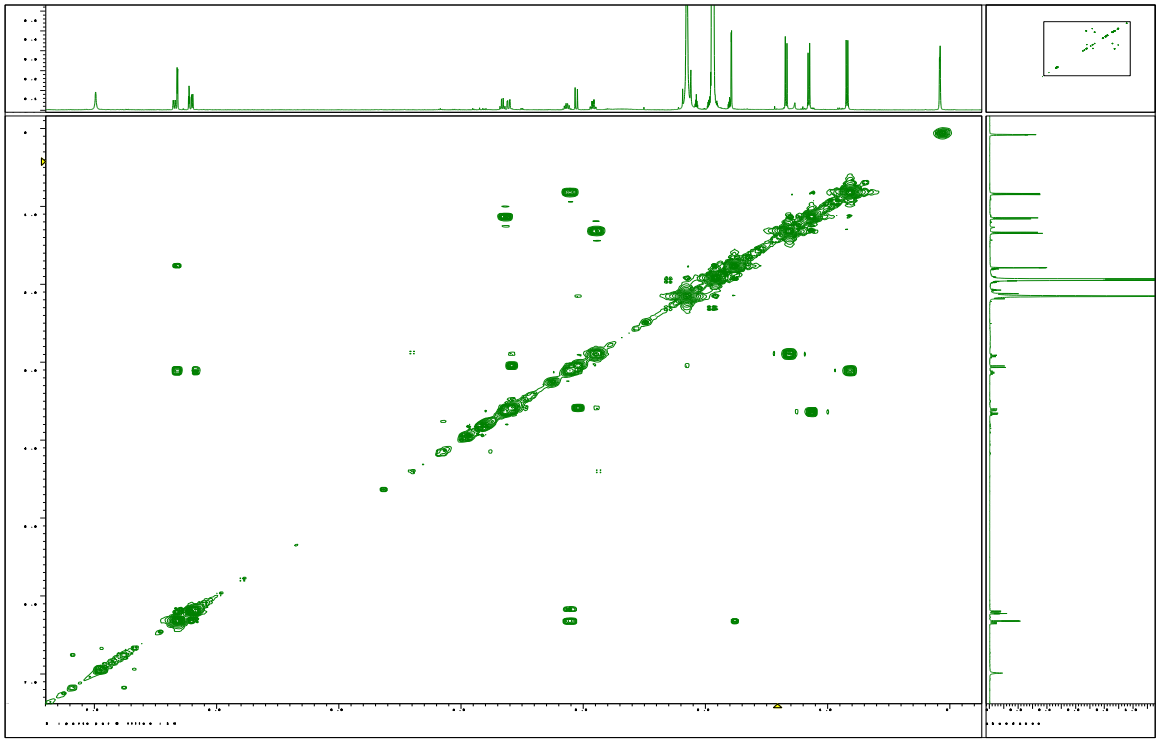

Figure S45. HMQC spectrum of precursor A (**9**) in acetonitrile-d_3.

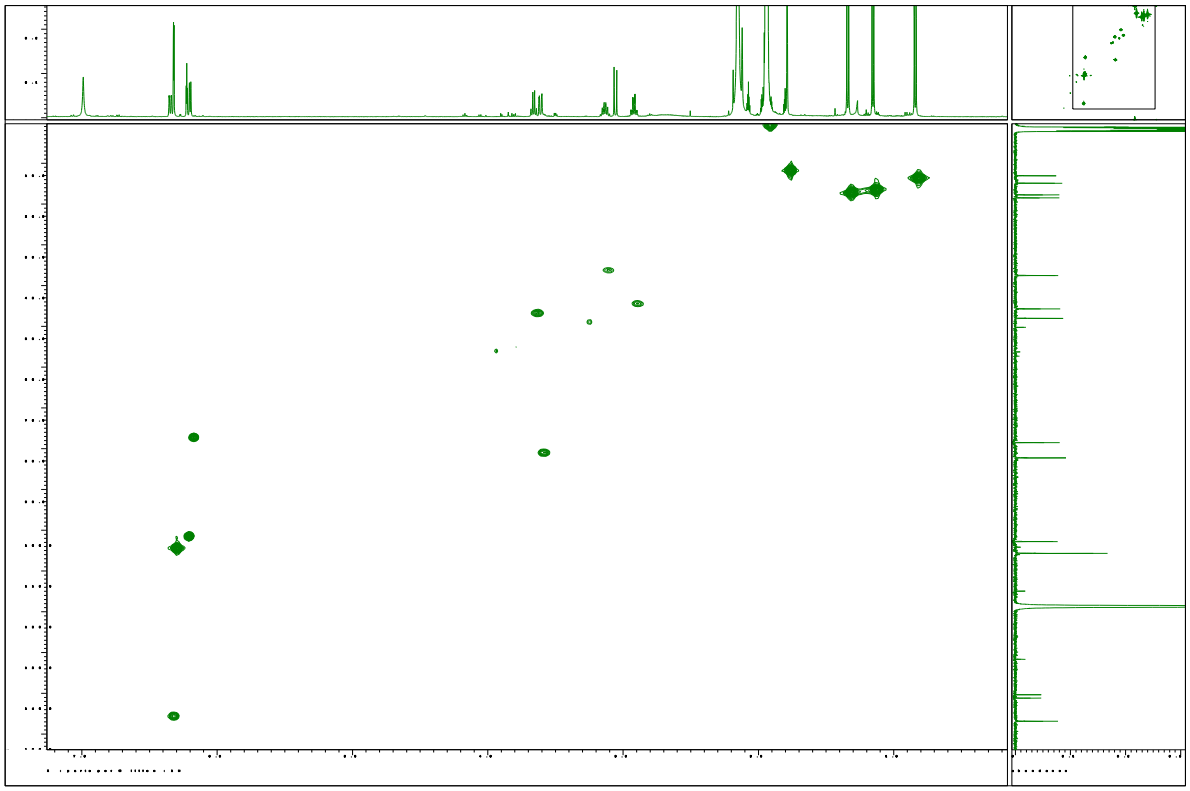

Figure S46. HMBC spectrum of precursor A (**9**) in acetonitrile-d_3.

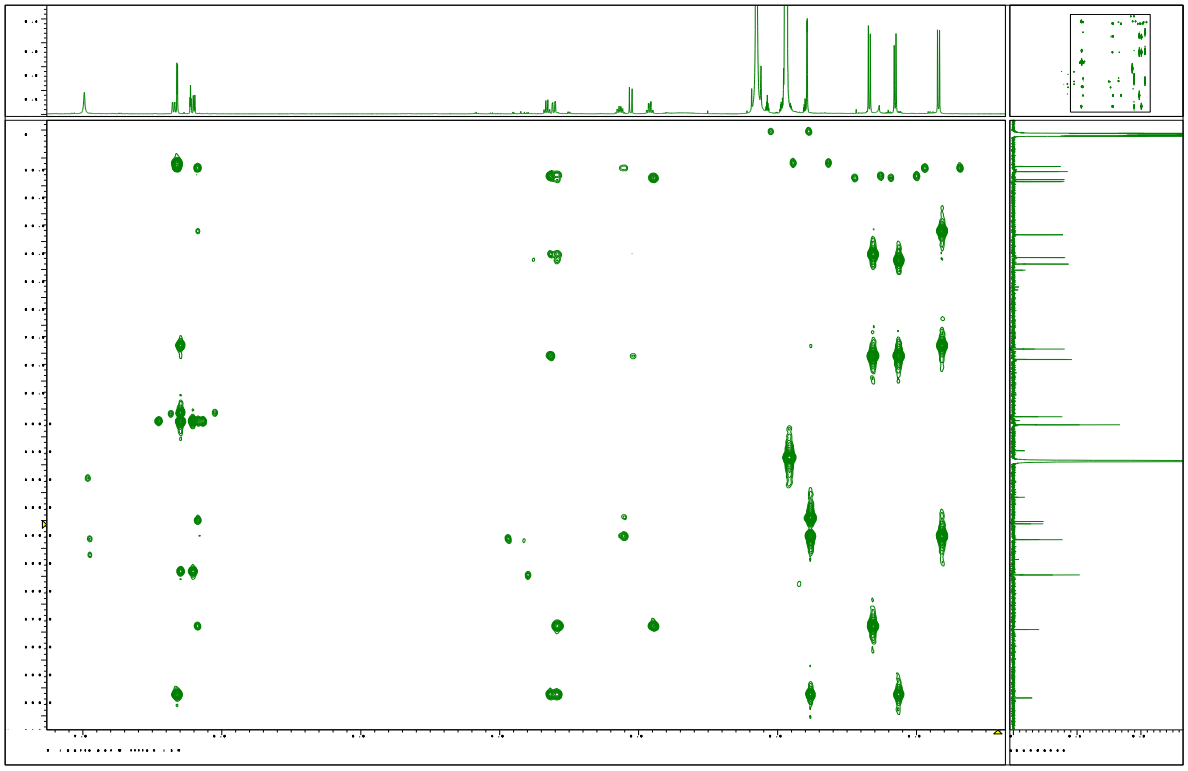

Figure S47. NOESY spectrum of precursor A (**9**) in acetonitrile-d_3.

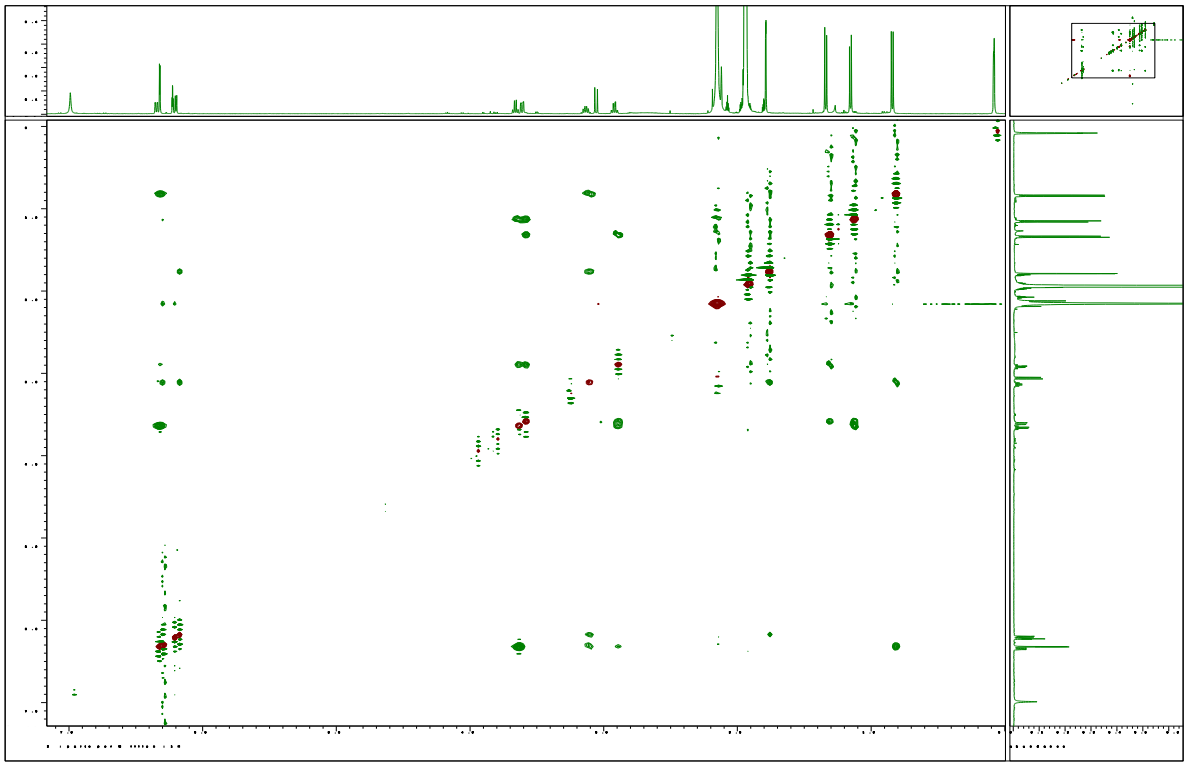

Figure S48. Comparison of ^{1}H and ^{13}C NMR chemical shifts of saccharothriolide analogs.

(a) Differences between ^{1}H and ^{13}C NMR chemical shifts of saccharothriolides G (**10**) and B (**2**).

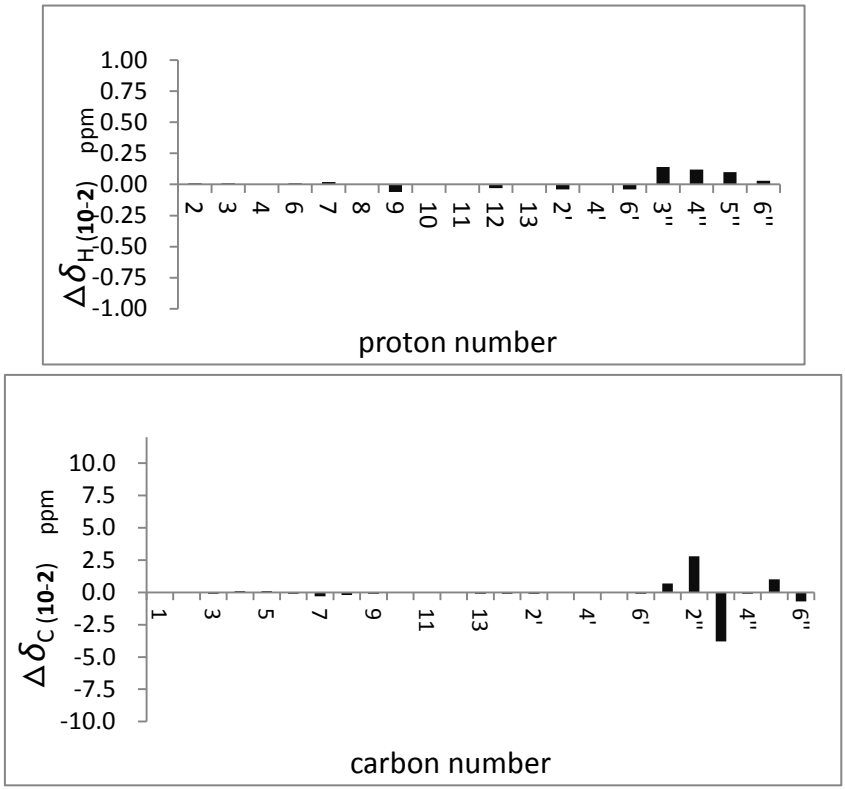

(b) Differences between ^{1}H and ^{13}C NMR chemical shifts of saccharothriolides H (**11**) and E (**5**).

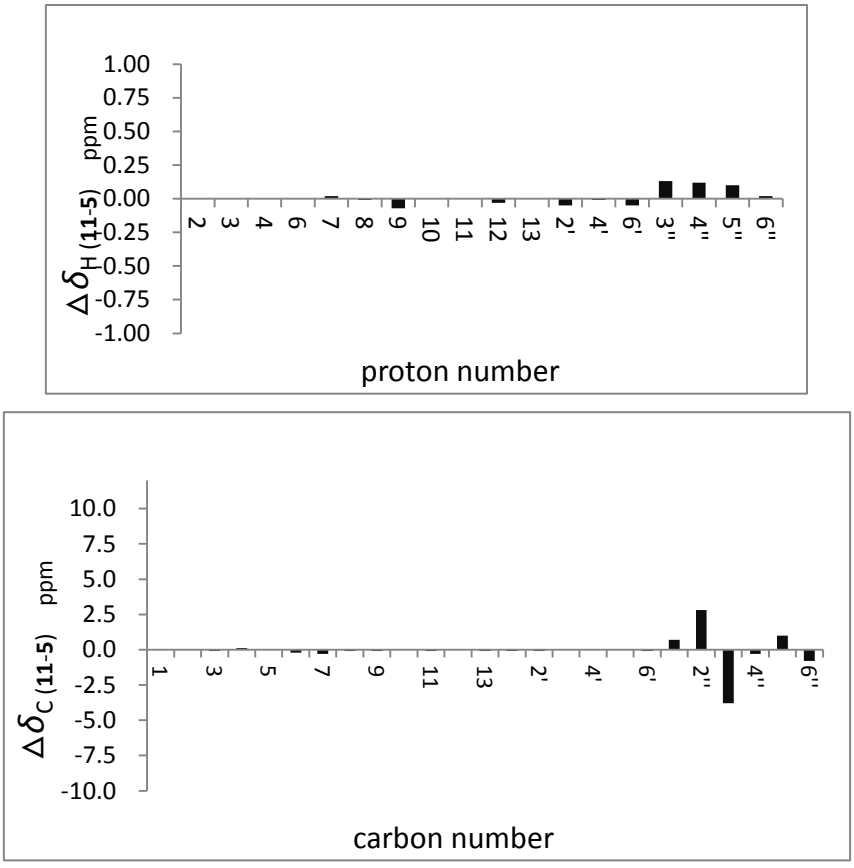

Figure S49. HR-ESI-MS spectrum of saccharothriolides G-J (**10-13**).

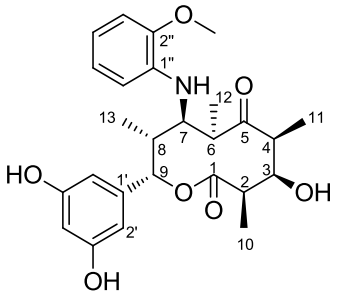

saccharothriolide G (**10**)

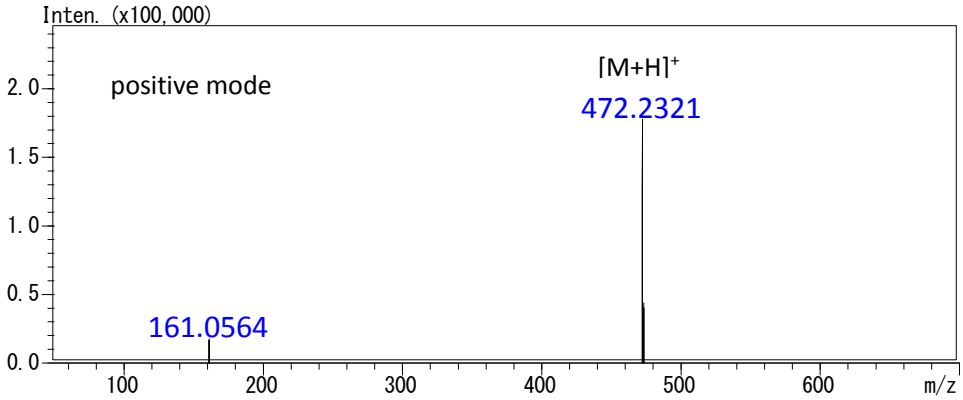

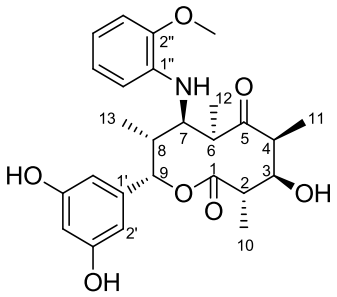

saccharothriolide H (**11**)

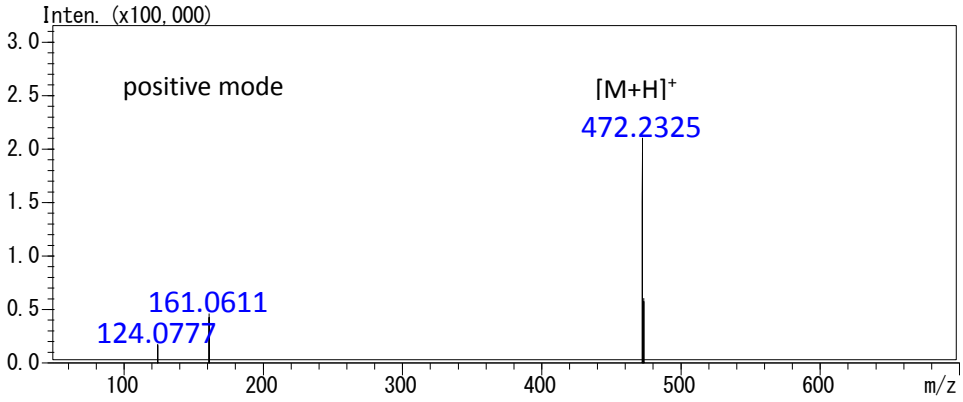

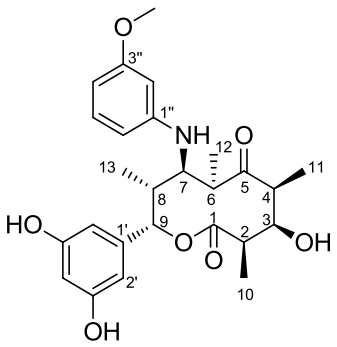

saccharothriolide I (**12**)

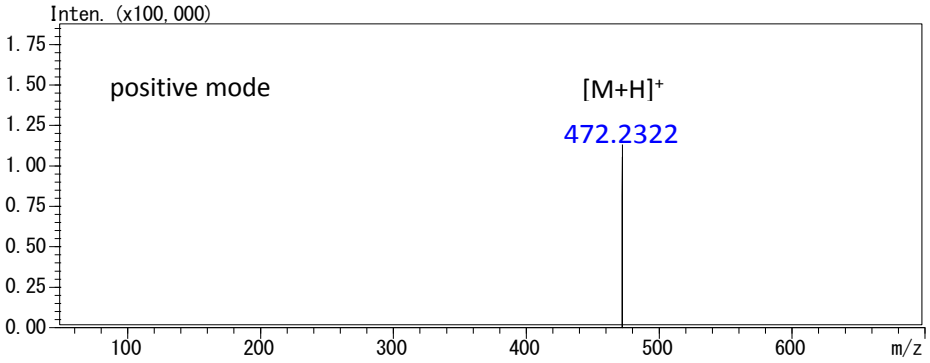

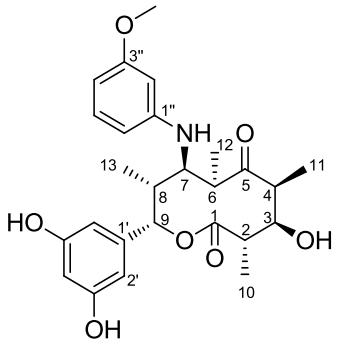

saccharothriolide J (**13**)

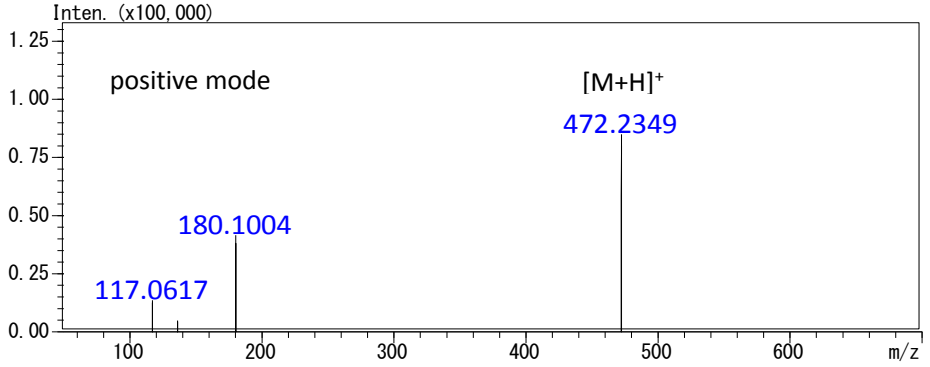

Figure S50. UV spectra of saccharothriolides G-J (**10**-**13**) in methanol.

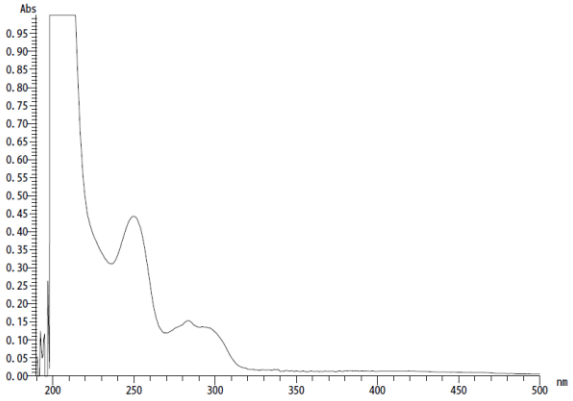

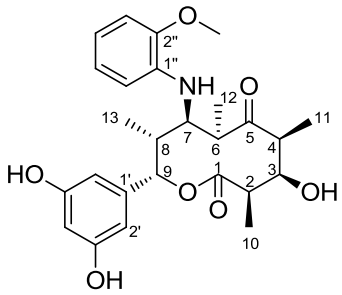

saccharothriolide G (**10**)

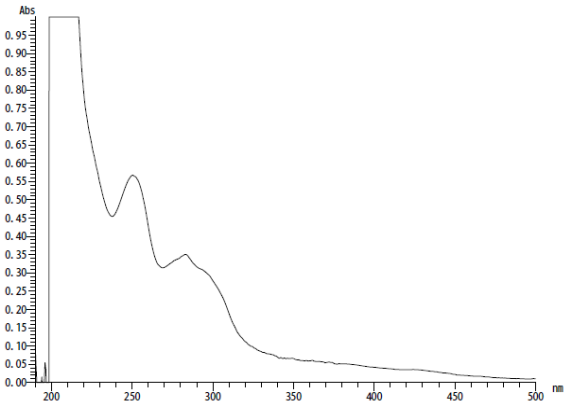

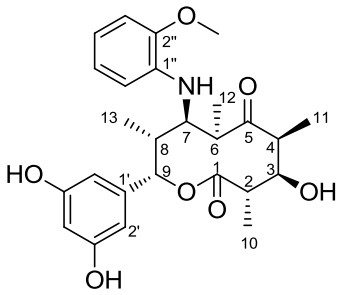

saccharothriolide H (**11**)

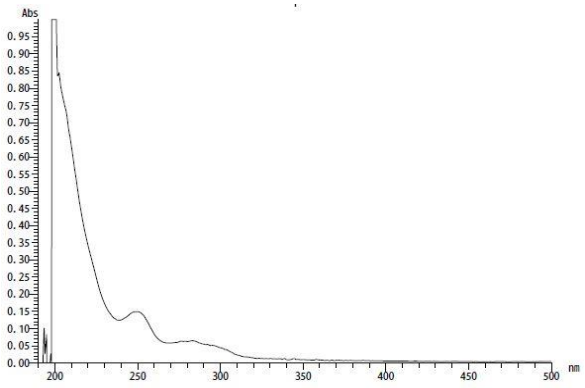

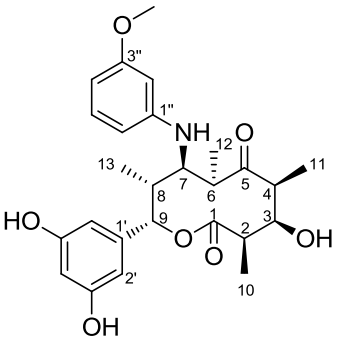

saccharothriolide I (**12**)

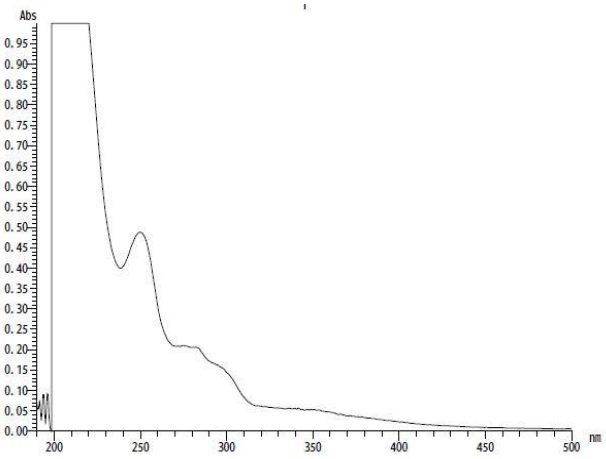

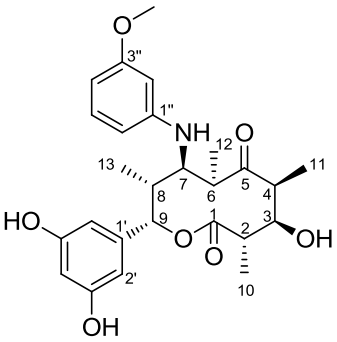

saccharothriolide J (**13**)

Figure S51. ^{1}H NMR spectrum of saccharothriolide G (**10**) in methanol-d_4.

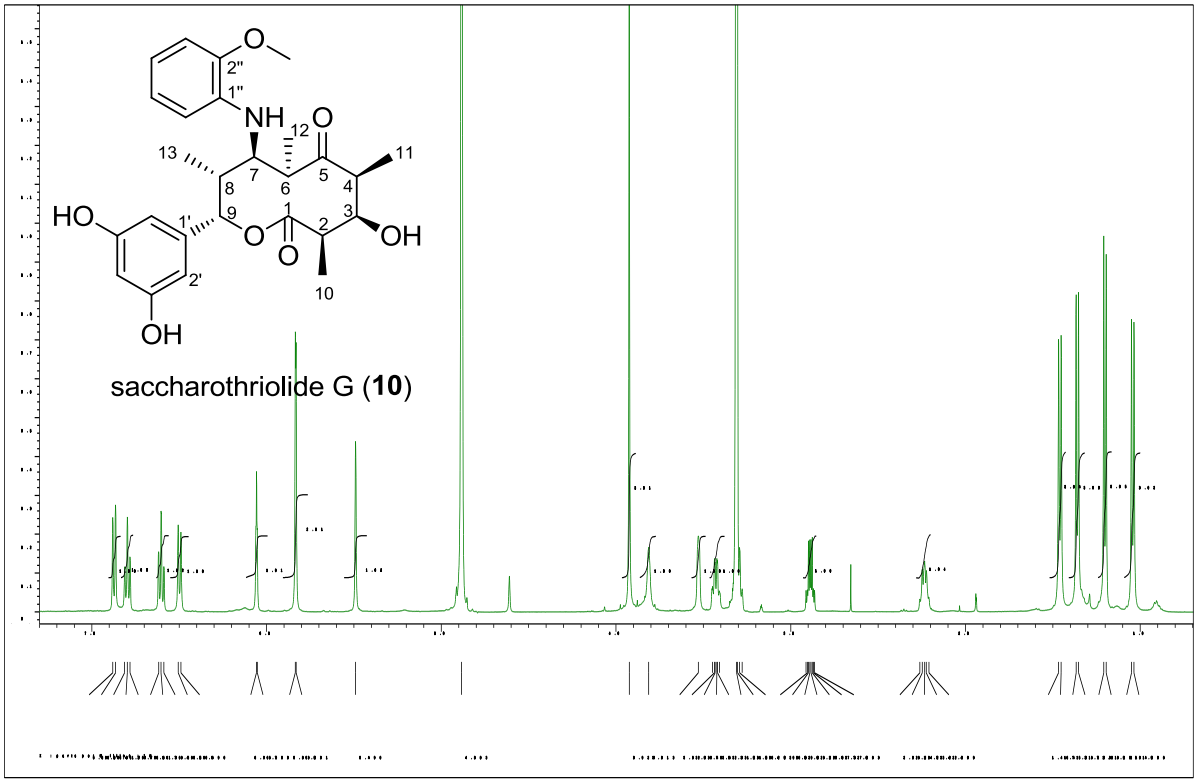

Figure S52. ^{13}C NMR spectrum of saccharothriolide G (**10**) in methanol-d_4.

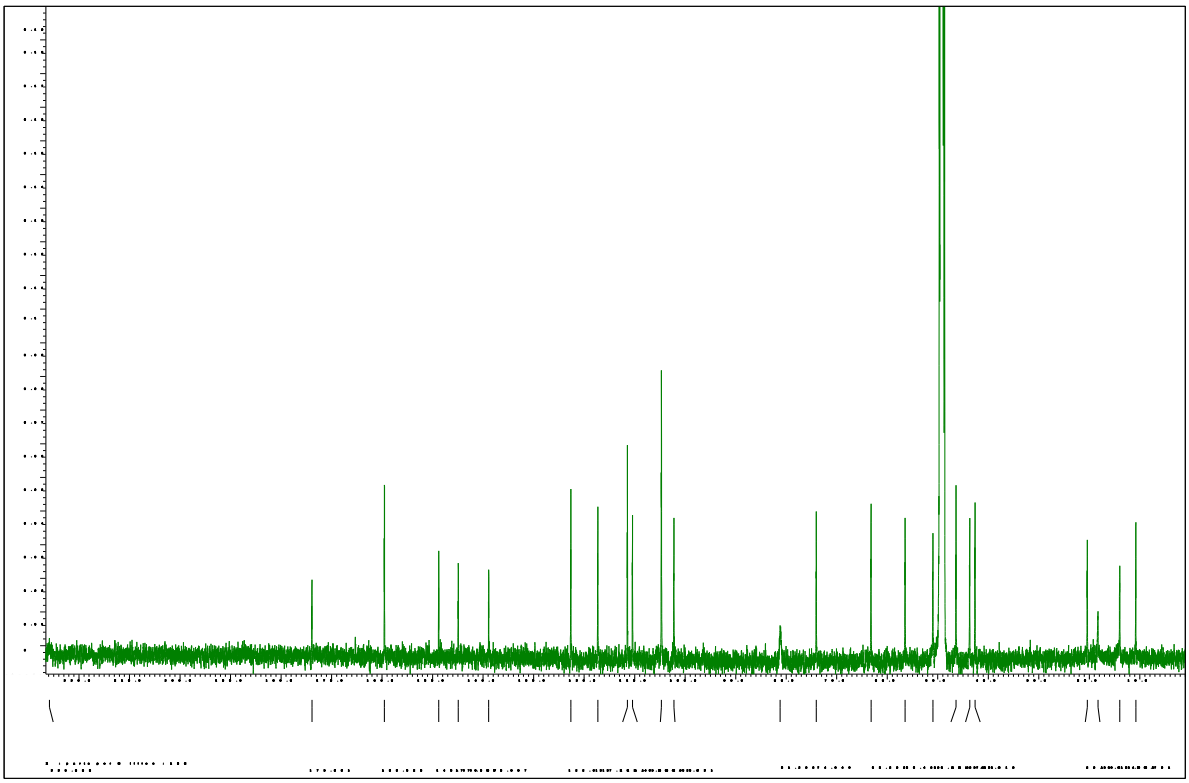

Figure S53. ^{1}H-^{1}H COSY spectrum of saccharothriolide G (**10**) in methanol-d_4.

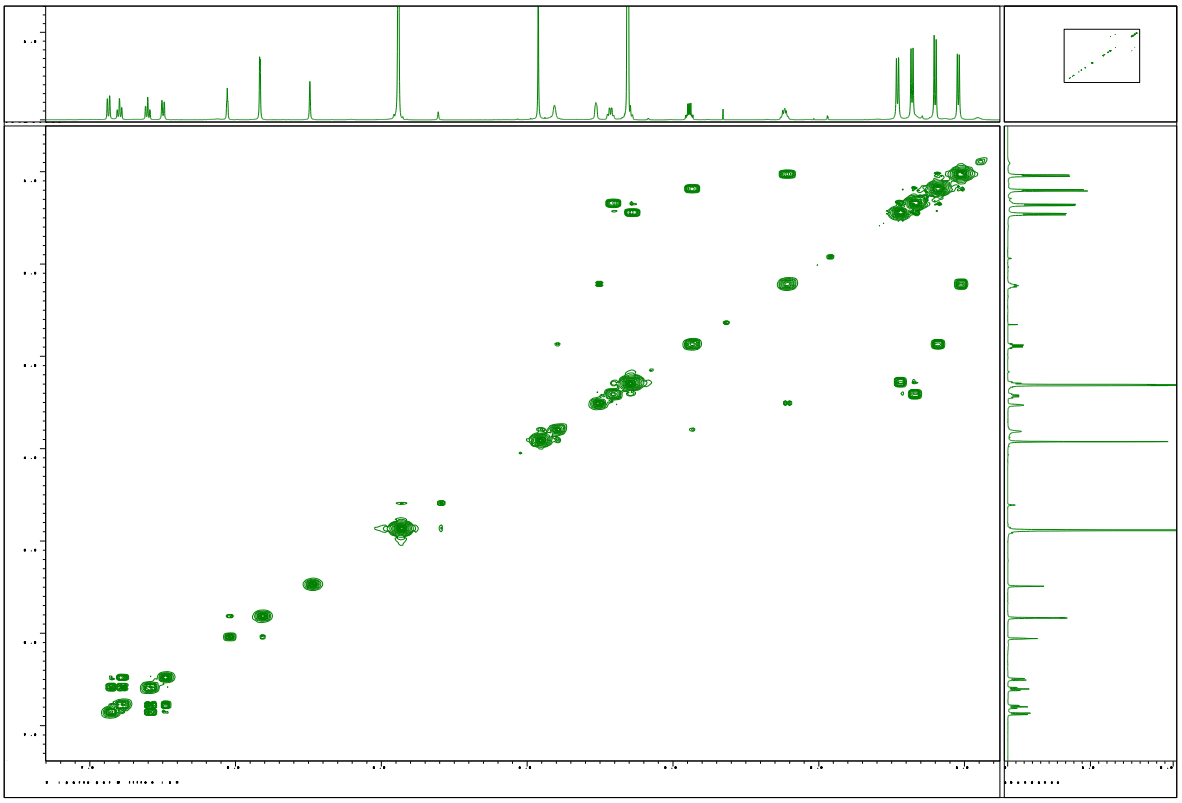

Figure S54. HMQC spectrum of saccharothriolide G (**10**) in methanol-d_4.

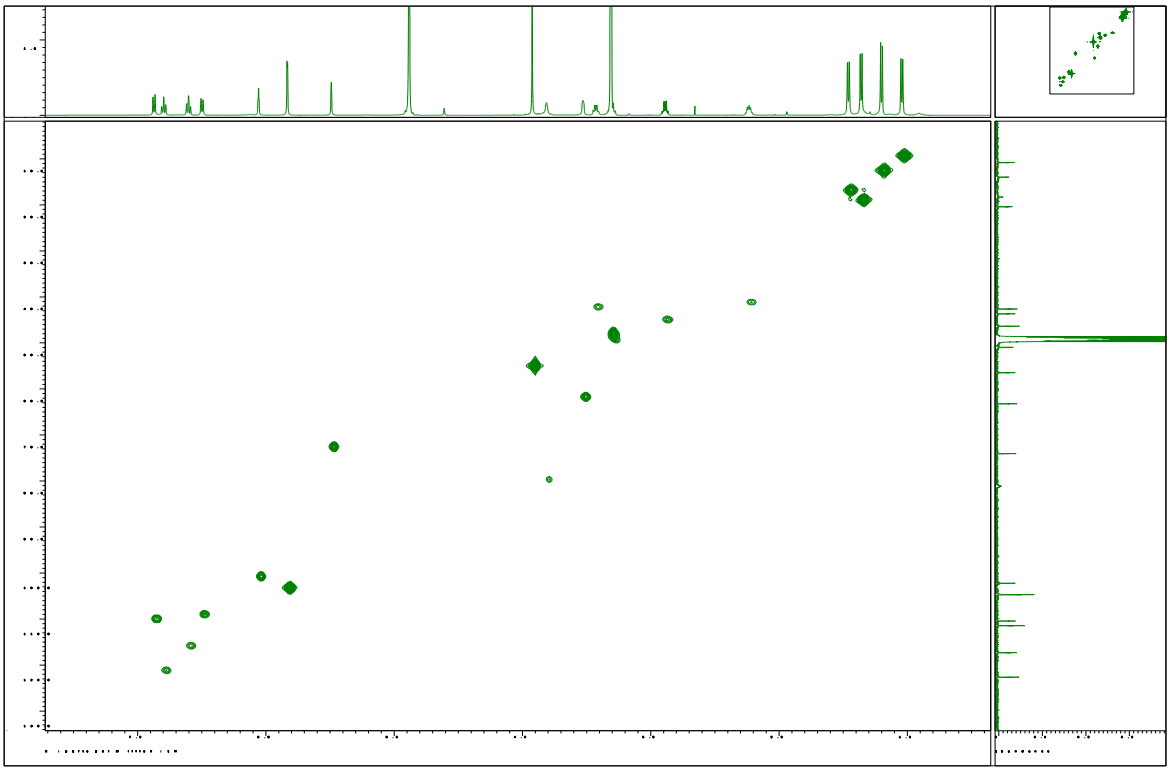

Figure S55. HMBC spectrum of saccharothriolide G (**10**) in methanol-d_4.

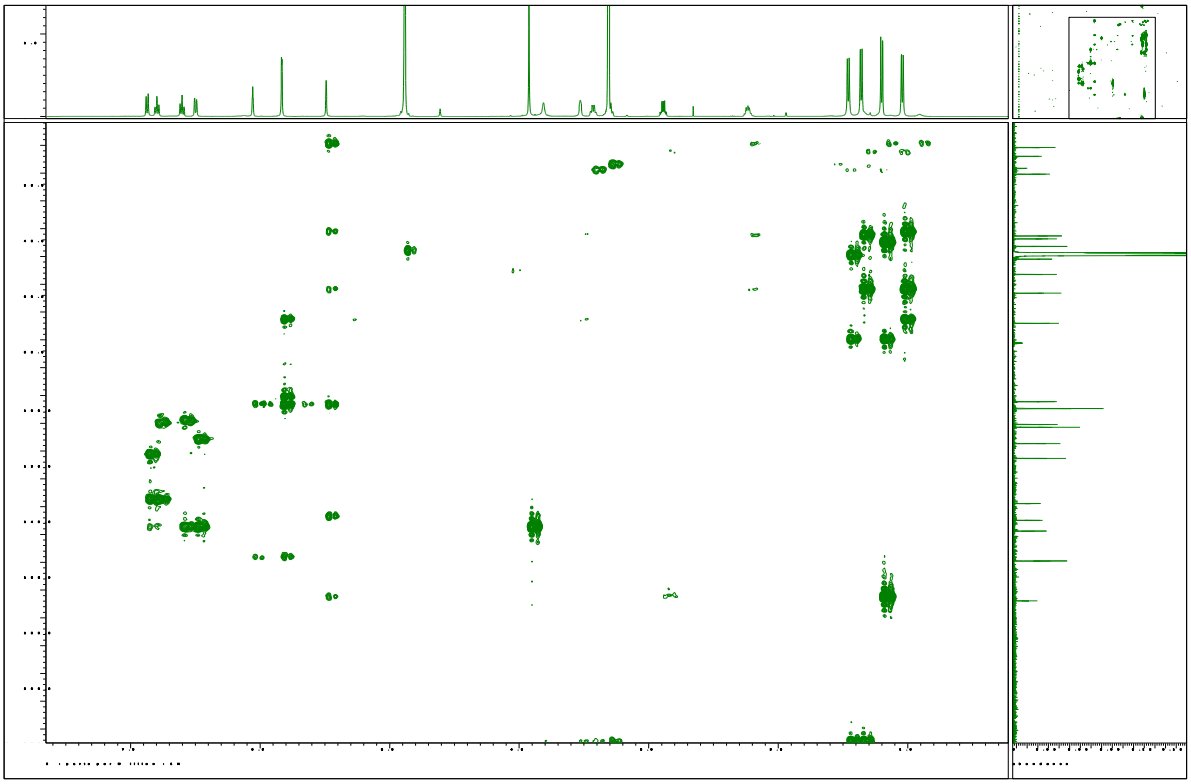

Figure S56. NOESY spectrum of saccharothriolide G (**10**) in methanol-d_4.

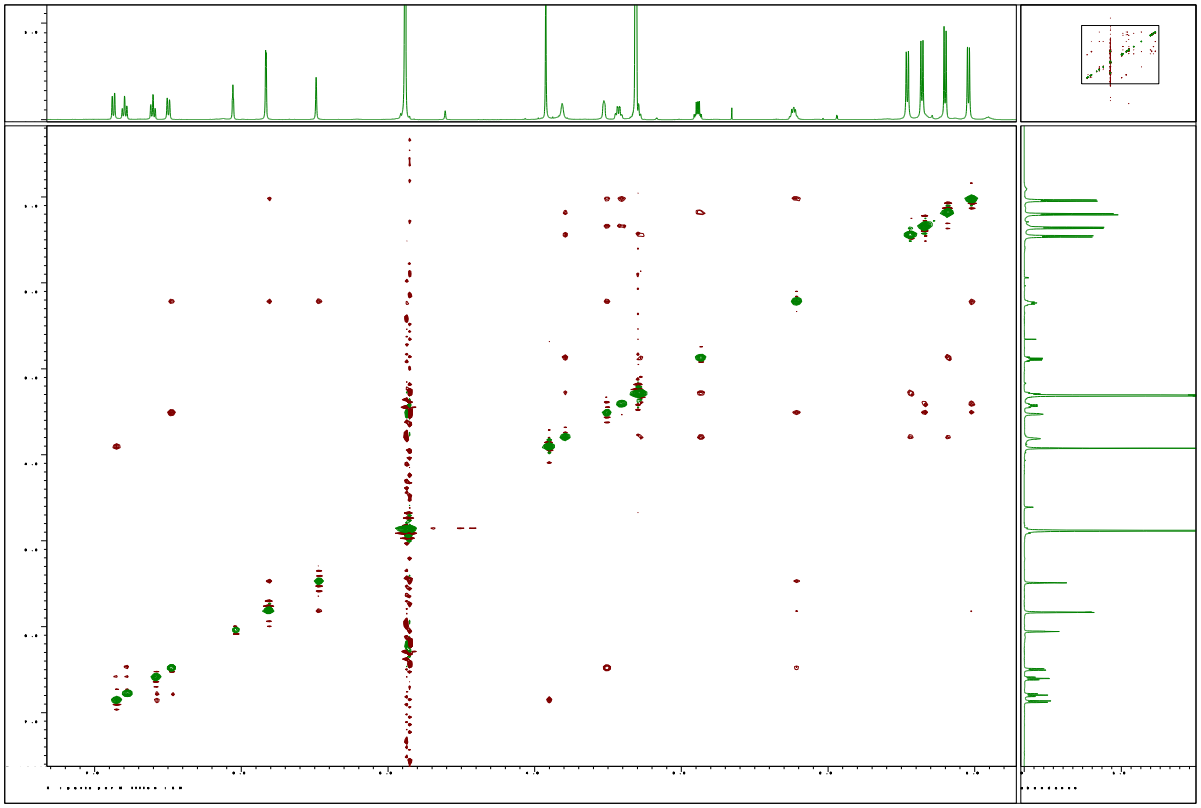

Figure S57. [1]H NMR spectrum of saccharothriolide H (**11**) in methanol-d_4.

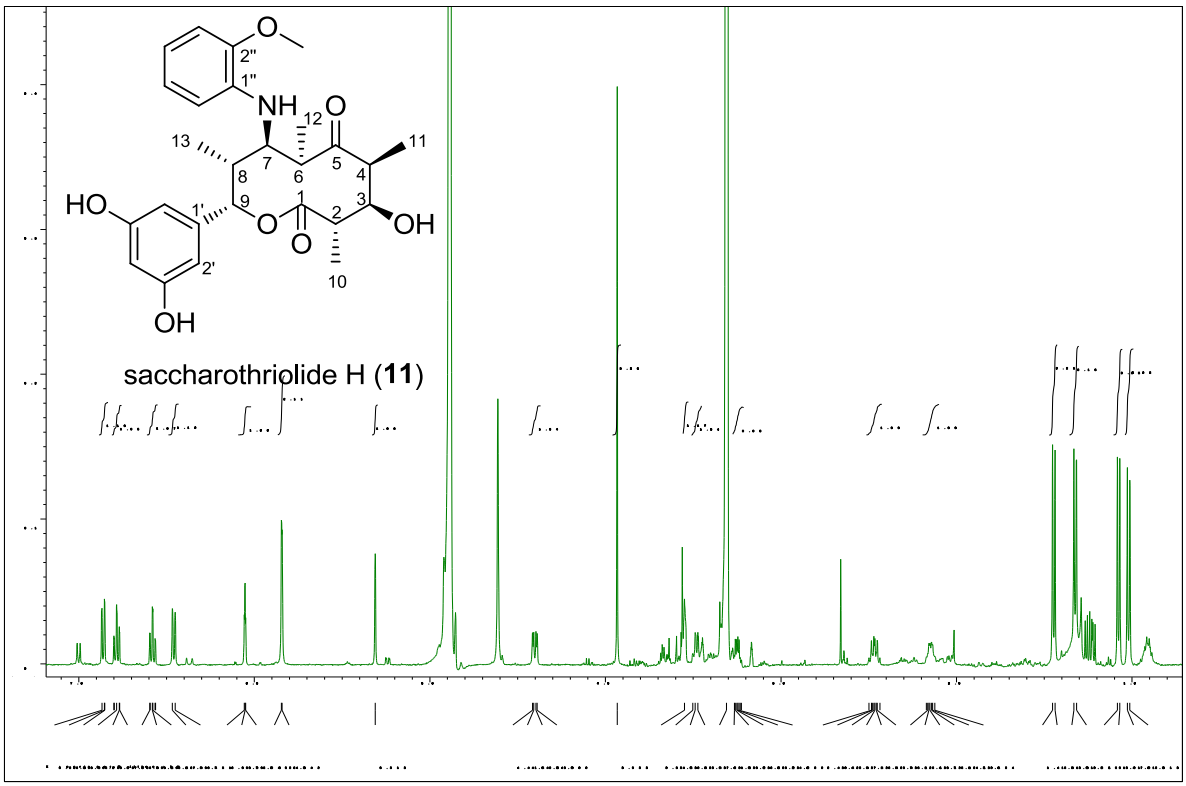

Figure S58. [13]C NMR spectrum of saccharothriolide H (**11**) in methanol-d_4.

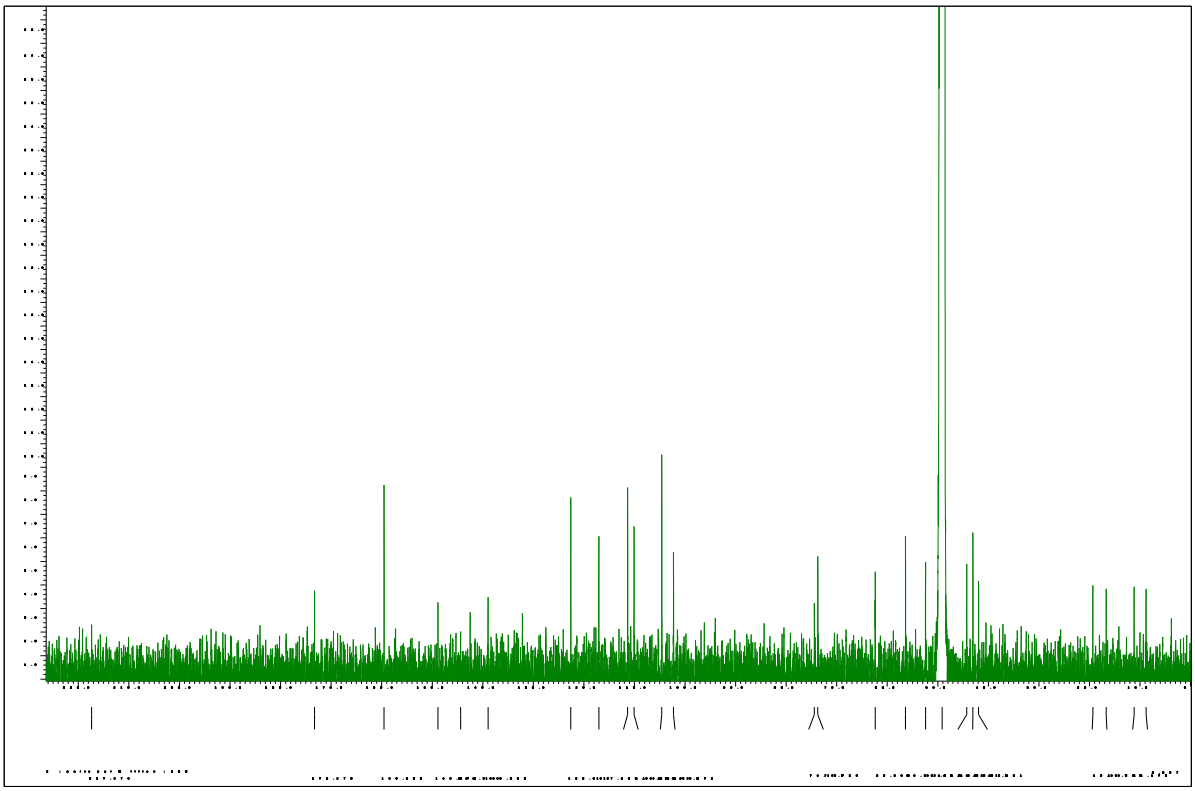

Figure S59. ^{1}H NMR spectrum of saccharothriolide I (**12**) in methanol-d_4.

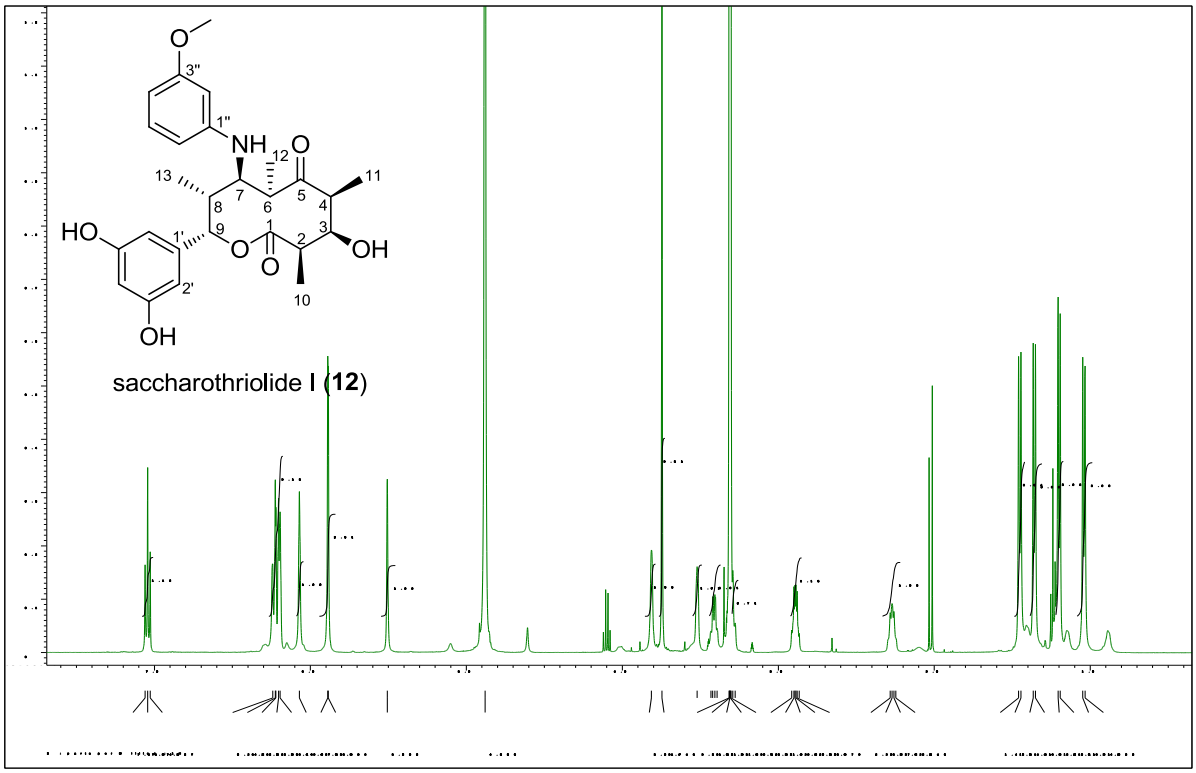

Figure S60. ^{13}C NMR spectrum of saccharothriolide I (**12**) in methanol-d_4.

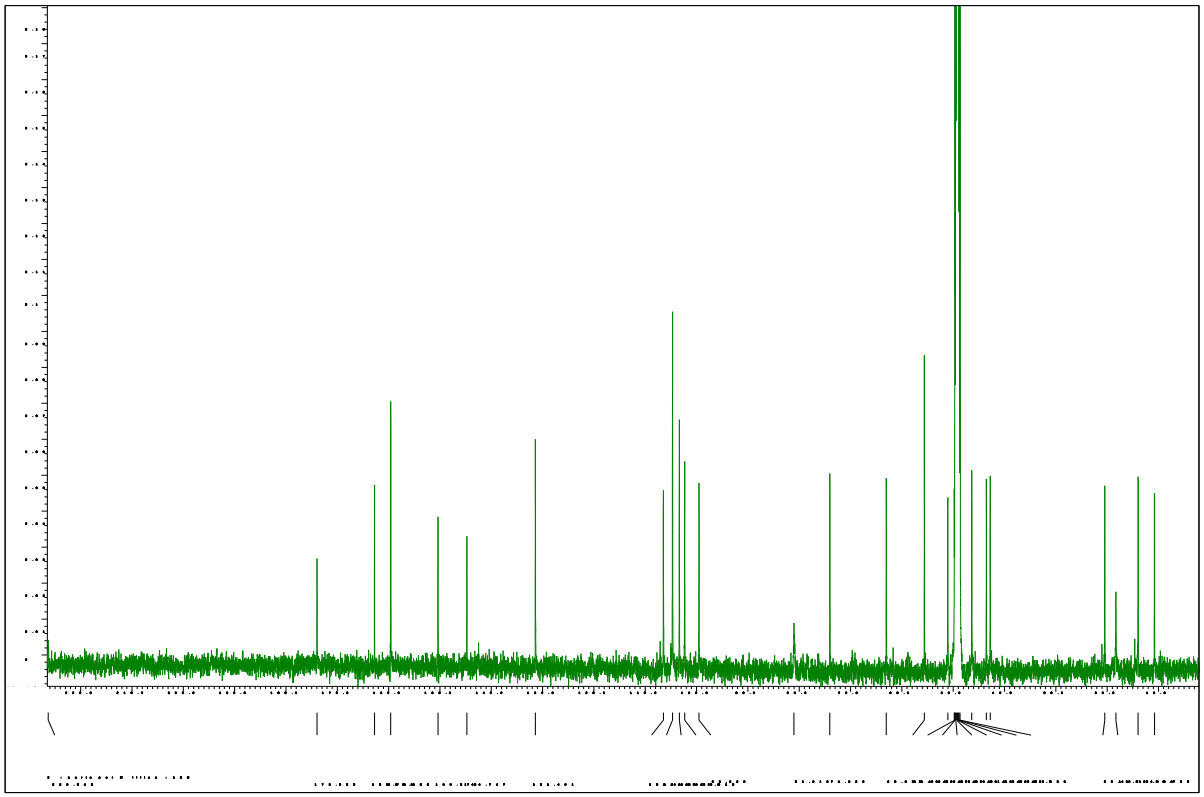

Figure S61. ^{1}H-^{1}H COSY spectrum of saccharothriolide I (**12**) in methanol-d_4.

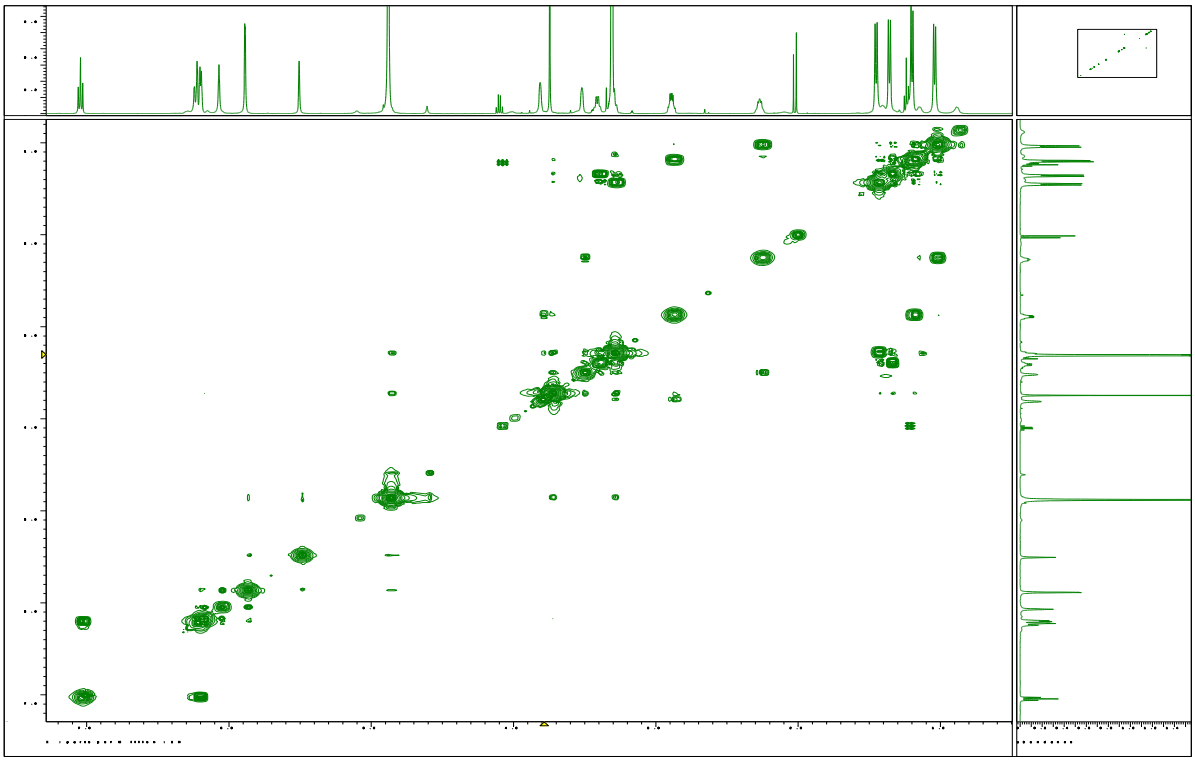

Figure S62. HMQC spectrum of saccharothriolide I (**12**) in methanol-d_4.

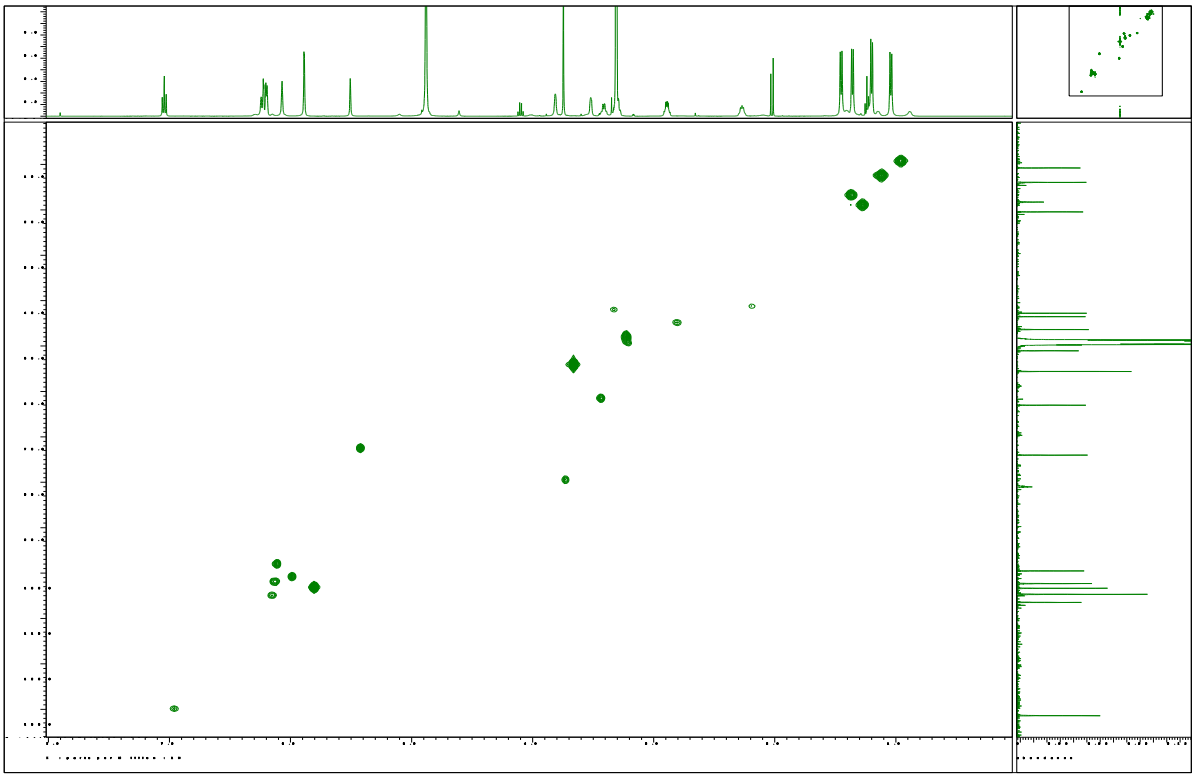

Figure S63. HMBC spectrum of saccharothriolide I (**12**) in methanol-d_4.

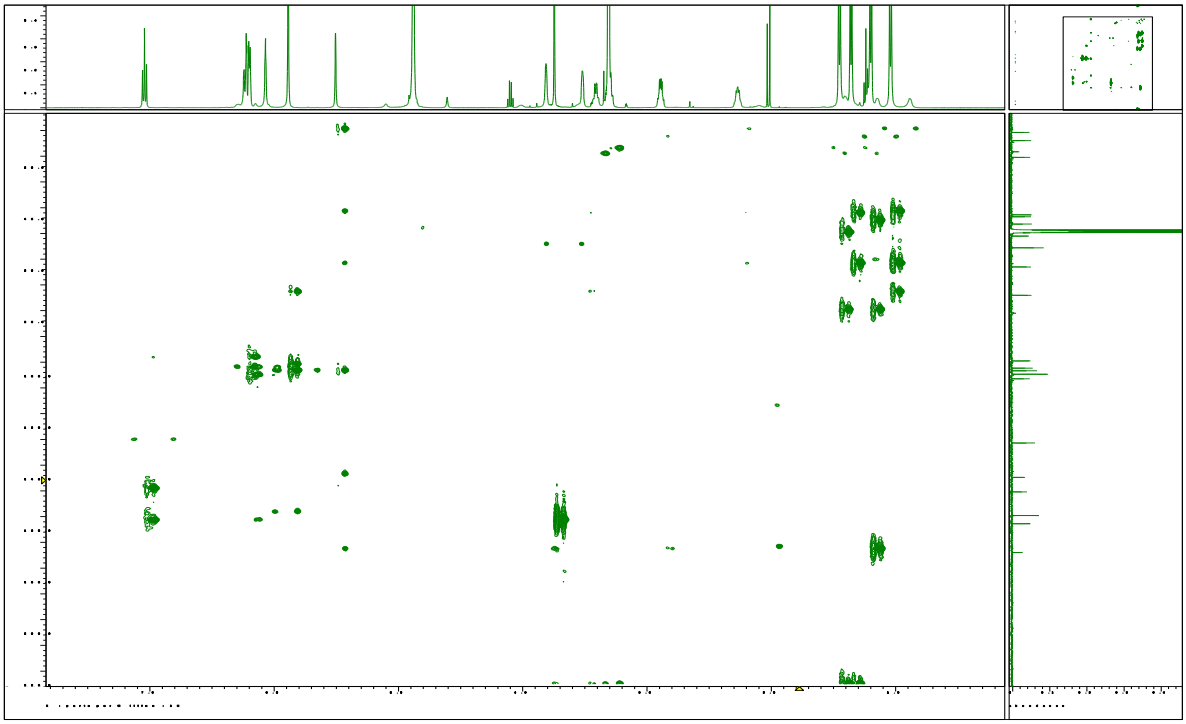

Figure S64. NOESY spectrum of saccharothriolide I (**12**) in methanol-d_4.

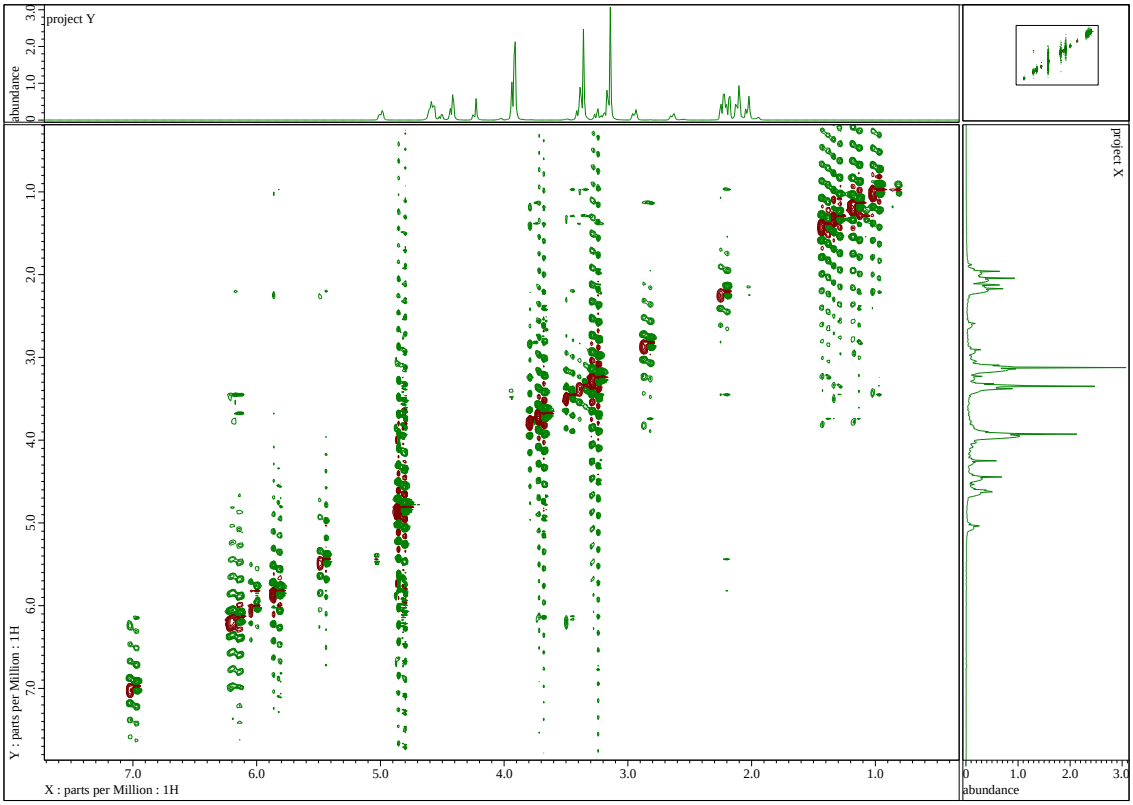

Figure S65. ^{1}H NMR spectrum of saccharothriolide J (**13**) in methanol-d_4.

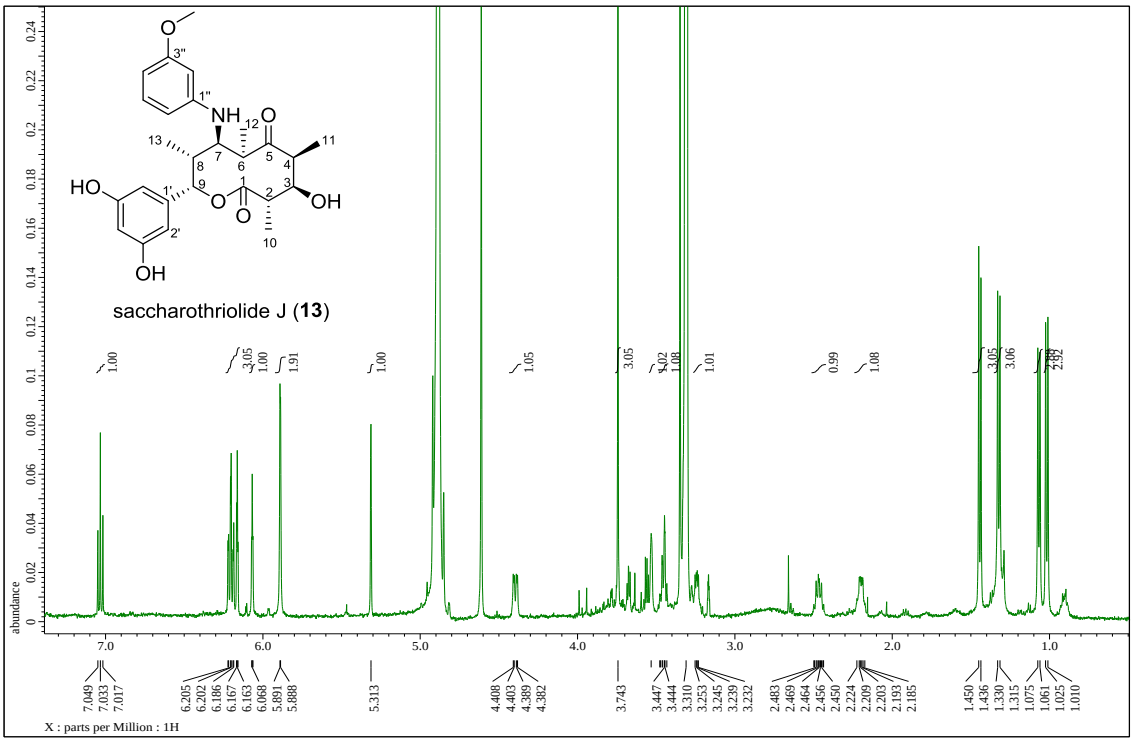

Figure S66. ^{13}C NMR spectrum of saccharothriolide J (**13**) in methanol-d_4.

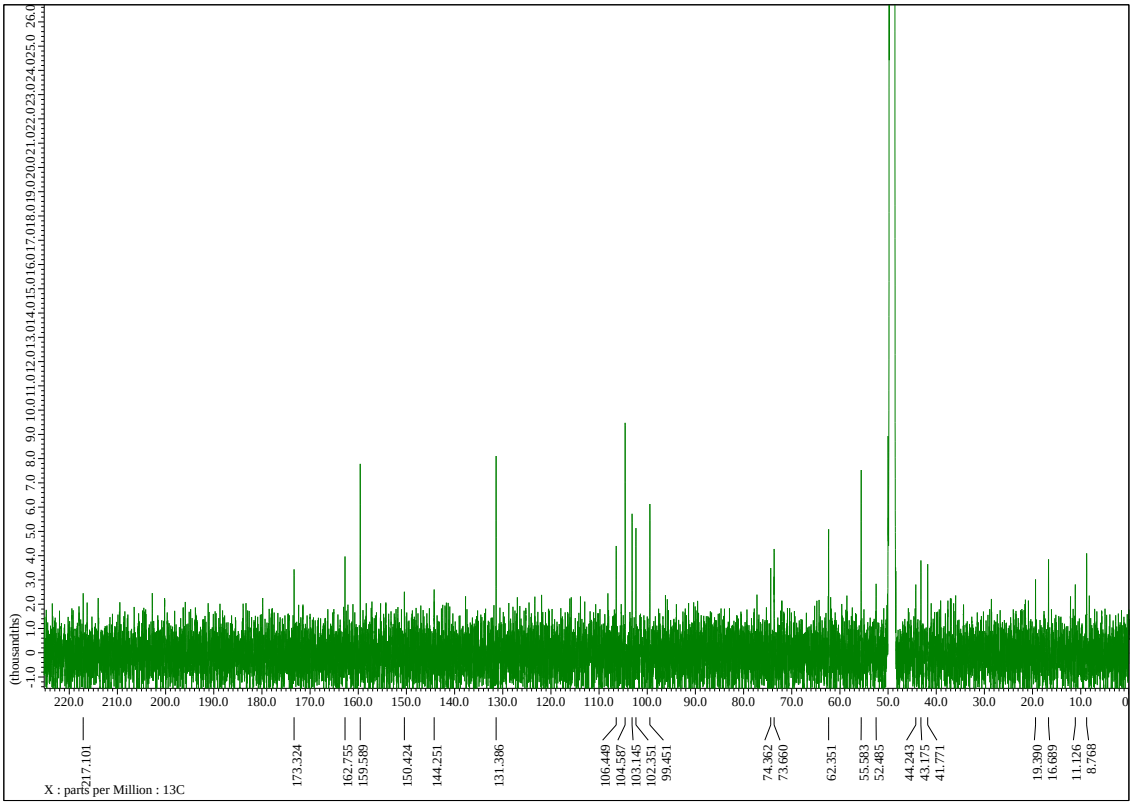

Acknowledgements

First and foremost I would like to thank my supervisor, professor Hideaki Kakeya for giving me the opportunity to complete my PhD degree in Kyoto University, and carry out this research. I would also like to thank him for providing generous funding for my research and numerous travel opportunities at conferences to present my work.

Secondly, special thanks should go to Shinichi Nishimura for his encouragement and guidance throughout all difficult situations. Thank you for his tremendous academic and personal support throughout the last four years.

I would like to thank everyone past and present in kakeya's lab. The seemingly long four years of research life was filled with countless happy memories.

I wish to acknowledge all collaborators, and my examination committee members, professors Kiyosei Takasu and Hiroaki Ohno, for all their profound and carefully aimed comments and suggestions.

I also should acknowledge China Scholarship Council (CSC) and Japanese Government (MEXT) Scholarship support for carrying out this research.

Finally, a special gratitude and love goes to my family for their unfailing support. I thank my parents for their abiding love. I thank my lovely son, Jiyang Mao, for his sweet smile and waking up early. I thank my husband, Di Mao, for his understanding, academic discussion and sharing the housework.